

VU Research Portal

Hypergranulatory tissue in breast implant surgery and skin scar formation

de Bakker, Erik

2023

DOI (link to publisher)
[10.5463/thesis.145](https://doi.org/10.5463/thesis.145)

document version
Publisher's PDF, also known as Version of record

[Link to publication in VU Research Portal](#)

citation for published version (APA)
de Bakker, E. (2023). *Hypergranulatory tissue in breast implant surgery and skin scar formation*. [PhD-Thesis - Research and graduation internal, Vrije Universiteit Amsterdam]. s.n. <https://doi.org/10.5463/thesis.145>

General rights

Copyright and moral rights for the publications made accessible in the public portal are retained by the authors and/or other copyright owners and it is a condition of accessing publications that users recognise and abide by the legal requirements associated with these rights.

- Users may download and print one copy of any publication from the public portal for the purpose of private study or research.
- You may not further distribute the material or use it for any profit-making activity or commercial gain
- You may freely distribute the URL identifying the publication in the public portal ?

Take down policy

If you believe that this document breaches copyright please contact us providing details, and we will remove access to the work immediately and investigate your claim.

E-mail address:
vuresearchportal.ub@vu.nl

Hypergranulation tissue
in breast implant surgery
and skin scar formation



Erik de Bakker

**Hypergranulation tissue in breast implant
surgery and skin scar formation**

Erik de Bakker

Author: Erik de Bakker
Cover design: Lisette Langenberg, www.medschets.nl
Layout design: Concept: Erik de Bakker
Finalisation: Erwin Timmerman, persoonlijkproefschrift.nl

Provided by thesis specialist Ridderprint, ridderprint.nl
Printing: Ridderprint

ISBN: 978-94-6458-947-4

Printing of this thesis was financially supported by: Nederlandse Vereniging voor Plastische Chirurgie, Vakgroep Plastisch, Reconstructieve en Handchirurgie Amsterdam UMC, Amsterdam Movement Sciences, Amsterdam UMC, BlooMEDical BV, BAP Medical, ChipSoft, Merz Pharma Benelux BV, EmdaPlast, MedConsult BV and Dermatologisch Centrum Utrecht

Copyright © E. de Bakker, Amsterdam 2023

All rights reserved. No part of this publication may be reproduced, stored or transmitted in any form or by any means without prior permission of the author.

The research in this thesis was embedded in Amsterdam Movement Sciences Research Institute, at the departments of Plastic, Reconstructive and Handsurgery and the Molecular Cell Biology and Immunology, Amsterdam UMC, location VUmc, the Netherlands

VRIJE UNIVERSITEIT

**HYPERGRANULATION TISSUE IN BREAST IMPLANT
SURGERY AND SKIN SCAR FORMATION**

ACADEMISCH PROEFSCHRIFT

ter verkrijging van de graad Doctor aan
de Vrije Universiteit Amsterdam,
op gezag van de rector magnificus
prof.dr. J.J.G. Geurts,
in het openbaar te verdedigen
ten overstaan van de promotiecommissie
van de Faculteit der Geneeskunde
op vrijdag 17 maart 2023 om 9.45 uur
in een bijeenkomst van de universiteit,
De Boelelaan 1105

door

Erik de Bakker

geboren te Blaricum

Promotiecommissie:

promotoren: prof.dr. M.J.P.F. Ritt
 prof.dr. S. Gibbs

copromotor: dr. F.B. Niessen

promotiecommissie: prof.dr. J.W.M. Niessen
 prof.dr. E. Middelkoop
 prof.dr. M.A.M. Mureau
 prof.dr. R.R.J.W. Van der Hulst
 dr. C. van Montfrans

TABLE OF CONTENTS

Chapter 1	General introduction	6
Part I: hypergranulation tissue in breast implant surgery		
Chapter 2	The Histological Composition of Capsular Contracture Focussed on the Inner Layer of the Capsule: An Intra-Donor Baker-I Versus Baker-IV Comparison.	22
Chapter 3	A case of silicone and sarcoid granulomas in a patient with 'highly cohesive' silicone breast implants: a histopathologic and laser raman microprobe analysis.	38
Chapter 4	Label-free stimulated Raman scattering imaging reveals silicone breast implant material in tissue.	56
Chapter 5	Baker-IV capsular contracture is correlated with an increased amount of silicone material: an intra-patient study.	80
Chapter 6	The Baker classification for capsular contracture in breast implant surgery is unreliable as a diagnostic tool.	100
Part II: hypergranulation tissue in skin scar formation		
Chapter 7	Prognostic tools for hypertrophic scar formation based on fundamental differences in systemic immunity.	116
Chapter 8	Summary and general discussion	142
Chapter 9	List of publications	163
	Dankwoord	165
	About the author	173

I

Every person will be confronted repeatedly during their life with wound healing when they are faced with small, large, or surgical wounds. At its very core, wound healing is a mechanism of repair to return the tissue to homeostasis and normal function after injury. Although the owner may not be consciously aware of it, wound healing is a continuously active process. The repair of small defects in the skin, vessels, and all other tissues in the human body occurs with negligible scarring and is no longer visible to the eye. On the other hand, normal healing of deeper injuries will result in the repair of the defect at the expense of a visible scar.

Wound healing can be divided into a number of phases and is an intricate balance between many cells and cytokines. Traditionally, the scientific field divided wound healing into three distinctive phases; inflammation, proliferation, and tissue remodelling or maturation (fig 1). As our knowledge expands, it is now realized that wound healing is more complex, that these phases overlap and their duration depends on the extent of the trauma and type of wound¹⁻³.

The inflammatory phase has a rapid onset after injury and begins directly after haemostasis. With capillary damage, blood loss results in activation of the intrinsic coagulation pathway to form a blood clot. The function of the blood clot is to stop further blood loss and provide an initial quick closure of the defect by depositing fibrin and fibronectin. The platelets within the clot, together with cells within the damaged tissue, are responsible for triggering the inflammatory cascade by releasing chemokines that attract inflammatory cells such as neutrophils and monocytes, and later endothelial cells and fibroblasts. Neutrophils clear the matrix and kill bacteria, while monocytes attracted to the wound bed will transform to macrophages to clear away debris. Several days after the start of this process there is a transition to the proliferation phase, which can take up to six weeks and is meant to restore the skin barrier function². In the case of the skin, keratinocytes migrate into the wound bed and proliferate to re-epithelialize the area⁴. Fibroblasts are pivotal from this time on as they are responsible for creating the provisional collagen matrix. Stimulated by their surroundings fibroblasts transform to myofibroblasts, synthesizing a more definitive extracellular matrix. As the myofibroblasts also show contrac-

tile properties, they are a major factor in the contraction and maturation of the granulation tissue³. Angiogenesis is an important part of this phase, as vascular perfusion is vital in delivering oxygen and nutrients necessary for, amongst other things, the proliferation of fibroblasts and keratinocytes. The final maturation or remodelling phase of the damaged tissue can take up to 24 months in which the (myo)fibroblasts will construct a definitive collagen matrix which is what we know as the scar⁴⁵. Proteolytic enzymes, mainly metalloproteinases and their inhibitors, are important in this phase. Elastin, which is responsible for elasticity of the skin and tissue, can be found again after being absent in the granulation tissue³. Apoptosis is the final important process as it significantly reduces the number of both vascular cells and myofibroblasts within the tissue.

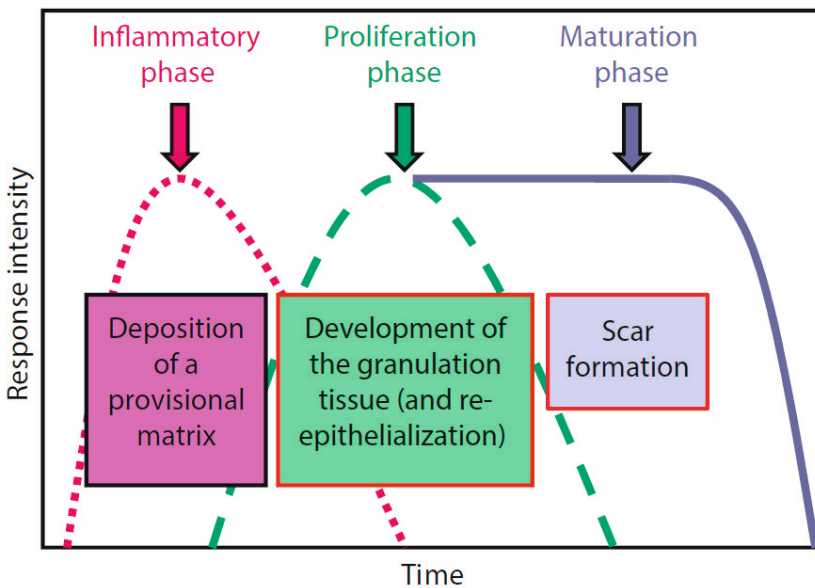


Figure 1: Overview of the various phases of wound healing. Adapted from Darby and Desmoulière³

The favourable outcome, resulting in wound closure with a minimum scar requires all elements in this chain of wound healing to work together optimally to produce just the right amount of granulation tissue. Therefore, it should come as no surprise that aberrant wound healing exists on both sides of a spectrum. When wounds fail to proceed through all steps of normal wound healing they become chronic wounds, inducing significant complaints and morbidity⁶.

At the other end of the spectrum, when there is ‘too much’ tissue formed, known as hypergranulation, fibrosis (excessive scar formation) can occur. Fibrosis can occur in all organs and can subsequently cause a myriad of health problems.

This thesis focuses on fibrosis after breast surgery resulting in I) capsular contracture, and II) skin hypertrophic scarring.

Part I: hypergranulation tissue in breast implant surgery

The absence of a thriving breast enhancement business since the early 20th century is not for a lack of trying. As early as 1895, Czerny performed a reasonably successful autologous fat transfer by moving a lipoma to the breast after having removed a breast tumor⁷. Subsequently, he and many others proceeded to experiment with a plethora of materials to augment or correct the form of the female breast. This resulted in paraffin injections, glass and ivory balls, and sponge implants made from varying chemicals being implanted, all of which had significant risks and morbidity^{7,8}. As a result, these procedures were far from popular. Nonetheless, there was an evident demand, which just needed a suitable material.

The medical use of silicone took off in the 1940s, with free silicone injections being used in breast augmentation. Like free silicone injections today, these procedures led to many complications including pain, chronic infections, and subsequent loss of the breast^{7,9,10}. In 1963 the breast implant, made from silicone and more or less the same as we know it today, was introduced by the Dow Corning Corporation, paving the way for widespread use⁷.

The increase in the use of silicone breast implants in cosmetic breast augmentation surgery and breast reconstructive surgery has been very significant

worldwide ever since their introduction. In the Netherlands alone, about 3.3% of women have breast implants and 26.740 implants in 11.660 patients were placed in²⁰¹⁹¹¹. In the USA, 313.000 breast augmentations and 78.000 breast reconstruction procedures using silicone implants were performed in 2018. Worldwide, a staggering 1.8 million breast augmentations were performed in 2018 alone, a number that is increasing year by year and the majority of which involves using silicone breast implants¹².

Although these numbers are impressive, their use has sparked much controversy and many questions still remain, some of which this thesis aims to answer.

The foreign body reaction

While capsular contracture is undoubtedly one of the most discussed subjects concerning breast implants, it is important to emphasize that capsule formation is a completely normal, physiological process of the healthy human body reacting to a foreign object.

Capsule formation is not unique to breast implant surgery, occurs as the final stage of the normal wound healing process and is a reaction to any foreign body, whether it is a splinter or a cochlear implant¹³⁻¹⁵.

Our body is constantly faced with potential threats in the form of micro-organisms and foreign substances. The way our innate immune system handles these foreign substances and intruders is very much like the security of many companies is handled; instead of recognizing each threat it will instead recognize anything being not part of the body and will try to eliminate this. Elimination is handled by phagocytosis and phagolysosomal digestion of the intruder¹⁵. This works very well against micro-organisms but fails with larger objects like foreign bodies. Macrophages will try to eat away the object and will form a fibrous capsule around the object, to effectively exclude it from the body. In short, the immune system wants to get rid of all unfamiliar elements it encounters and in the case of implants or foreign bodies, it cannot do this and does the next best thing, it forms a capsule.

If the formed fibrous capsule around an implant after the initial wound healing would be definitive and truly exclude the implant from the body, that would be

that and there would have been no reason for this thesis (and the many before and probably after this one). However, this is not the case.

The symptomless capsule

In the symptomless capsule formation, three layers form (see figure 1). There is a clear distinction between the layer most adjacent to the implant and those further away from it. The inner layer consists of a thin layer of cells, mostly fibrocytes, histiocytes and/or macrophages, sometimes arranged in a palisaded manner to form an epithelial like layer (see figure 2a, layer A)¹⁶. This layer is not consistently reported in all histological research, but seems to be more prevalent in capsules from textured implants and polyurethane implants¹⁷⁻¹⁹. Beyond this layer is the intermediate layer with fibrils aligned with the implant and an outer layer with extracellular matrix aligned perpendicular to the implant (layers B and C respectively).

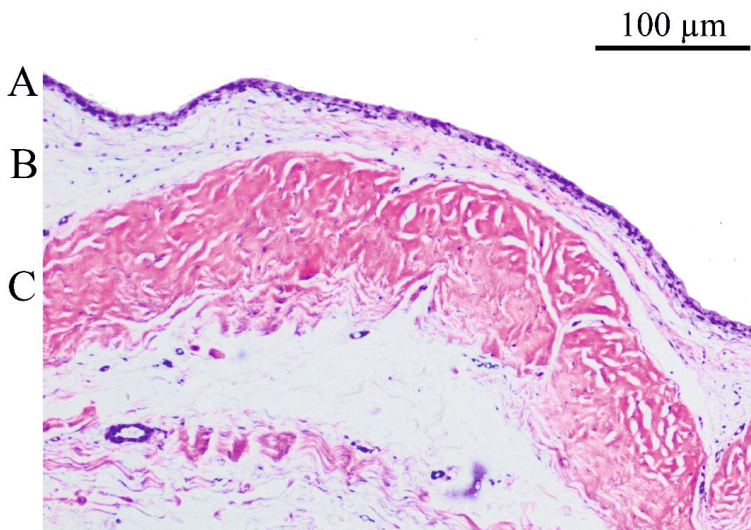


Figure 2a: Baker-I (symptomless) capsule with **A** inner layer, **B** intermediate layer, **C** outer layer. Implant was adjacent to the inner layer.

The symptomatic capsule

If too much fibrotic tissue is formed around the implant, thickening and contracture may occur and this is the most prevalent complication following breast implant surgery¹⁶. The complaints experienced vary depending on the severity of thickening and contracture, ranging from just mild hardening or increased visibility or sensibility of the implant to significant deformation and pain. Needless to say, these complaints are a major contributor to loss of quality of life for patients and they are usually the primary reason for revision surgery²⁰. Moreover, patients who have already been shown to develop capsular contracture (CC) are more likely to have recurring instances of CC after revision surgery¹⁶. The reported incidence rates vary widely, ranging from 0.6 to 17.4 percent for primary cosmetic augmentation and 21.1 to 47.7 percent for breast reconstructive surgery²¹.

The classification introduced by dr. Baker in 1978 proposed a four-point scale ranging from grade I (natural look and feel), to grade IV (severe contracture), as shown in table I.

Table I: Baker classification of capsular contracture after augmentation mammoplasty *

Class I	Breast absolutely natural, no one could tell breast was augmented
Class II	Minimal contracture; I can tell surgery was performed, but patient has no complaint
Class III	Moderate contracture; patient feels some firmness
Class IV	Severe contracture; obvious just from observation

**From Baker JL Jr. Augmentation mammoplasty. In: Owsley JQ Jr, Peterson RA, eds. Symposium on aesthetic Surgery of the Breast. St. Louis: Mosby; 1978:256–263*

This classification has remained the de facto standard to evaluate capsular problems, although the scale does not mention pain or discerns between capsule thickening and contracture^{16,22,23}. While this classification is widely used clinically and in scientific literature to correlate a clinical grade with (bio)medical data (e.g. histology, immunologic data, type of implant, or type of surgery), it has never been critically assessed for reliability¹⁶. See also figure 2 for an example of a Baker-IV CC.



Figure 2: Baker-IV (capsular contracture) visible on both breasts. Note the position of the nipple on the left and the distortion of the area under the areola. Image added to this thesis with written consent of the patient.

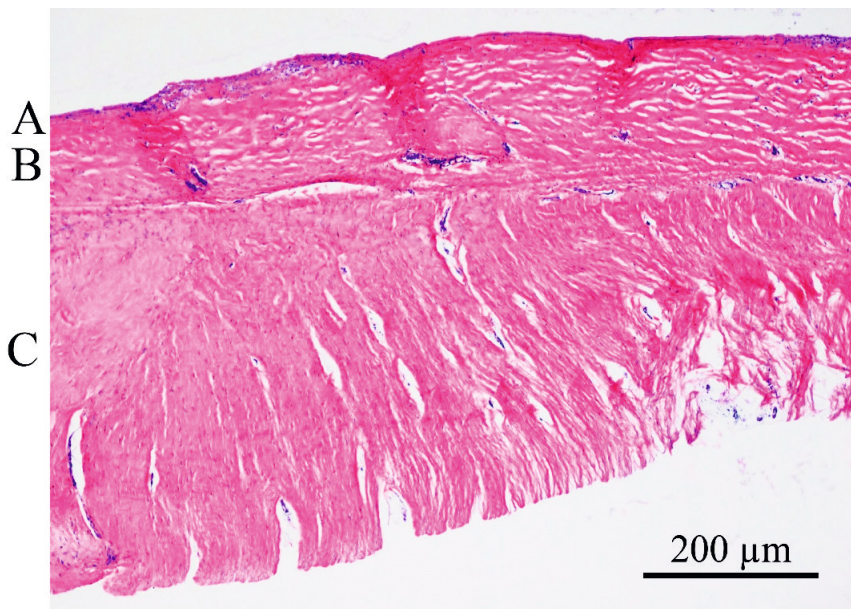


Figure 3: Baker-IV (capsular contracture) capsule with A inner layer, B intermediate layer, C outer layer. Implant was adjacent to the inner layer.

Histologically, the Baker-IV capsules are found to have more, and thicker bands of collagen fibers. The same layers as in the Baker-I capsules are found, although the sum is significantly thicker (figure 3)^{16,24}. In some cases, myofibroblasts are found, which could be contributing to the contracture side of the capsular complaints²⁴.

Multiple risk factors for developing CC have been identified over the years. These can be divided into roughly three categories; surgical factors, patient bound factors and the implant type^{21,25,26}. Surgical factors include subglandular placement of the implant, antibiotic and/or steroid pocket irrigation and postoperative hematoma. Patient bound factors include breast reconstructive surgery after breast cancer, irradiation of the breast and implant age (how long the implant has been in the body). The implant factors include a smooth implant surface, type of implant (saline filled vs. silicone) and implant generation. The first generations of implants contained liquid silicone causing significant silicone gel bleed through the shell and were prone to rupturing thanks to a relatively vulnerable shell, and these factors were deemed to be responsible for high CC rates. With the introduction of high cohesive silicone gels and more durable shells, indeed a lower CC rate was achieved^{16,27-29}. These improvements notwithstanding, however, the prevalence of CC is still relatively high. It should be noted that to date no direct link between the use of silicone and CC has been demonstrated.

Contributing to this lack of correlation, especially in the early years of silicone implant usage, is the fact that it was difficult to prove any silicone content in capsules. Silicone was assumed to be in the capsule because there were intracellular clear spaces consistent with silicone, vacuolated macrophages with retractile material, or silicone was seen as birefringent material with brightfield microscopy^{18,30}.

On the staining front, progress has been made by Dijkman who uses a Modified Oil Red O staining (MORO) with Transmission Electron Microscopy (TEM) in combination with Energy Dispersive X-ray microanalysis (EDX) to confirm the specificity of the silicone staining³¹.

As silicone is a non-organic material, normal immunohistochemical staining is less likely to specifically detect it. Progress has been made in other fields of detection, such as the above mentioned Energy Dispersive X-ray analysis, infrared spectroscopy (30) and confocal laser Raman-microspectroscopy (CLRM)^{17,32}. These methods are capable of identifying silicone with molecular specificity and have been used to detect silicone in tissue. They are, however, quite time-consuming and are at a disadvantage compared to normal histology because only specific points in the tissue can be measured and only after specific preparation of the tissue.

Gaps of evidence and specific aims of this thesis:

Although a lot has been written on the histology of CC, there is a lack in direct comparisons between asymptomatic capsules (Baker-I) and symptomatic (Baker-IV) capsules. This is true especially for the inner layer sometimes observed in the capsules, described as an epithelial like or synovial metaplasia like layer. The role of silicone in the pathophysiology of CC can only be better understood by identifying the material accurately in the tissue and, again, comparing Baker-I and Baker-IV type capsules.

The Baker scale itself, although widely used has not been the subject of critical investigation. As much of the scientific literature and clinical documentation comparing asymptomatic with symptomatic capsules is dependent on the Baker scale for capsular contracture, more knowledge is necessary on its reliability and reproducibility.

Therefore the specific research questions of this thesis are:

- Is there a difference in the prevalence of a metaplasia-like synovial layer/epithelium between Baker-I and Baker-IV capsules?
- Is Raman microscopy able to detect silicone in tissue reliably and (relatively) fast?
- Is an increased silicone content correlated with Baker-IV capsular contracture?
- Is the Baker scale for capsular contracture reliable as a diagnostic tool?

Part II: hypergranulation tissue in skin scar formation

Fibrosis of the skin is called hypertrophic scar tissue (HS), while normal scar tissue is called normotrophic scar tissue (NS). Figure 3 gives a side-by-side comparison between normal scar tissue and hypertrophic scar tissue. The third type of aberrant scar, the keloid, is not within the scope of this thesis. The primary differentiation between HS and keloids has traditionally been that an HS remains within the confine of the wound, whereas a keloid may grow outside its confines. No scientific consensus has been reached on the subject of how different these types of scars are^{4,33}. Since normotrophic scars (NS) are flat, pale, and consisting out of pliable tissue they are of little to no nuisance to their owner. In contrast, HS are raised, appear red, non-pliable and may be itchy or even painful². Over joints HS can cause significant physiological complaints like joint immobility and pain. The psychological impact of HS is associated with symptoms of depression, anger, anxiety and post-traumatic stress^{34,35}.



Figure 3: a normotrophic scar (left), side to side with a hypertrophic scar (right). Both scars resulting from breast reduction surgery, inframammary scar.

Gaps of evidence and specific aims of this thesis:

Despite being a subject with a substantial body of research, many questions remain unanswered. While risk factors like wound location, tension and mechanical loading, age and bacterial colonization are helpful in the sense that we know a wound on the sternum or the outside of an elbow is at risk of becoming a HS, they do not help to identify the patient that does actually develop a HS^{4,36-38}. Patients undergoing breast reduction surgery for example do not fit this

profile, neither do many other patients who have HS. People getting accidental cuts, burn wounds or in need of emergency surgery have no choice in receiving these wounds, but at the moment we do not have any tools to predict HS formation for this group and therefore cannot anticipate treatments to prevent HT scar forming. People undergoing elective, cosmetic surgery do have a choice in whether or not to get the surgery, so being able to better predict if they are at risk of developing HS can be a very helpful tool. Since an early treatment start is preferred in HS a good prognostic tool would be useful for both groups³⁹. The underlying problem, of course, is that a true pathophysiological mechanism has not been found for HS. Finding true prognostic (biological) markers will probably also help in identifying underlying mechanisms in HS formation.

Therefore the specific research questions of this thesis are:

- Is there a correlation between HS and patient dependent, easily testable biomarkers?
- Can an immunological or systemic basis for HS formation be established?
- Can these differences be exploited to predict HS formation

REFERENCES

1. Broughton, II, G., Janis, J. E. & Attinger, C. E. The basic science of wound healing. *Plast. Reconstr. Surg.* **117**, 12–34 (2006).
2. Finnerty, C. C. *et al.* Hypertrophic scarring: the greatest unmet challenge after burn injury. *Lancet (London, England)* **388**, 1427–1436 (2016).
3. Darby, I. A. & Desmoulière, A. Scar Formation: Cellular Mechanisms. in *Textbook on Scar Management* 19–26 (Springer International Publishing, 2020). doi:10.1007/978-3-030-44766-3_3
4. Slemper, A. E. & Kirschner, R. E. Keloids and scars: a review of keloids and scars, their pathogenesis, risk factors, and management. *Curr. Opin. Pediatr.* **18**, 396–402 (2006).
5. van der Veer, W. M. *et al.* Potential cellular and molecular causes of hypertrophic scar formation. *Burns* **35**, 15–29 (2009).
6. Frykberg, R. G. & Banks, J. Challenges in the Treatment of Chronic Wounds. *Adv. Wound Care* **4**, 560–582 (2015).
7. Patel, B. C., Wong, C. S., Wright, T. & Schaffner, A. D. *Breast Implants. StatPearls* (2021).
8. Perry, D. & Frame, J. D. The history and development of breast implants. *Ann. R. Coll. Surg. Engl.* **102**, 478–482 (2020).
9. Bhardwaj, P., Greenwalt, I., Ko, K., Sher, S. R. & Tsiapali, E. Free Silicone Injections to the Breast: Delayed Complications and Surgical Management of Sequelae. *Plast. Reconstr. surgery. Glob. open* **8**, e3208 (2020).
10. Leyva, A. *et al.* Filler Migration and Granuloma Formation After Gluteal Augmentation with Free-silicone Injections. *Cureus* **10**, e3294 (2018).
11. DBIR. Dutch Breast Implant Registry (DBIR) Annual Report 2019. (2020).
12. Jalalabadi, F., Doval, A. F., Neese, V., Andrews, E. & Spiegel, A. J. Breast Implant Utilization Trends in USA versus Europe and the Impact of BIA-ALCL Publications. *Plast. Reconstr. Surg. - Glob. Open* 1–9 (2021). doi:10.1097/GOX.0000000000003449
13. Kastellorizios, M., Tipnis, N. & Burgess, D. J. Foreign Body Reaction to Subcutaneous Implants. *Adv. Exp. Med. Biol.* **865**, 93–108 (2015).
14. Ebramzadeh, E., Campbell, P., Tan, T. L., Nelson, S. D. & Sangiorgio, S. N. Can We Explain the Histological Variation Around Metal-on-metal Total Hips? *Clin. Orthop. Relat. Res.* **473**, 487–494 (2014).
15. Klopffleisch, R. & Jung, F. The pathology of the foreign body reaction against biomaterials. *J. Biomed. Mater. Res. - Part A* **105**, 927–940 (2017).
16. Berry, M. G., Cucchiara, V. & Davies, D. M. Breast augmentation: Part II – adverse capsular contracture. *J. Plast. Reconstr. Aesthetic Surg.* **63**, 2098–2107 (2010).
17. Luke, J. L. *et al.* Pathological and biophysical findings associated with silicone breast implants: a study of capsular tissues from 86 cases. *Plast. Reconstr. Surg.* **100**, 1558–65 (1997).
18. Prantl, L. *et al.* Clinical and morphological conditions in capsular contracture formed around silicone breast implants. *Plast. Reconstr. Surg.* **120**, 275–84 (2007).
19. Bassetto, F., Scarpa, C., Caccialanza, E., Montesco, M. C. & Magnani, P. Histological Features of Periprosthetic Mammary Capsules: Silicone vs. Polyurethane. *Aesthetic Plast. Surg.* **34**, 481–485 (2010).
20. Handel, N., Cordray, T., Gutierrez, J., Jensen, J. A. & Arthur Jensen, J. A Long-Term Study of Outcomes, Complications, and Patient Satisfaction with Breast Implants. *Plast. Reconstr. Surg.* **117**, 757–67; discussion 768–72 (2006).
21. Bachour, Y. *et al.* Risk factors for developing capsular contracture in women after breast implant surgery: A systematic review of the literature. *J. Plast. Reconstr. Aesthetic Surg.* **71**, e29–e48 (2018).
22. Baker JL, J. Augmentation mammoplasty. in *Symposium on Aesthetic Surgery of the Breast. St Louis: Mosby.* (ed. JQ Owsley, R. P.) 256 (1978).
23. Malahias, M., Jordan, D. J., Hughes, L. C., Hindocha, S. & Juma, A. A literature review and summary of capsular contracture: An ongoing challenge to breast surgeons and their patients. *International Journal of Surgery Open* **3**, 1–7 (2016).

24. Bui, J. M. *et al.* Histological characterization of human breast implant capsules. *Aesthetic Plast. Surg.* **39**, 306–15 (2015).
25. Stevens, W. G. *et al.* Risk Factor Analysis for Capsular Contracture. *Plast. Reconstr. Surg.* **132**, 1115–1123 (2013).
26. Benediktsson, K. & Perbeck, L. Capsular contracture around saline-filled and textured subcutaneously-placed implants in irradiated and non-irradiated breast cancer patients: Five years of monitoring of a prospective trial. *J. Plast. Reconstr. Aesthetic Surg.* **59**, 27–34 (2006).
27. Bachour, Y. *et al.* The aetiopathogenesis of capsular contracture: A systematic review of the literature. *J. Plast. Reconstr. Aesthetic Surg.* (2017). doi:10.1016/j.bjps.2017.12.002
28. Hillard, C., Fowler, J. D., Barta, R. & Cunningham, B. Silicone breast implant rupture: A review. *Gland Surg.* **6**, 163–168 (2017).
29. Caffee, H. H. The influence of silicone bleed on capsule contracture. *Ann. Plast. Surg.* **17**, 284–7 (1986).
30. Potter, E. H., Rohrich, R. J. & Bolden, K. M. The Role of Silicone Granulomas in Recurrent Capsular Contracture. *Plast. Reconstr. Surg.* **131**, 888e–895e (2013).
31. Kappel, R. ., Boer, L. L. & Dijkman, H. Gel Bleed and Rupture of Silicone Breast Implants Investigated by Light-, Electron Microscopy and Energy Dispersive X-ray Analysis of Internal Organs and Nervous Tissue. *Clin. Med. Rev. Case Reports* **3**, (2016).
32. Kidder, L. H., Kalasinsky, V. F., Luke, J. L., Levin, I. W. & Lewis, E. N. Visualization of silicone gel in human breast tissue using new infrared imaging spectroscopy. *Nat. Med.* **3**, 235–7 (1997).
33. Mahdavian Delavary, B., van der Veer, W. M., Ferreira, J. A. & Niessen, F. B. Formation of hypertrophic scars: evolution and susceptibility. *J. Plast. Surg. Hand Surg.* **46**, 95–101 (2012).
34. Ngaage, M. & Agius, M. The psychology of scars: A mini-review. *Psychiatr. Danub.* **30**, S633–S638 (2018).
35. Lawrence, J. W., Mason, S. T., Schomer, K. & Klein, M. B. Epidemiology and impact of scarring after burn injury: a systematic review of the literature. *J. Burn Care Res.* **33**, 136–46
36. Butzelaar, L., Ulrich, M. M. W., Mink van der Molen, A. B., Niessen, F. B. & Beelen, R. H. J. Currently known risk factors for hypertrophic skin scarring: A review. *J. Plast. Reconstr. Aesthet. Surg.* **69**, 163–9 (2016).
37. Chiang, R. S. *et al.* Current concepts related to hypertrophic scarring in burn injuries. *Wound Repair Regen.* **24**, 466–477 (2016).
38. Monstrey, S. *et al.* Updated Scar Management Practical Guidelines: Non-invasive and invasive measures. *Journal of Plastic, Reconstructive and Aesthetic Surgery* **67**, 1017–1025 (2014).
39. Lee, H. J. & Jang, Y. J. Recent Understandings of Biology, Prophylaxis and Treatment Strategies for Hypertrophic Scars and Keloids. *Int. J. Mol. Sci.* **19**, (2018).

2

The histological composition of capsular contracture focussed on the inner layer of the capsule; an intra-donor Baker-I versus Baker-IV comparison.

E. de Bakker

L.J. van den Broek

M.J.P.F. Ritt

S. Gibbs

F.B. Niessen

ABSTRACT

Background Capsular contracture remains one of the major complications after breast implantation surgery. The extent of capsular contraction is scored using the Baker scale. The aim of this study was to compare intra-individual Baker-I with Baker-IV capsules, and in particular the prevalence and histological properties of the inner capsule layer.

Methods Twenty capsules from ten patients were included after bilateral explantation surgery due to unilateral capsular contracture (Baker-IV) after cosmetic augmentation with textured implants. All capsules underwent (immune-) histochemical analysis: haematoxylin-eosin (morphology), CD68 (macrophages), cytokeratin (epithelial cells) and vimentin (fibroblasts), and were visually scored for cell density, presence of an inner layer and measured for thickness.

Results Baker-IV (n=10) capsules were significantly thicker compared to Baker-I (n=10) capsules ($P=0.004$). An inner layer was present in 8 Baker-I capsules. All Baker-I capsules were vimentin and CD68 positive and cytokeratin negative. Positive vimentin was seen throughout the inner layer and CD-68 staining was observed adjacent to the intermediate capsule layer. In contrast, only 2 Baker-IV capsules had an inner layer, of which only 1 showed the same profile as Baker-I capsules ($P=0.016$). No cytokeratin positivity was seen in any capsule. In Baker-IV capsules outer layers showed more positivity for both vimentin and CD68.

Conclusions The inner layer is morphologically consistent with synovial metaplasia and is more prevalent in healthy, uncontracted Baker-I capsules. This inverse relation between the presence of the inner layer and higher Baker classification or pathological contracture could indicate a protective role of the inner layer against capsular contracture formation.

INTRODUCTION

Since the first silicone breast implants were used in surgery, capsular contracture has been a serious adverse outcome resulting in significant aesthetic and functional complications¹. Capsular contraction is therefore the subject of numerous studies to understand and prevent its formation²⁻¹⁰. The type of implant, implantation technique and post-operative radiotherapy are all factors described to influence the formation of capsular contracture¹¹. One of the most striking aspects of capsular contracture is that some patients develop unilateral contracture even though both breasts have been augmented or reconstructed in a similar fashion during the same procedure¹²⁻¹⁴. The capsules of these patients could provide useful intra-donor comparison opportunities, but until now these have not been explored. The pathohistological mechanisms involved in capsular contracture remain unclear despite numerous studies^{1,12,15-19}. Histologically, the capsules have been described as consisting of 3 layers: an inner layer adjacent to the implant consisting of fibrocytes and histiocytes which forms an epithelial-like or pseudo-epithelial layer (PSE), an intermediate layer of smaller fibrils in a vessel-rich network and an outer collagen-dense layer¹⁷. Furthermore, this PSE is not consistently reported although there appears to be a higher prevalence with textured implants^{20,21}. While not used as frequently as textured or smooth implants, polyurethane foam-coated implants have been reported to generate a similar layer²². More recently, the inner layer has been identified as a metaplasia like synovial layer^{3,9,24} consisting of macrophages and fibroblasts²³, at this point, both names are used to describe the same layer²¹. Since very few studies report immunohistochemical stainings targeted specifically at the inner layer, histological information on this specific layer is limited^{18,20,21,24-26}. Therefore, the aim of this study was to compare, for the first time, intra-individual Baker-I with Baker-IV capsules. In particular, the focus will be on the prevalence and (immuno-)histological properties of the inner capsule layer and to determine whether this is indeed a metaplasia-like synovial layer or has more epithelial-like characteristics.

MATERIALS AND METHODS

Patients and Tissue Collection

Donor-matched Baker-I and Baker-IV capsules were collected from patients undergoing explantation surgery between 2010 and 2014 due to capsular contracture complaints. All capsules were obtained from adult women who primarily underwent plastic surgery for cosmetic breast augmentation and subsequently developed unilateral complaints, i.e. Baker-I on the one side and Baker-IV on the other. Only cosmetic breast augmentation patients were included to exclude any effects that the breast cancer treatment can have on the tissue. All patients had received high cohesive gel-textured implants in the past with the submuscular method in various clinics within the Netherlands. All complaints were graded with the Baker classification scale, and only matched capsules of patients with Baker-I and Baker-IV grade were included. The discarded capsule tissue was coded to enable the collection of additional relevant information (e.g. type and size of implant, duration of implant placement, age of patient and comorbidity). Clinical grading, the explantation of implants and the collection of capsules, was performed by an experienced plastic surgeon (FBN) and included only after oral informed consent. Tissue collection procedures were performed in compliance with the 'Code for Proper Secondary Use of Human tissue' as formulated by the Dutch Federation of Medical Scientific Organization. In total, 10 patients and 20 capsules were included. Patients who had received PIP implants or with a history of (breast) cancer were excluded. Patient characteristics at inclusion are shown in Table 1.

Table 1: Patient characteristics

Number of patients	10
Age (years)	47.5 +/- 8.9
BMI	24.2 +/- 4.1
Duration of implant placement (months)	161 +/- 71
Size of implant (cc)	306 +/- 10.5
Smoker	3 /10
Diabetic	2/10
Tear of implant on Baker-IV side	3 /10
Tear of implant on Baker-I side	1/10
More than one augmentation	1/10

Mean +/- SD is shown. Tear in implant seen during explantation.

Histological Analysis

Tissue samples were fixed in 4% formaldehyde for 24 h, then routinely processed and embedded in paraffin. Sections of 5 μ m were then used for haematoxylin and eosin (HE) staining²⁷. The HE-stained capsules were photographed at 10-fold magnification (Nikon Eclipse 80i, Düsseldorf, Germany). The thickness was quantified using NIS-Elements AR 2.10 software (Nikon). Of each capsule, at least 5 measurements were made to obtain a representative mean thickness of the capsule. A visual separation was made between the inner, intermediate and outer layers. Each capsule was scored visually for the presence of a visible inner, pseudo-epithelial layer or synovium-like, layer. Cell density was scored for the two outer layers because of the denser nature of an inner layer. Scoring was done independently by two authors.

Immunohistochemical Analysis

Immunohistochemical analysis was performed to ascertain the composition of the inner layer and to determine whether it had a more epithelial-like or a more synovial-like phenotype where there are type A cells (macrophages) and type B cells (fibroblast-like) present while epithelial-like cells should be cytokeratin positive. Immunohistochemical staining on paraffin-embedded

5µm sections was performed with cytokeratin, vimentin and CD68 as described previously²⁸ (all Dako/Agilent, Santa Clara, California, USA, dilution 1:100). For each staining, a positive control normal human skin sample was included. Quantification for positivity was done visually and independently by two authors, noting whether the positivity was in the inner layer or a different part of the capsule and whether the sample showed no, a little, intermediate or a lot of positive cells.

Statistical Analysis

All mean thickness results were paired for each patient and were analysed with the Student's two tailed *t* test for paired variables. The related-samples McNemar test was used to determine correlation between Baker score and presence of an inner layer and presence of an inner layer with a synovial metaplasia-like phenotype. A *p* value of less than 0.05 was considered significant. All statistics were performed with IBM SPSS Statistics for Windows version 22.0 (IBM Corp. Released 2013. Armonk, NY: IBM Corp.)

RESULTS

Patient Characteristics

In total, 10 patients with a Baker-I and Baker-IV capsule were included. In total 20 capsules were analysed. The mean duration of implantation was 156 months; 3 were smokers and 2 had type II diabetes (Table 1). Out of all explanted implants, 4 had signs of a tear, out of which 3 were on the affected, Baker-IV, side. One patient had a breast augmentation prior to the one of which the capsules were removed for this study. The prior augmentation was also revised because of capsular contracture.

Capsular Thickness and Morphology

In general, a large variation between samples was observed, both between patients and Baker classification. This included variance between cell density,

capsule thickness and organisation. The thickness of capsules was determined by assessment of HE-stained tissue sections (Figure 1).

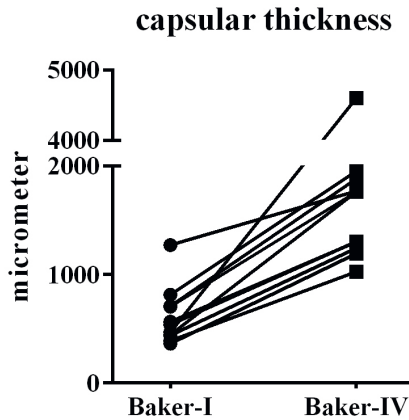


Figure 1: Intra-donor differences in Baker-I and Baker-IV capsular thickness. Average of 5 different measurements within a tissue section is shown for each capsule. Each line represents one donor with a Baker-I and a Baker-IV capsule. Thickness is shown in micrometre (μm).

The Baker-IV capsules were on average 3.3-fold thicker in comparison with the Baker-I capsules ($P = 0.004$, Table 2). The increase in thickness was comparable for all paired capsules as is visually shown in Figure 1. All capsules were organised in multiple layers (Figure 2). Some of the capsules containing an internal layer, directly adjacent to the implant, consisting of cells arranged in a palisaded manner (Figs. 2, 3). In the current literature, this inner layer is sometimes called a pseudo-epithelial or synovial metaplasia-like layer. Beyond this layer, more outer wards, all capsules contained two thicker layers. The intermediate layer was generally organised in line with the border of the capsule. The outermost layer appears more loosely organised and is aligned perpendicular to the implant (Figure 2).

Table 2: Capsule characteristics

Characteristic	B1	B4	<i>p</i>
Entire capsule			
Thickness	543 ±152 μm	1802 ±1035 μm	0.004
Inner layer			
Present	Y (8/10)	Y (2/10)	0.031
Vimentin	Y (8/8)	Y (1/2)	
CD68	Y (8/8)	Y (2/2)	
Cytokeratin	N (8/8)	N (2/2)	
Vim+/CD68+/Cytokeratin-	8/10	1/10	0.016
Intermediate and Outer layer			
Vimentin	+(3/10)	+(0/10)	
	++(3/10)	++(4/10)	
	+++ (4/10)	+++ (6/10)	
CD68	+(8/10)	+(5/10)	
	++(1/10)	++(3/10)	
	+++ (1/10)	+++ (2/10)	
Cytokeratin	- (10/10)	- (10/10)	
Cell density	+ (7/10)	+(3/10)	
	++ (2/10)	++(6/10)	
	+++ (1/10)	+++ (1/10)	

Summary of morphologic and histologic characteristics of the capsules; Thickness in μm ± standard deviation, measured at 4-fold magnification using NIS-Elements AR 2.10 software (Nikon). In each photo at least 5 measurements were made. Cell density, Inner layer presence and positive staining scored visually by two independent authors noting if an inner layer was present (Y), if that layer showed positivity (Y) or not (N) and for the outer layer if it had low (+), medium (++) or high cell density (+++), positivity for the staining and whether it showed no(-), low(+), intermediate(++) or a lot(+++) of positive cells.

The Baker-I capsules more frequently showed the inner layer (8/10) compared to Baker-IV capsules (2/10) (Figure 3 and Table 2). The McNemar test showed that this result was significant ($P = 0.03$, Table 2). When an inner layer was present in the Baker-IV capsule, it was less consistent in nature and not present on the entire border of the capsule.

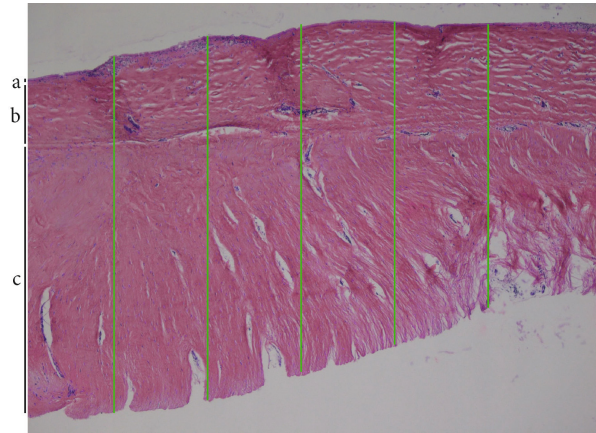


Figure 2: Capsule thickness measurement and layers.

Representative photograph of Baker-IV capsule is shown with a) inner layer, b) intermediate layer; note extracellular matrix is aligned in line with the implant; and c) outer layer: note extracellular matrix is aligned perpendicular with the implant. The five thickness measurements used in figure 1 are indicated with green bars.

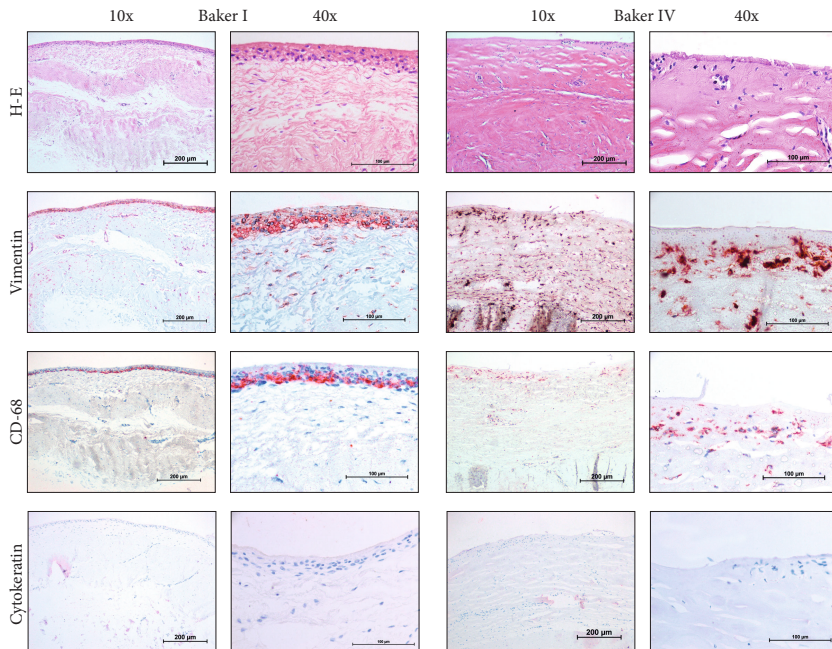


Figure 3: (Immuno-)histochemical Staining results of a representative Baker-I and Baker-IV capsule from the same donor. Shown are 10x and 40x magnifications.

In contrast, most Baker-I capsules showed very consistent and continuous inner layers (Figure 3). As can clearly be seen in Figure 3, an inner layer is an extremely cell-dense region consisting of up to four stratified cell layers. In contrast, the outer layers consisted of single cells dispersed throughout the tissue. In cell density, there was again a large variance between Baker-I and Baker-IV capsules. In general, cell density is higher for the Baker-IV capsules (Table 2).

Phenotype of Cells

Next, the phenotype of the inner layer was determined. Cytokeratin, which identifies epithelial cells, was negative in all capsules while being positive in our control skin sample. This implied that a synovial metaplasia may be present²⁹. Out of the 10 Baker-I capsules, 8 showed an inner layer out of which all were indeed vimentin and CD68-positive and cytokeratin negative. These inner layers showed positive vimentin throughout the inner layer, and CD-68 staining was observed in the lowest cell layer adjacent to the intermediate capsule layer (Table 2; Figure 3). In contrast, in the Baker-IV capsules, only 2 capsules had an inner layer out of which only 1 showed the same profile as the Baker-I capsules; this is a statistically significant result ($P = 0.016$, Table 2). Finally, the phenotype of the outer layers was determined. In nearly all capsules, vimentin positive cells were observed as single cells throughout the intermediate and outer capsule layers (Table 2, Figure 3). Overall, there were more vimentin positive cells in the Baker-IV capsules compared to Baker-I. With regard to CD68, only very few cells stained positive in the outer layer of Baker-I, in contrast to the densely stained inner cell layer. For Baker-IV, positive staining cells were found throughout the intermediate and outer layer. No significant correlation was found between the presence of an inner layer and positivity for CD-68 or vimentin in the outer layers.

CONCLUSION

These findings suggest that a synovial metaplasia-like inner layer is more often present than previously thought and is more prevalent in healthy, uncontracted Baker-I capsules. Morphologically, this layer is consistent with a synovial metaplasia-like nature rather than an epithelial-like layer. There is an inverse relation between the presence of this inner layer and higher Baker classification or pathological contracture, and it could therefore play a protective role against the formation of capsular contracture. A clear relation between Baker grade and the presence of a synovial metaplasia-like layer has not been found until now. Future research should focus on the mechanism of loss of this inner layer and whether preventing the loss of this layer could prevent capsular contracture.

DISCUSSION

This present study highlights the differences between Baker-I and Baker-IV capsules within the same donor. All patients had developed unilateral local contracture complaints, which is one of the most striking characteristics of the aetiology of capsular contracture. For the first time, these differences are shown in a donor-matched group. We also show that even within the same donor, there can be a large variance in morphology of the capsules. The finding of a significant difference in capsule thickness reaffirms earlier studies³⁰. This study shows a significant difference between the Baker-I and Baker-IV capsules concerning the presence and form of a synovial metaplasia-like layer. This inner layer, when present, consists of vimentin (mesenchymal cells) and CD68 (macrophages)-positive and cytokeratin (epithelial)-negative cells, closely stacked together towards the implant in a palisaded manner. This cytology is in line with earlier publications about synovial metaplasia in breast implant capsules and is also found with other foreign body reactions³¹. Because the synovial metaplasia-like layer in the Baker-IV capsules is less congruent in

comparison with the Baker-I capsules, it could be hypothesised that these are remnants of previously intact synovial metaplasia-like layers. It could be possible that this inner layer either fulfils a protective role against contracture and that, when lost, the continuous contact with the prosthesis activates a secondary pathway leading to contracture. It is also possible that this layer is lost due to the increasing amount of tissue in the outer layers and the loss of nutrition to the inner layer. A theory is that this inner layer is a specialised form of repair and disappears over time²⁹. However, since the average duration of implant placement in this study is 13 years with the inner layer still showing in the Baker-I capsules, it seems unlikely that this layer would disappear over time. The stronger overall positivity in all layers for vimentin could correlate with more fibroblasts present in the Baker-IV capsules. Fibroblasts are responsible for production of extracellular matrix, and this study showed that Baker-IV capsules are significantly thicker than Baker-I capsules.

Macrophages play a key role to stimulate fibroblasts in the formation of granulation tissue and fibrosis, and their role in foreign body reactions is a very actual topic³². While macrophage presence and key role seem evident, different subtypes and reactions might be causal to the actual formation of capsular contracture. If the macrophage in the Baker-I capsule is anti-fibrotic and protective (M1), in the Baker-IV capsule, this role could be reversed (M2). In our experience, there are cases in which women had experienced an event which might have led to this shift in behaviour of the cells surrounding the implant such as direct trauma to the breast or pregnancy. This repeated exposure of the implant to stress could be the start of a more, secondary, profibrotic process. The macrophage seems to be susceptible to modulation and has already been suggested as a target for a therapeutic approach to prevent capsular contraction³³. Our results indicate only a slight increase in CD68 positivity in the outer layers of the Baker-IV capsules, and therefore, it is likely that one or more other types of immune cells, like different T-cell subsets, are also involved in this process³⁴. This study only included capsules of textured implants due to the fact that these are used nearly exclusively in the Netherlands, a comparison with capsules of smooth implants should be pursued in the future.

REFERENCES

1. Araco A, Caruso R, Araco F, et al. Capsular Contractures: A Systematic Review. *Plast Reconstr Surg.* 2009;124(6):1808-1819.
2. Collis N, Coleman D, Foo IT, et al. Ten-year review of a prospective randomized controlled trial of textured versus smooth subglandular silicone gel breast implants. *Plast Reconstr Surg.* 2000;106(4):786-791.
3. Fernandes JR, Salinas HM, Broelsch GF, et al. Prevention of capsular contracture with photochemical tissue passivation. *Plast Reconstr Surg.* 2014;133(3):571-577.
4. Forsberg CG, Kelly D a, Wood BC, et al. Aesthetic Outcomes of Acellular Dermal Matrix in Tissue Expander/Implant-Based Breast Reconstruction. *Ann Plast Surg.* 2013;72(June):0-4.
5. Giordano S, Peltoniemi H, Lilius P, et al. Povidone-Iodine Combined With Antibiotic Topical Irrigation to Reduce Capsular Contracture in Cosmetic Breast Augmentation: A Comparative Study. *Aesthetic Surg J.* 2013;33(5):675-680.
6. Contracture C, Rossi F, Novellis V De, et al. Modification of Cysteinyl Leukotriene Receptors Expression in. *Ann Plast Surg.* 2009;63(2):206-208.
7. Jacombs A, Tahir S, Hu H, et al. In vitro and in vivo investigation of the influence of implant surface on the formation of bacterial biofilm in mammary implants. *Plast Reconstr Surg.* 2014;133(4):471e-80e.
8. Marques M, Brown S a, Cordeiro NDS, et al. Effects of fibrin, thrombin, and blood on breast capsule formation in a preclinical model. *Aesthet Surg J.* 2011;31(3):302-309.
9. Marques M, Brown SA, Rodrigues-pereira P, et al. Animal Model of Implant Capsular Contracture : Effects of Chitosan. *Aesthetic Surg J.* 2011;31(5):540-550.
10. Reid RR, Greve SD, Casas LA. The effect of Zafirlukast (Accolate) on early capsular contracture in the primary augmentation patient: A pilot study. *Aesthetic Surg J.* 2005;25(1):26-30.
11. Whitfield GA, Horan G, Irwin MS, et al. Incidence of severe capsular contracture following implant-based immediate breast reconstruction with or without postoperative chest wall radiotherapy using 40 Gray in 15 fractions. *Radiother Oncol.* 2009;90(1):141-147.
12. Stevens WG, Nahabedian MY, Calobrace MB, et al. Risk Factor Analysis for Capsular Contracture. *Plast Reconstr Surg.* 2013;132(5):1115-1123.
13. Veras-Castillo ER, Cardenas-Camarena L, Lyra-Gonzalez I, et al. Controlled Clinical Trial With Pirfenidone in the Treatment of Breast Capsular Contracture. *Ann Plast Surg.* 2011;70(1):1.
14. Rieger UM, Mesina J, Kalbermatten DF, et al. Bacterial biofilms and capsular contracture in patients with breast implants. *Br J Surg.* 2013;100(6):768-774.
15. Steiert AE, Boyce M, Sorg H. Capsular contracture by silicone breast implants: Possible causes, biocompatibility, and prophylactic strategies. *Med Devices Evid Res.* 2013;6(1):211-218.
16. Dancey A, Nassimzadeh A, Levick P. Capsular contracture - What are the risk factors? A 14 year series of 1400 consecutive augmentations. *J Plast Reconstr Aesthetic Surg.* 2012;65(2):213-218.
17. Berry MG, Cucchiara V, Davies DM. Breast augmentation: Part II - Adverse capsular contracture. *J Plast Reconstr Aesthetic Surg.* 2010;63(12):2098-2107.
18. Wilflingseder P, Propst a., Mikuz G. Constrictive fibrosis following silicone implants in mammary augmentation. *Chir Plast.* 1974;2(4):215-229.
19. Collis N, Coleman D. Ten-year review of a prospective randomized controlled trial of textured versus smooth subglandular silicone gel breast implants. *Plast Reconstr* 2000.
20. Luke JL, Kalasinsky VF, Turnicky RP, et al. Pathological and biophysical findings associated with silicone breast implants: a study of capsular tissues from 86 cases. *Plast Reconstr Surg.* 1997;100(6):1558-1565.

21. Prantl L, Schreml S, Fichtner-Feigl S, et al. Clinical and morphological conditions in capsular contracture formed around silicone breast implants. *Plast Reconstr Surg.* 2007;120(1):275-284.
22. Bassetto F, Scarpa C, Caccialanza E, et al. Histological Features of Periprosthetic Mammary Capsules: Silicone vs. Polyurethane. *Aesthetic Plast Surg.* 2010;34(4):481-485.
23. Zheng M, Cai W, Weng H, et al. Determination of serum fibrosis indexes in patients with chronic hepatitis and its significance. *Chin Med J (Engl).* 2003;116(3):346-349.
24. Moyer KE, Ehrlich HP. Capsular Contracture after Breast Reconstruction. *Plast Reconstr Surg.* 2013;131(4):680-685.
25. Kamel M, Protzner K, Fornasier V, et al. The peri-implant breast capsule: An immunophenotypic study of capsules taken at explantation surgery. *J Biomed Mater Res.* 2001;58(1):88-96.
26. Potter EH, Rohrich RJ, Bolden KM. The Role of Silicone Granulomas in Recurrent Capsular Contracture. *Plast Reconstr Surg.* 2013;131(6):888e-895e.
27. Waaijman T, Breetveld M, Ulrich M, et al. Use of a collagen-elastin matrix as transport carrier system to transfer proliferating epidermal cells to human dermis in vitro. *Cell Transplant.* 2010;19(10):1339-1348.
28. Ouwehand K, Oosterhoff D, Breetveld M, et al. Irritant-induced migration of Langerhans cells coincides with an IL-10-dependent switch to a macrophage-like phenotype. *J Invest Dermatol.* 2011;131(2):418-425.
29. Fowler MR, Nathan CAO, Abreo F. Synovial metaplasia, a specialized form of repair: A case report and review of the literature. *Arch Pathol Lab Med.* 2002;126(6):727-730.
30. Bui JM, Perry T, Ren CD, et al. Histological characterization of human breast implant capsules. *Aesthetic Plast Surg.* 2015;39(3):306-315.
31. Stone JL, Boost T. Cytological features of breast peri-implant synovial metaplasia. *Acta Cytol.* 2014;58(5):511-513.
32. Klopfleisch R. Macrophage reaction against biomaterials in the mouse model – Phenotypes, functions and markers. *Acta Biomater.* 2016;43:3-13.
33. Huang Y-J, Hung K-C, Hung H-S, et al. Modulation of Macrophage Phenotype by Biodegradable Polyurethane Nanoparticles: Possible Relation between Macrophage Polarization and Immune Response of Nanoparticles. *ACS Appl Mater Interfaces.* 2018;10(23):19436-19448.
34. Wolfram D, Rabensteiner E, Grundtman C, et al. T Regulatory Cells and TH17 Cells in Peri-Silicone Implant Capsular Fibrosis. *Plast Reconstr Surg.* 2012;129(2):327e-337e.

3

A Case of Silicone and Sarcoid Granulomas in a Patient with “Highly Cohesive” Silicone Breast Implants: A Histopathologic and Laser Raman Microprobe Analysis

T.I. Todorov

E. de Bakker

L.C. Langenberg

L.A. Murakata

M.H.H. Kramer

P.W.B. Nanayakkara

J.A. Centeno

International journal of Enviromental research and Public Health 2021 18 4526.

doi: 10.3390/ijerph18094526

Foreign body giant cell (FBGC) reaction to silicone material in the lymph nodes of patients with silicone breast implants has been documented in the literature, with a number of case reports dating back to 1978. Many of these case reports describe histologic features of silicone lymphadenopathy in regional lymph nodes from patients with multiple sets of different types of implants, including single lumen smooth surface gel, single lumen textured surface gel, single lumen with polyethylene terephthalate patch, single lumen with polyurethane coating, and double lumen smooth surface. Only one other case report described a patient with highly-cohesive breast implants and silicone granulomas of the skin¹. In this article, we describe a patient with a clinical presentation of systemic sarcoidosis following highly cohesive breast implant placement. Histopathologic analysis and Confocal Laser Raman Microprobe (CLRM) examination were used to confirm the presence of silicone in the axillary lymph node and capsular tissues. This is the first report where chemical spectroscopic mapping has been used to establish and identify the coexistence of Schaumann bodies, consisting of calcium oxalate and calcium phosphate minerals, together with silicone implant material.

Keywords: breast implant; silicone; sarcoidosis, Raman, Schaumann bodies

INTRODUCTION

Silicone gel breast implants have been subject to controversies since their introduction by Cronin and Gerow in the early 1960s². The safety of these implants first came into question after several reports were published on a possible association between silicone breast implants and the development of connective tissue disease in the 1980s^{1,3-6}. Other possible adverse effects of silicone implants include capsular contracture, rupture⁷, locoregional complications, silicone migration to the lung, skin, and lower extremities^{8,9}, and interference with cancer detection¹⁰. To reduce these probable adverse effects, ‘highly cohesive’ implants were introduced into the market in 1994. The cohesiveness of the silicone polydimethylsiloxane (PDMS) polymer and a specially designed outer membrane in these implants were developed to reduce the incidence of rupture and gel bleeds, characterized by gel leakage through the shell of the implant¹¹⁻¹³. Several authors reported systemic responses in patients with silicone breast implants, including PDMS prostheses¹³⁻¹⁵. We now report the first case of a patient with highly cohesive breast implants who exhibited a sarcoidosis-like clinical presentation and silicone-containing granulomas at a distant site from her breasts. This case is especially enlightening in the context of the current attention around a number of other reported adverse effects related to breast implants. Therefore, we acknowledge the importance of sharing this account in the present climate of the enhanced understanding regarding exposure to such materials.

Case report

A 40-year-old Nigerian born woman, living in the Netherlands since 1985, underwent bilateral breast augmentation in 1996. The implants that she received were the ‘highly-cohesive’ silicone gel implants. Postoperatively, no complications were reported, except for occasional short-lived episodes of breast hardening.

In July 2001, she developed stone-hard tender breasts, which predominantly on the right side. A few weeks later she noticed multiple firm, non-tender skin

nodules that were located between the breasts and under the right breast. The nodules were approximately 0.5 cm in diameter, and after several days they began to ulcerate and produced a 'whitish' fluid. She was seen by her plastic surgeon who concluded that she had eczema. In the following eight months, the ulcerations and symptoms worsened, and the implants had to be surgically removed. During the procedure, the surgeon noted that the fibrous capsule surrounding the implant was severely contracted around the implants. A biopsy was taken from the lymph node located in the left axillary and cultures were sent for fungi and mycobacteria. Macroscopic examination of the breast explants showed no obvious leakage. PCR for mycobacteria was negative and cultures for fungi and bacteria were also negative.

Six months after the removal of the breast implants, the patient presented to the internal medicine outpatient clinic with an increasing number of nodules scattered all over her body. Her eyes and mouth were dry, her appetite reduced, she lost 2 kilograms of weight over 2 months and she complained of extreme lassitude. She had no fever or night sweats but had slight dyspnea on exertion. The patient denied a history of intravenous drug use or liquid silicone injections. On physical examination, she had firm, non-tender skin nodules about 1 cm in diameter on her face (upper eyelids, nose, cheeks), arms, and legs. The nodules were moveable and did not appear to be attached to the skin surface or underlying structures. Both breasts were hard and tender on palpation. In addition, she had swelling in both her upper eyelids, which became so severe that she could barely open her eyes at times. She also had a moderate visual impairment in her left eye and ophthalmological examination showed features of panuveitis. There was generalized lymphadenopathy. The axillary and inguinal lymph nodes were firm, non-tender, and approximately 2 cm in diameter, while a left supraclavicular lymph node was about 1.5 cm in diameter. Other physical findings included normal heart and lung sounds, mild hepatomegaly, and the spleen was not palpable.

A chest x-ray and CT scan of the thorax showed multiple enlarged lymph nodes in the hilum and axilla bilaterally, and fine nodular interstitial infiltrates in her lungs. Her sedimentation rate was 23 mm/hr (normal < 10 mm/hr), c-re-

active protein 25 mg/l (normal < 8 mg/l), Hb 7.8 mmol/l (normal 7.5-10 mmol/l), WBC count $4.7 \times 10^9/l$ (normal $3-10 \times 10^9/l$), creatinine 88 $\mu\text{mol/l}$ (normal 60-110 $\mu\text{mol/l}$), gamma glutamyltransferase 201 μl (normal 10-50 μl), alanine aminotransferase 66 μl (normal 4-36 μl), and the angiotensin converting enzyme (ACE) level was 63 μl (normal < 25 μl).

The patient was diagnosed with sarcoidosis. She refused to take prednisone and was treated with minocycline, an antibiotic with presumed anti-granulomatous activity, 100 mg twice per day during 7 months with moderate improvement in her condition. She did not develop any new nodules and the existing nodules became smaller. She also noted a decrease in the amount of dryness of her eyes and mouth.

MATERIALS AND METHODS

Histology

Biopsies were taken from the fibrous capsule surrounding the implants, a lymph node in the left axillary, a nodule on the left lower leg, and a nodule on the eyelid. This study was based on the evaluation of sections of capsular tissue, axillary lymph node, eyelid and a leg nodule. For each type of tissue, sections 4 - 6 μm in thickness were stained with hematoxylin and eosin (HE) and evaluated using ordinary light microscopy. The presence or absence of the following histologic features were evaluated: 1) silicone-induced granuloma reaction; 2) sarcoid-like granulomas; 3) giant cells; and 4) refractile material consistent with silicone. Sections (2-6 μm thick) were also prepared for the CLRM experiments.

Additional case material consisted of the implant removed from the patient, herein referred to as the “explant”. The explant was received and maintained without addition of fixative solutions. The explant material was examined using CLRM.

Chemical Microspectroscopy

CLRM measurements were conducted as published elsewhere^{16,17}. Briefly, CLRM experiments were performed on sections prepared from capsular tissue, axillary lymph node, eyelid nodule, and leg nodule using a LabRAM spectrograph (Jobin Yvon Horiba and Dilor, France). The instrument is equipped with a He:Ne laser having an excitation wavelength at 632 nm. The spectrograph is interfaced to a high stability BX 40 Olympus microscope equipped with objectives at 10X, 50X and 100X. Laser spot diameters of approximately 2 and 1 μm could be obtained using the 50 and 100x objectives, respectively. The 100X objective was used to focus the laser beam onto the sample and to collect the Raman spectral images. The microscope system is also equipped with an adjustable confocal hole ranging from 100 – 1000 μm aperture size, allowing for reduction on stray light and the removal of unwanted laser plasma lines. Once the laser is focused onto the sample using the 100X objective, the scattered light is collected using the same objective, collimated and focused on the entrance slit of the spectrograph. The spectrometer was equipped with two gratings mounted on the same shaft blazed at 1800 grooves/nm (holographic) and 950 grooves/nm, respectively. The Raman signal is then measured with a detection system consisting of a charge-couple detector with an active detector window of 1024 X 256 pixels. The viewing area containing the foreign materials was approximately 5 X 5 μm . Each spectrum was the result of 12 scans, at a spectral resolution of 4 cm^{-1} .

Raman microspectroscopy chemical finger printing has been used to identify silicone migration away from the implant¹⁶⁻¹⁹. This chemical characterization technique is an inelastic light scattering method that allows for the identification of functional groups that have an inducible dipole moment. When incident coherent light interacts with molecule, much of the light scatters with the same frequency as that of the incident light, referred to as elastic scattering. A small portion of the scattered photons have a frequency greater or less than that of the incident light, known as inelastic scattering. The difference is equal to the vibrational frequency of the molecular bond with which the photons interacted. The frequency of this scattered light contains information

that can be correlated to the molecular species that led to the frequency shift²⁰. This frequency shift arises from polarizable molecules, or those that have an inducible dipole moment. This phenomenon was first characterized by C.V. Raman, and has been developed into a characterization tool that can be used to identify chemical signatures of organic and inorganic material relevant to the present investigation^{21,22}.

In this study, we have used the mapping capabilities of the Raman microprobe system to study the multi-compositional characteristics of foreign inclusions associated with breast implants and mineral deposition, allowing us to simultaneously identify silicone, calcium oxalate and other compounds associated with the appearance of Schaumann bodies.

RESULTS

Histology

Capsule surrounding the implant, bilateral

Hematoxylin-eosin (HE) stained sections showed a thick fibrous capsular wall with an inner lining of amorphous eosinophilic material, mononuclear cells, and congested blood vessels forming a ‘pseudosynovium’ (Figure 1A)²³. There were numerous non-caseating granulomas, foreign body and Touton-type giant cells, and scattered chronic inflammatory cells within fibrous tissue. The granulomas were more prominent in the mid-section of the capsule wall, and their composition varied from a few epithelioid cells to large nodular aggregates surrounded by a thick fibrous collar. The foreign-body and Touton-type giant cells contained vacuoles with occasional Schaumann bodies, birefringent crystalline material, and clear refractile, non-birefringent material. The clear refractile material was confirmed as PDMS (Figure 1B) by confocal Raman microprobe analysis. Occasionally, all three of the inclusions were seen in the same giant cell (Figure 1C).

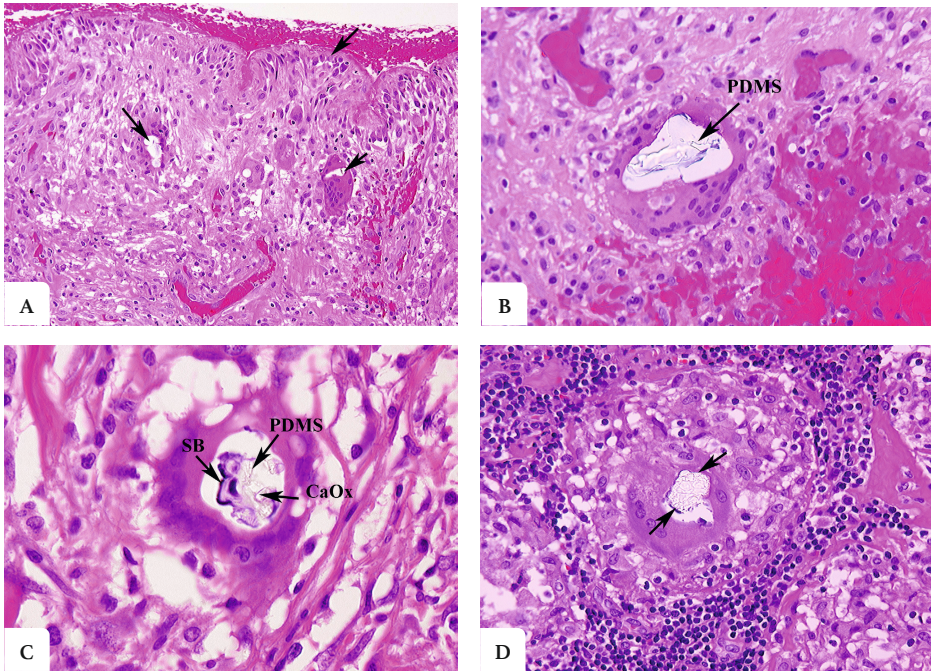


Figure 1. (A) Fibrous capsule surrounding the implant, right. The surface of the tissue lies adjacent to the silicone breast implant and forms the 'pseudosynovium'. This 'pseudosynovium' is composed of amorphous eosinophilic material and mononuclear cells. Of note are several foreign body giant cells containing clear silicone gel. There is a chronic inflammatory infiltrate scattered among the fibroblasts, fibrous tissue, and collagen. (HE, low power). (B) Fibrous capsule surrounding implant, right. A high power view of the above tissue shows silicone gel within the giant cell that is embedded in fibrous tissue. There are also scattered chronic inflammatory cells, congested blood vessels, and surgical related hemorrhage. (HE, high power). (C) Fibrous capsule surrounding implant, left. High power view of previous section. In the center of the multinucleated giant cell are fragments of Schaumann body, and refractile clear crystalline material consistent with calcium oxalate. (HE, high power). (D) Axillary lymph node, left. There is clear refractile globular material in the center of the giant cell of the epithelioid granuloma consistent with silicone gel. In addition, fragments of a Schaumann body can be seen around the outer edge of the silicone gel. (HE, high power).

Axillary lymph node, left

The lymph nodes were almost totally replaced by non-caseating epithelioid granulomas of varying sizes and contained the same type of PDMS-based inclusions as seen in the fibrous capsule surrounding the implants (Figure 1D). Granulomas were also seen in the lymph node hilum.

Eyelid nodule

The biopsy showed multiple epithelioid granulomas, septa of dense fibrous tissue, and lobules of serous (lacrimal) glands with focal lymphocytic infiltration (Figure 2A). In some foci there were degenerating ducts and glands admixed with chronic inflammation. Many of the epithelioid cells had clearing of the cytoplasm (‘clear-cells’), and a rare Schaumann body was seen (Figure 2B). One small focus of necrosis was found in one granuloma; but special stains were negative for fungi and bacteria.

Leg nodule

The majority of tissue was replaced by sheets of non-caseating granulomas (Figure 2C), histologically typical of sarcoidosis. Some smaller nodules were surrounded by fibrous tissue with thick fibrous septae and contained varying amounts of chronic inflammatory cells. Multinucleated, foreign-body giant cells with an occasional Schaumann body was present, as well as scattered lymphocytes, plasma cells, and occasional eosinophils and neutrophils (Figure 2D).

Confocal Laser Raman Microscopy

Figure 3 illustrates four different Raman microprobe studies. Trace A is the Raman spectrum of PDMS in the breast capsular connective tissue, while trace B is the Raman spectrum obtained from the surface of the “explant” shell. Trace C is the Raman spectrum of the silicone gel obtained from the inside of the “explant” (i.e., inner gel). Trace D (bottom trace) is the Raman spectrum of commercially obtained medical-grade silicone gel (Aldrich, Milwaukee, WI) and is used as a reference for comparison.

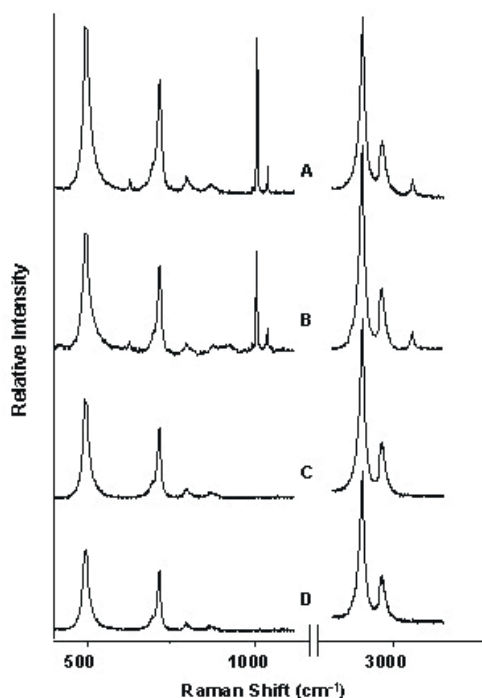


Figure 3. (A) Raman spectra of the silicone breast “explant” and fibrous tissue surrounding implant: (A) spectrum of silicone migrated to fibrous tissue surrounding the implant; (B) spectrum of silicone obtained from the shell of the “explant”; (C) spectrum of silicone gel obtained from the inside of the “explant”; (D) reference PDMS material.

It is worth noting that the inner gel of the “explant” (C) showed the same spectrum as the commercially available (reference) PDMS (D), while the spectrum of PDMS that had migrated to the capsular breast tissue (A), and the spectrum from the outer surface of the explant capsule (B, implant shell), demonstrated new Raman lines at 621, 1031 (breathing vibration of the aromatic ring), 3056 (aromatic CH stretch), and one strong line at 1000 cm⁻¹ (breathing vibration of the aromatic ring). The new bands are characteristic for the presence of aromatic groups bound to silicone based compounds. This spectrum is consistent with the study by Keizers et al in which the compound was identified as diphenylsilicone¹⁹.

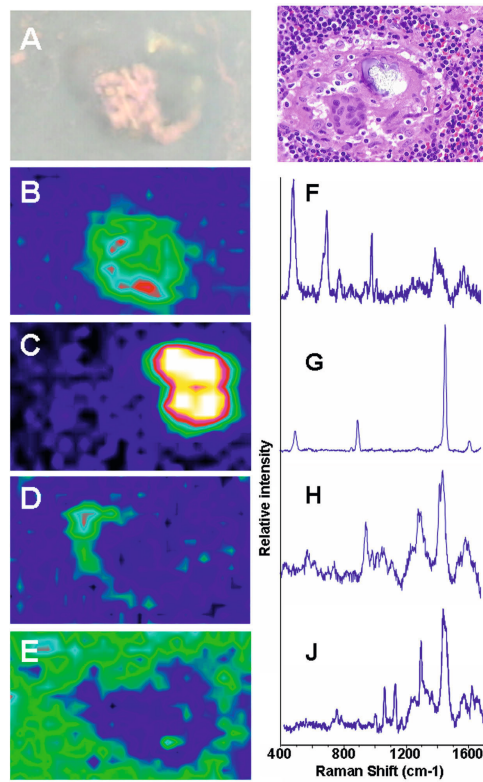


Figure 4. Raman spectroscopy generated images of silicone migrated to axillary lymph node: (A) white light image; (B) Raman generated image based on the distribution of silicone shown in spectrum (F); (C) Raman image based on distribution of oxalate shown in spectrum (G); (D) Raman image based on the distribution of phosphate shown in spectrum (H); (E) Raman image of tissue around the migrated silicone; (J) Raman spectrum from the tissue surrounding the phenylsilicone and Schaumann body.

The presence of diphenylsilicone in the axillary lymph node section was also demonstrated employing CLRM (see Figure 4). The Raman spectroscopy generated images show the presence of diphenylsilicone, image B, surrounded by calcium phosphate (image C) and calcium phosphate mineral deposit (image D). The mineral deposits are identified histologically as Schaumann bodies. The Raman spectra (see Figure 4, traces G and H) unequivocally identify these Schaumann body inclusions as containing mineral deposition based on calcium oxalate and calcium phosphate minerals. The spectra of calcium oxalate

and phosphate spectra are consistent with prior studies by Pestaner et al and Calzolari et al²⁴. The spectra of calcium oxalate and phosphate spectra are consistent with prior studies by Pestaner et al and Calzolari et al^{24,25}. These findings suggest that not only inner silicone gel in the “highly cohesive” implant migrates to the surrounding tissues, but that axillary lymph nodes may also contain implant shell diphenylsilicone particles.

DISCUSSION

Silicone leakage from traditional breast implants is frequent⁴ but data on “highly cohesive” breast implants are scarce²⁶. This type of implant was first introduced into the market in the early 90`, claiming to reduce the amount of leakage of PDMS and thereby decreasing the possibility of local or systemic effects. A large follow-up study by Heden in 2012 showed a rupture rate of 1.7% in type 410 PDMS implants²⁷.

The relationship between silicone implants and systemic disease has been under investigation for many years⁷. Migration of silicone from implant “bleeds” typically follows the lymphatic pathway and is rarely found in tissue beyond the axillary lymph nodes²⁸. Metastatic silicone granulomas have been described in patients who have had silicone oil injections for cosmetic reasons^{29,30}. Initially, the risk of silicone leakage from highly cohesive implants was considered to be low, but case reports describing silicone spread from the reported generation of breast implants are rising in number^{11,31-35}. In our case, the patient denied ever having silicone injections of any kind. After augmentation with the “highly cohesive” silicone gel implants, the woman described in this case study developed multifocal nodules consistent with sarcoidosis. PDMS was found in the fibrous capsules surrounding the implants and axillary lymph nodes both histologically and by CLRM spectroscopy.

There are over 48 case reports of sarcoidosis of the breast³⁵⁻⁴³. There are two reports of patients with breast sarcoidosis who had silicone implants without exacerbation of their disease and who did not experience any unusual peripros-

thetic complications. One patient with silicone implants had progressive and non-responsive symptoms of sarcoidosis that did not remit until the implants were removed. One report describes a patient who presented with sarcoidosis of the skin, without systemic involvement⁴³⁻⁴⁶. A large study by Watad et al. in a cohort that contained over 24,000 women with breast implants matched with over 98,000 women without breast implants, showed a higher risk of developing sarcoidosis following silicone breast prosthesis implantation (OR 1.98)⁴⁷.

The etiology of sarcoidosis is unknown. It is a multisystem granulomatous disease that rarely involves the breast⁴⁸. Immunologic abnormalities are the hallmark of sarcoidosis with the principal feature being non-caseating granulomas that somehow influence the function of the immune system by activating chemical mediators of inflammation or altering the function of lymphocytes^{44,49}.

It has been suggested that immunomodulation by foreign bodies such as silicone has a potential pathogenic role in the development of sarcoidosis⁴⁶. Recently, silicone gel was shown to enhance both the humoral and the delayed-type hypersensitivity response of rats to bovine serum albumin, and therefore may also have a direct effect on macrophages with local release of various cytokines and subsequent recruitment and activation of lymphocytes⁵⁰. The foreign body response to silicone or perhaps a direct adjuvant action of silicone may contribute to systemic activation of macrophages and T-helper cells, serving as a stimulus in the progression of sarcoidosis⁴⁵. Resolution of the patient's illness following removal of the breast implants supports this observation.

CONCLUSIONS

This is the fifth in a series of individual case reports that links silicone breast implants to the development of sarcoidosis. There were non-caseating granulomas in four different body sites, an infectious work-up was negative, radiographic evidence of bilateral hilar lymphadenopathy, and an elevated ACE level and panuveitis of the left eye. This combination of findings is consistent

with sarcoidosis. This is the first report where chemical spectroscopic mapping has been used to establish and identify the coexistence of Schaumann bodies, consisting of calcium oxalate and calcium phosphate minerals, in the presence of silicone. Whether the silicone in the tissues increased modulation of the immunologic response leading to the discovery of previously undiagnosed sarcoidosis, or whether it catalyzed the development of sarcoidosis is unknown.

REFERENCES

1. Sun, H.H.; Sachanandani, N.S.; Jordan, B.; Myckatyn, T.M. Sarcoidosis of the Breasts Following Silicone Implant Placement. *Plast. Reconstr. Surg.* 2013, 131, 939e–940e, doi:10.1097/PRS.0b013e31828bd964.
2. Perry, D.; Frame, J. The History and Development of Breast Implants. *Ann. R. Coll. Surg. Engl.* 2020, 102, 478–482, doi:10.1308/rcsann.2020.0003.
3. Cuellar, M.L.; Gluck, O.; Molina, J.F.; Gutierrez, S.; Garcia, C.; Espinoza, R. Silicone Breast Implant — Associated Musculoskeletal Manifestations. *Clin. Rheumatol.* 1995, 14, 667–672, doi:10.1007/BF02207934.
4. Gabriel, S.E.; O’fallon, W.M.; Kurland, L.T.; Beard, C.M.; Woods, J.E.; Melton, L.J. Risk of Connective-Tissue Diseases and Other Disorders after Breast Implantation. *N. Engl. J. Med.* 1994, 330, 1697–1702.
5. Spiera, H. Scleroderma after Silicone Augmentation Mammoplasty. *J. Am. Med. Assoc.* 1988, 260, 236–238.
6. Nunen, S.A.V.; Gatenby, P.A.; Basten, A. Post-Mammoplasty Connective Tissue Disease. *Arthritis Rheum.* 1982, 25, 694–697, doi:https://doi.org/10.1002/art.1780250613.
7. Beekman, W.H.; Feitz, R.; van Diest, P.J.; Hage, J.J. Migration of Silicone Through the Fibrous Capsules of Mammary Prostheses. *Ann. Plast. Surg.* 1997, 38, 441–445.
8. Muñoz, F.G.; Hermoso, F.A.; Cano, M.A. Lung Siliconoma, a Rare Complication of Breast Prosthesis Rupture. *Archivos de bronconeumologia* 2018, 54, 580–581.
9. Dragu, A.; Theegarten, D.; Bach, A.D.; Polykandriotis, E.; Arkudas, A.; Kneser, U.; Horch, R.E.; Ingianni, G. Intrapulmonary and Cutaneous Siliconomas after Silent Silicone Breast Implant Failure. *Breast J.* 2009, 15, 496–499, doi:https://doi.org/10.1111/j.1524-4741.2009.00765.x.
10. Brown, S.L. Epidemiology of Silicone-Gel Breast Implants. *Epidemiol.* 2002, 13, S34–S39.
11. Handel, N.; Garcia, M.E.; Wixtrom, R. Breast Implant Rupture: Causes, Incidence, Clinical Impact, and Management. *Plast. Reconstr. Surg.* 2013, 132, 1128–1137, doi:10.1097/PRS.0b013e3182a4c243.
12. Zambacos, G.J.; Molnar, C.; Mandrekas, A.D. Silicone Lymphadenopathy after Breast Augmentation: Case Reports, Review of the Literature, and Current Thoughts. *Aesthetic Plast. Surg.* 2013, 37, 278–289.
13. Kappel, R.M.; Klunder, A.J.; Pruijn, G.J. Silicon Chemistry and Silicone Breast Implants. *Eur. J. Plast. Surg.* 2014, 37, 123–128.
14. Kivity, S.; Katz, M.; Langevitz, P.; Eshed, I.; Olchovski, D.; Barzilai, A. Autoimmune Syndrome Induced by Adjuvants (ASIA) in the Middle East: Morphea Following Silicone Implantation. *Lupus* 2012, 21, 136–139.
15. Majjers, M.C.; de Blok, C.J.M.; Niessen, F.B.; van der Veldt, A.A.M.; Ritt, M.J.P.F.; Winters, H.A.H.; Kramer, M.H.H.; Nanayakkara, P.W.B. Women with Silicone Breast Implants and Unexplained Systemic Symptoms: A Descriptive Cohort Study. *Neth. J. Med.* 2013, 71, 534–540.
16. Katzin, W.E.; Centeno, J.A.; Feng, L.-J.; Kiley, M.; Mullick, F.G. Pathology of Lymph Nodes from Patients with Breast Implants: A Histologic and Spectroscopic Evaluation. *Am. J. Surg. Pathol.* 2005, 29, 506–511.
17. Centeno, J.A.; Mullick, F.G.; Panos, R.G.; Miller, F.W.; Valenzuela-Espinoza, A. Laser-Raman Microprobe Identification of Inclusions in Capsules Associated with Silicone Gel Breast Implants. *Mod. Pathol.* 1999, 12, 714–721.
18. Luke, J.L.; Kalasinsky, V.F.; Turnicky, R.P.; Centeno, J.A.; Johnson, F.B.; Mullick, F.G. Pathological and Biophysical Findings Associated with Silicone Breast Implants: A Study of Capsular Tissues from 86 Cases. *Plast. Reconstr. Surg.* 1997, 100, 1558–1565.
19. Keizers, P.H.; Vredendregt, M.J.; Bakker, F.; de Kaste, D.; Venhuis, B.J. Chemical Fingerprinting of Silicone-Based Breast Implants. *J. Pharm. Biomed. Anal.* 2015, 102, 340–345.

20. Kneipp, K.; Kneipp, H.; Itzkan, I.; Dasari, R.R.; Feld, M.S. Surface-Enhanced Raman Scattering and Biophysics. *J. Phys.: Condens. Matter* 2002, 14, R597–R624, doi:10.1088/0953-8984/14/18/202.
21. Hamada, K.; Fujita, K.; Smith, N.I.; Kobayashi, M.; Inouye, Y.; Kawata, S. Raman Microscopy for Dynamic Molecular Imaging of Living Cells. *J. Biomed. Opt.* 2008, 13, 044027-1–044027-4, doi:10.1117/1.2952192.
22. Spiro, T.G.; Gaber, B.P. Laser Raman Scattering as a Probe of Protein Structure. *Annu. Rev. Biochem.* 1977, 46, 553–570, doi:10.1146/annurev.bi.46.070177.003005.
23. Bachour, Y.; Heinze, Z.; van Selms, G.; Ritt, M.; Niessen, F.; Keizers, P. Poly Implant Prothèse Silicone Breast Explants: Chemical Analysis of Silicone Gel and Implant Shell. *Plast. Reconstr. Surg. Global Open* 2019, 7, 1–6.
24. Pestaner, J.P.; Mullick, F.G.; Johnson, F.B.; Centeno, J.A. Calcium Oxalate Crystals in Human Pathology - Molecular Analysis with the Laser Raman Microprobe. *Arch. Pathol. Lab. Med.* 1996, 120, 537–540.
25. Calzolari, A.; Pavan, B.; Curtarolo, S.; Nardelli, M.B.; Fornari, M. Vibrational Spectral Fingerprinting for Chemical Recognition of Biominerals. *ChemPhysChem* 2020, 21, 770–778.
26. Hedén, P.; Boné, B.; Murphy, D.K.; Slicton, A.; Walker, P.S. Style 410 Cohesive Silicone Breast Implants: Safety and Effectiveness at 5 to 9 Years after Implantation. *Plast. Reconstr. Surg.* 2006, 118, 1281–1287.
27. Hedén, P.; Bronz, G.; Elberg, J.J.; Deraemaecker, R.; Murphy, D.K.; Slicton, A.; Brenner, R.J.; Svarvar, C.; van Tetering, J.; van der Weij, L.P. Long-Term Safety and Effectiveness of Style 410 Highly Cohesive Silicone Breast Implants. *Aesthetic Plast. Surg.* 2009, 33, 430–436.
28. Van Diest, P.J.; Beekman, W.H.; Hage, J.J. Pathology of Silicone Leakage from Breast Implants. *J. Clin. Pathol.* 1998, 51, 493–497.
29. Suzuki, K.; Aoki, M.; Kawana, S.; Hyakusoku, H.; Miyazawa, S. Metastatic Silicone Granuloma Lupus Miliaris Disseminatus Faciei-like Facial Nodules and Sicca Complex in a Silicone Breast Implant Recipient. *Arch. Dermatol.* 2002, 138, 537–538.
30. Rapaport, M.J.; Vinnik, C.; Zarem, H. Injectable Silicone: Cause of Facial Nodules, Cellulitis, Ulceration, and Migration. *Aesthetic Plast. Surg.* 1996, 20, 267–276.
31. Tebbetts, J. Failure of a “Highly Cohesive Implant”: What Does It Really Mean? *Plast. Reconstr. Surg.* 2009, 124, 323–325.
32. Accurso, A.; Rocco, N.; Feleppa, C.; Palumbo, A.; D’Andrea, F. Spread of Silicone to Axillary Lymph Nodes after High Cohesive Gel Silicone Implant Rupture. *Plast. Reconstr. Surg.* 2008, 122, 221e–222e.
33. Shaaban, H.; Jmor, S.; Alvi, R. Leakage and Silicone Lymphadenopathy with Cohesive Breast Implant. *Br. J. Plast. Surg.* 2003, 56, 518–519.
34. Lahiri, A.; Waters, R. Locoregional Silicone Spread after High Cohesive Gel Silicone Implant Rupture. *J. Plast. Reconstr. Aesthetic Surg.* 2006, 59, 885–886, doi:10.1016/j.bjps.2005.12.014.
35. Kappel, R.; Boer, L.L.; Dijkman, H. Gel Bleed and Rupture of Silicone Breast Implants Investigated by Light-, Electron Microscopy and Energy Dispersive X-Ray Analysis of Internal Organs and Nervous Tissue. *Clin. Med. Rev. Case Rep.* 2016, 3, 3–9.
36. Fitzgibbons, P.L.; Smiley, D.F.; Kern, W.H. Sarcoidosis Presenting Initially as Breast Mass: Report of Two Cases. *Hum. Pathol.* 1985, 16, 851–852, doi:10.1016/S0046-8177(85)80259-8.
37. Gansler, T.; Wheeler, J. Mammary Sarcoidosis. Two Cases and Literature Review. *Arch. Pathol. Lab. Med.* 1984, 108, 673–675.
38. Banik, S.; Bishop, P.W.; Ormerod, L.P.; O’Brien, T.E. Sarcoidosis of the Breast. *J. Clin. Pathol.* 1986, 39, 446–448, doi:10.1136/jcp.39.4.446.
39. McPherson 3rd, J.; Yeoh, C.B. Rare Manifestations of Sarcoidosis. *J. Natl. Med. Assoc.* 1993, 85, 869–872.
40. Donaldson, B.A.; Polynice, A. Sarcoidosis of the Breast: Case Report and Chart Review. *Am. Surg.* 1995, 61, 778–780.
41. Ojeda, H.; Sardi, A.; Totoonchie, A. Sarcoidosis of the Breast: Implications for the General Surgeon. *Am. Surg.* 2000, 66, 1144–1148.

42. Takahashi, R.; Shibuya, Y.; Shijubo, N.; Asaishi, K.; Abe, S. Mammary Involvement in a Patient with Sarcoidosis. *Intern. Med.* 2001, 40, 769–771.
43. Lower, E.; Hawkins, H.; Baughman, R. Breast Disease in Sarcoidosis. *Sarcoidosis Vasc. Diffuse Lung Dis.* 2001, 18, 301–306.
44. Riefkohl, R.; Roberts 3rd, T.; McCarty Jr, K.S. Lack of Adverse Effect of Silicone Implant on Sarcoidosis of the Breast. *Plast. Reconstr. Surg.* 1985, 76, 296–298.
45. Teuber, S.S.; Howell, L.P.; Yoshida, S.H.; Gershwin, E. Remission of Sarcoidosis Following Removal of Silicone Gel Breast Implants. *Int. Arch. Allergy Immunol.* 1994, 105, 404–407.
46. Yoshida, T.; Tanaka, M.; Okamoto, K.; Hirai, S. Neurosarcoidosis Following Augmentation Mammoplasty with Silicone. *Neurol. Res.* 1996, 18, 319–320.
47. Watad, A.; Rosenberg, V.; Tiosano, S.; Cohen Tervaert, J.W.; Yavne, Y.; Shoenfeld, Y.; Shalev, V.; Chodick, G.; Amital, H. Silicone Breast Implants and the Risk of Autoimmune/Rheumatic Disorders: A Real-World Analysis. *Int. J. Epidemiol.* 2018, 47, 1846–1854.
48. Dilaveri, C.A.; Mac Bride, M.B.; Sandhu, N.P.; Neal, L.; Ghosh, K.; Wahner-Roedler, D.L. Breast Manifestations of Systemic Diseases. *Int. J. Women's Health* 2012, 4, 35–43.
49. Marcoval, J.; Maná, J.; Moreno, A.; Gallego, I.; Fortuno, Y.; Peyrí, J. Foreign Bodies in Granulomatous Cutaneous Lesions of Patients with Systemic Sarcoidosis. *Arch. Dermatol.* 2001, 137, 427–430.
50. Hajdu, S.D.; Agmon-Levin, N.; Shoenfeld, Y. Silicone and Autoimmunity. *Eur. J. Clin. Invest.* 2011, 41, 203–211.

4

Label-free Stimulated Raman Scattering imaging reveals silicone breast implant material in tissue

L. van Haasterecht

L. Zada

R.W. Schmidt

E. de Bakker

E. Barbé

H.A. Leslie

A. Dick Vethaak

S. Gibbs

J.F. de Boer

F.B. Niessen

P.P.M. van Zuijlen

M. L. Groot

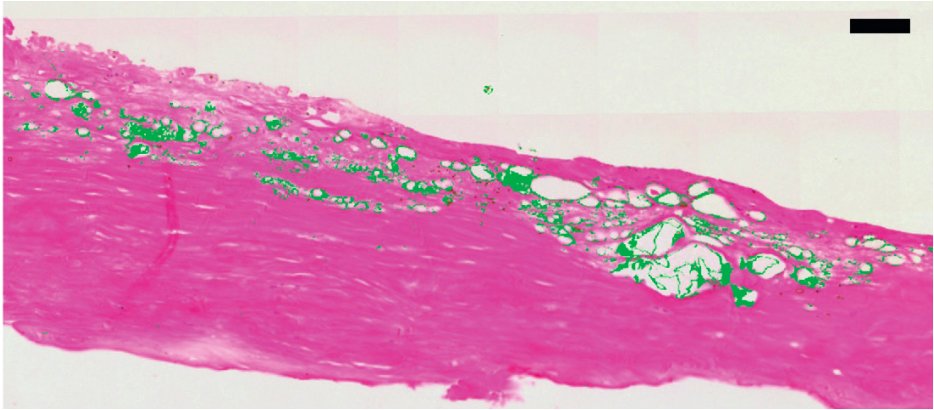
F. Ariese

Millions of women worldwide have silicone breast implants. Implant failure occurs in approximately a tenth of patients within ten years,¹ and the consequences of dissemination of silicone debris are poorly understood. Currently, silicone detection in histopathological slides is based on morphological features as no specific immunohistochemical technique is available. Here we show the feasibility and sensitivity of Stimulated Raman Scattering (SRS) imaging to specifically detect silicone material in stained histopathological slides, without additional sample treatment. Histology slides of four periprosthetic capsules from different implant types were obtained after explantation, as well as an enlarged axillary lymph node from a patient with a ruptured implant. SRS images co-registered with bright-field images revealed the distribution and quantity of silicone material in the tissue. Fast and high-resolution imaging of histology slides with molecular specificity using SRS provides an opportunity to investigate the role of silicone debris in the pathophysiology of implant-linked diseases.

KEYWORDS:

capsular contraction, label-free histology, non-linear optics, plastic surgery, polymer detection, pathology, silicone bleeding

ABSTRACT FIGURE:



ABBREVIATIONS:

CC, Connected Component

OPO, Optical Parametric Oscillator

PDMS, Polydimethylsiloxane

PU, Polyurethane

ROI, Region Of Interest

RMSE, Root Mean Square Error

SRS, Stimulated Raman Scattering

INTRODUCTION

Breast augmentation is the most commonly performed plastic surgery procedure worldwide.² The majority of these implants are of the silicone gel type, with a small minority being saline-filled. The filling of modern cohesive gel implants is made up of short-chain polymers of polydimethylsiloxane (PDMS) gel, interspersed with short-chain PDMS fluid. The cover, or shell, is composed of a tougher, cross-linked silicone elastomer.³

Concerns over the safety of breast implants have conventionally focused on macroscopic rupture, in which structural failure of the shell leads to large amounts of silicone gel around the implant. Dissemination of silicone gel has been observed in the surrounding implant capsule and axillary lymph nodes in the case of implant rupture.⁴⁻⁸ Further migration to the lungs,⁹⁻¹¹ skin,¹² and the lower extremities¹³ has also been described. The use of a cohesive gel, and increased structural integrity of the implant shells because of barrier layers, have led to decreased rupture rates in modern adaptations.

Nevertheless, concern remains about the safety of long-term exposure to implant material. Silicone is regarded as a biologically inert material, although immunological reactions can result in complications, as demonstrated by the severe granulomatous reactions sometimes observed after liquid silicone injections.^{14,15} The role of free silicone in the development of capsular contraction,¹⁶ and in Breast Implant-Associated Anaplastic Large Cell Lymphoma¹⁷ is not fully understood. The type of implant has been shown to affect the risk of these conditions,^{18,19} however the exact role that silicone itself plays is still unconfirmed.^{20,21}

Large amounts of gel from ruptured implants are easily discernible using imaging techniques such as magnetic resonance imaging and high-resolution ultrasound.⁷ However, gel 'bleeding' or 'sweating', short-chain polymer fluid permeating through the shell, results in small particles or droplets that pose a diagnostic challenge.²² Even though fluorosiloxane barriers were introduced to reduce this bleeding phenomenon, it is unclear to what extent this bleeding still happens into the surrounding tissue.²³ The reference standard for such

evaluations, bright-field microscopic analysis of histology slides, relies on morphological clues of silicone particles but lacks a specific dye that reliably stains silicone only. Suspect structures are often described as amorphous, translucent material in apparent vacuoles.^{24,25} Non-specific stains that have been described to help visualize silicone include stamp pad ink and polymer-staining Oil Red O.^{10,24,26}

Several analysis techniques exist that exhibit chemical specificity. For instance, energy dispersive X-ray analysis has been used in the past for the detection of elemental silicon in silicone granulomas.^{10,26–28} Atomic absorption spectroscopy has also been described as quantitative tool for silicon detection.²² Besides not having molecular specificity, these techniques require additional sample preparation, and only a limited number of points can be analyzed. Attempts to detect silicone polymers with molecular specificity include NMR²⁹ and infrared spectroscopy.³⁰ These techniques are generally time-consuming and therefore impractical for analysis of larger tissues. They also lack the necessary micrometer spatial resolution.

Conventional Raman microscopy provides a non-destructive spectral analysis of chemicals at sub-micrometer resolution. However, excessively long acquisition times due to the low Raman cross section, and the strong fluorescence background make this technique less suitable for the large-scale mapping of tissues. Previous attempts at Raman spectroscopic analysis found additional disadvantages: tissue must remain unstained and uncovered, resulting in the tissue drying out and risking contamination.²⁵

Silicone detection in histological slides should ideally be specific, sensitive, non-destructive and fast. One technique that fulfills these requirements is Stimulated Raman Scattering (SRS) microscopy. SRS is based on the synchronized action of two overlapping laser beams of a different color, typically in the near-infrared range. SRS results in much stronger signals than conventional Raman scattering, circumvents fluorescence from the sample and the cover slip, while speeding up the detection significantly; pixel dwell times in the order of microseconds, compared to seconds for conventional Raman, are routinely achieved.^{31–33} Furthermore, the spectral response still follows the spontaneous

Raman spectral response.³¹ These characteristics make SRS an excellent technique for label-free vibrational imaging of biological tissues.^{31,33–37} In an earlier paper we established SRS as a suitable technique for the identification of micrometer-sized polymer particles (‘microplastics’) in environmental samples.³⁸

SRS is a four-wave mixing process that interacts with the third order susceptibility of a Raman active material. In short, two spatially and temporally overlapping pulsed laser beams concurrently arrive at a sample. When the photon energy difference of the beams matches a vibrational transition of a molecule, a signal is generated by intensity transfer from the pump beam to the Stokes beam. Modulation of one of the beams will therefore cause modulation transfer to the other beam. The amplitude of this modulation transfer will be proportional to both the Raman cross section of the molecule and the number of molecules in the focal volume.^{31,34,43}

In this paper, we introduce an SRS-based method for the detection of silicone in histological slides. We first record SRS-derived silicone and background tissue spectra in the C-H stretch region to select two wavenumber settings that maximize the contrast between silicone and the surrounding tissue. We show that sample deparaffinization and staining of the slides does not change the silicone content of these samples. We provide a framework for fast, high-volume analysis by showing the distribution map and quantified analysis of a full histological slide.

MATERIALS AND METHODS / EXPERIMENTAL

Sample preparation

Table 1 shows a list of samples used in this experiment. The periprosthetic capsules from four women with breast implants, collected during explantation, were analyzed for this study. In one case the reason for explantation was a clinical diagnosis of implant rupture. The second case involved an implant that was deemed during explantation to be ‘sweating’, a phenomenon in which, perioperatively, silicone gel is found to have permeated through the

implant shell, without a macroscopically visible rupture. Removal of the third, PU foam-covered, implant was not related to implant failure. A capsule from a non-ruptured implant (Sample #4) served as a potential negative control. Furthermore, an axillary lymph node from a patient with a ruptured implant was included (Sample #5). Informed consent was obtained in accordance with institutional guidelines.

Samples were fixed in 4% formaldehyde for 24 hours, then routinely processed for conventional paraffin embedding. Paraffin sections of 5 μm were cut. After deparaffinization and rehydration, slides were stained with hematoxylin and eosin (H&E).

To investigate the potential loss of silicone content during deparaffinization, one tissue section, known to contain silicone, was imaged before and after deparaffinization.

Table 1. Sample Description

Sample number	Tissue	Implant status	Implant type
#1	Implant capsule	Rupture	Silicone gel
#2	Implant capsule	'Sweating'	Silicone gel
#3	Implant capsule	Intact	PU-covered, Silicone gel
#4	Implant capsule	Intact	Silicone gel
#5	Axillary lymph node	Rupture	Silicone gel

List of all samples used in this study. Implant status indicates the perioperative evaluation of the macroscopic integrity of the explanted implant. PU: polyurethane

SRS microscopy setup

A modified version of a previously described setup^{38,39,43} was used (Figure 1), based on a Plecter Duo Nd:YAG laser (Lumera Laser, Kaiserslautern, Germany) with a repetition rate of 80 MHz and 8 ps pulse duration. The two output beams consisted of a 1064 nm laser which was sinusoidally amplitude-modulated at 3.636 MHz with a 3080-194 Acousto Optical Modulator (EQ Photonics GmbH, Eching Germany).

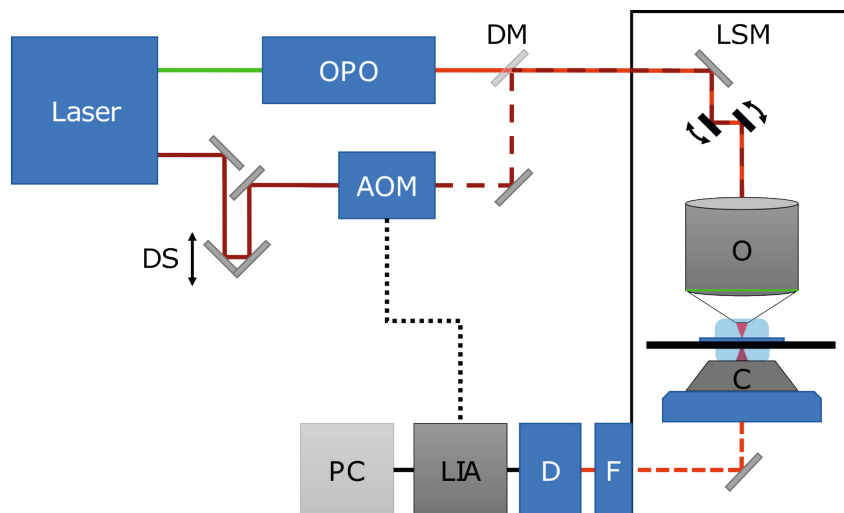


Figure 1. Schematic representation of the SRS setup

DS: Delay Stage, AOM: Acousto-Optic Modulator, OPO: Optical Parametric Oscillator, DM: Dichroic Mirror, LSM: Laser Scanning Microscope, O: Objective, C: Condenser, F: Short-pass filter, D: Photo-detector, LIA: Lock-in amplifier, PC: Computer. The black dashed line represents the reference frequency for the LIA.

The second, frequency-doubled output was used to pump a Levante Emerald Optical Parametric Oscillator (OPO) (APE, Berlin, Germany). The OPO (Pump beam) was tuned so that the photon energy difference with the fixed 1064-nm beam (Stokes) would correspond with the targeted molecular vibration, with a 4cm^{-1} spectral resolution. The OPO output beam and the laser beam at 1064 nm were overlapped temporally using a delay stage, and overlapped spatially with a dichroic mirror. Subsequently, the beams were sent into a 7MP laser scanning microscope (Zeiss, Oberkochen, Germany). Samples were scanned using a C-achroplan W 32 \times water immersion objective with a numerical aperture of 0.85 (Zeiss, Oberkochen, Germany). Tile scanning with an x-y raster stage was used to image areas larger than the field of view. A water immersion condenser with a numerical aperture of 1.2 was used to collect the forward-scattered light. The 1064 nm beam was blocked with a combination of a long-pass dichroic mirror and a short-pass optical filter. A DET36A photodetector (Thorlabs, USA), integrated with an in-house built trans-impedance amplifier, detected

the pump beam light. To reveal the stimulated Raman loss (SRL) the signal was demodulated using a HF2LI lock-in amplifier (Zurich instrument, Zürich, Switzerland) set to 13.75 μ s time constant and filter order 8. The microscope's ZEN2011 proprietary software was used to reconstruct images.

SRS spectra were compared to spontaneous Raman spectra obtained from silicone breast implant gel and from silicone particulates in a histology slide, using an inVia Reflex Raman microspectrometer (Renishaw, Wotton-under-Edge, UK) at a laser wavelength of 785 nm.

Image acquisition

For overview SRS images, the tile size was 128 x 128 pixels and corresponded to a field of view of 205 x 205 μ m, meaning a pixel size of 1.6 μ m. The measurement time was 100 μ s per pixel, which corresponded to under three seconds per tile in practice. Regions of interest (ROI) were rescanned at higher resolution, with a 0.52 μ m pixel size and 256 x 256 pixels per frame in approximately nine seconds. The average power applied to the sample was 14 mW for the 1064 nm beam, and 7 mW for the OPO output beam. Total laser power was limited to minimize damage to samples. A 2:1 power ratio for the two beams was chosen to maximize the signal-to-noise ratio under this power restriction.³⁹

Image acquisition consisted of obtaining a brightfield picture of the entire slide, after which the sample was scanned at two different wavenumbers that maximize the contrast between silicone and the surrounding tissue. To that end, a series of SRS images in the CH-stretch range (2800 – 3000 cm^{-1}) was acquired with five wavenumber increments. Regions suspected of containing silicone were chosen for this, and a spectrum was acquired for each spatial location. Subsequently, averaged spectra from silicone and from the tissue background were created. To determine the optimal wavenumbers for SRS discrimination, the Root mean square error (RMSE) analysis described by Lu et al. was used.⁴⁰

Image processing and analysis

The acquired SRS images were processed to remove false positives and to create a mask that can be overlaid on the histological image. First, an upper threshold ten percent higher than the expected maximum SRS signal from silicone was applied to remove sporadic thermal damage-induced saturated signals. The image at the background wavenumber was subsequently subtracted from the silicone image, creating a high contrast, silicone-specific SRS image. Adaptive thresholding was applied to this image, and the resulting binary mask was co-registered with the bright-field image using the Control Point Selection Tool for Matlab (Version R2018b for Windows, MathWorks). The color green was chosen for the silicone overlay to maximize contrast with the magenta-rich histology images. Particles smaller than eight pixels were deleted to further reject artifacts from sub-micron thermal damage. Setting a pixel size effectively determines the lower spatial detection limit. Given the pixel sizes of 1.6 μm and 0.52 μm for low- and high-resolution scanning, this means particles as small as 20 μm^2 and 2 μm^2 , respectively, can be detected. Connected Component analysis (CC) provided a list of all detected silicone particles. This resulted in histograms and total silicone areas expressed in μm^2 .

RESULTS AND DISCUSSION

Wavenumber selection

The SRS wavenumber run on sample #1 resulted in a series of images that agreed very well with the spontaneous Raman spectra of silicone gel and of silicone particles in tissue (Figure 2, Supplementary video S1). A higher baseline is seen in the spontaneous Raman spectrum from the histology slide due to the fluorescence background (Figure 2A). The C-H stretch vibrational frequency in PDMS is distinctly different from that of the major tissue constituents, lipids and proteins. RMSE analysis resulted in two wavenumbers for optimal contrast: 2905 cm^{-1} for silicone and 2933 cm^{-1} for the tissue background (Figure 2B).

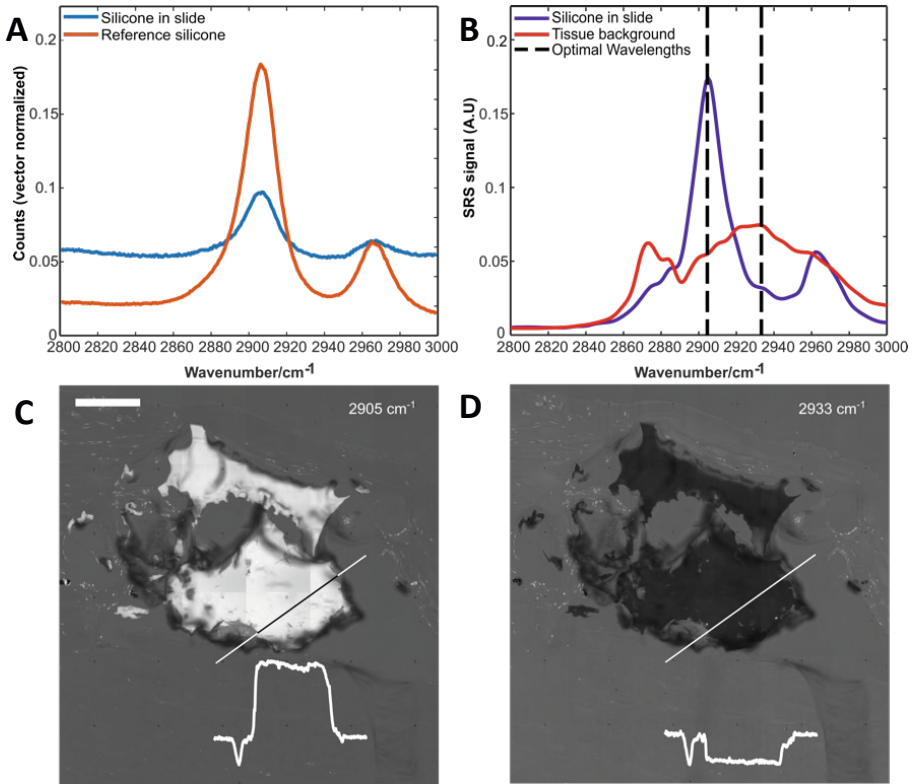


Figure 2. Optimal wavenumber determination.

Figure 2A depicts the spontaneous Raman spectra of silicone breast implant gel (for reference), and silicone in a histology slide from a ruptured implant (Sample # 1) in orange and blue, respectively. The SRS spectra of silicone in a histology slide and of the adjacent tissue areas can be seen in Figure 2B, in purple and red, respectively. The spontaneous Raman spectra from silicone has a high baseline in contrast to its SRS counterpart, due to the fluorescence background. Two dotted lines indicate the calculated optimal wavenumbers. The lower frames show SRS images of a silicone particle in an H&E stained histology slide at the two wavenumbers: Figure 2C for the silicone wavenumber at 2905 cm^{-1} , Figure 2D for the tissue background wavenumber at 2933 cm^{-1} . In both images, the pixel intensity along a line across the particle is plotted underneath this line. Scale bar: $250\text{ }\mu\text{m}$

Two SRS images of a silicone particle in histological tissue were then acquired at these two wavenumbers (Figures 2C and 2D). An intensity profile at the bottom of the images illustrates the contrast between a silicone particle and the surrounding tissue background.

Deparaffinization

SRS imaging of a silicone containing tissue slide before and after deparaffinization and staining was carried out to assess the possible washing out of silicone material during these steps. However side by side comparison of before (Figure 3A) and after SRS images (Figure 3C), does not show a decrease in silicone material.

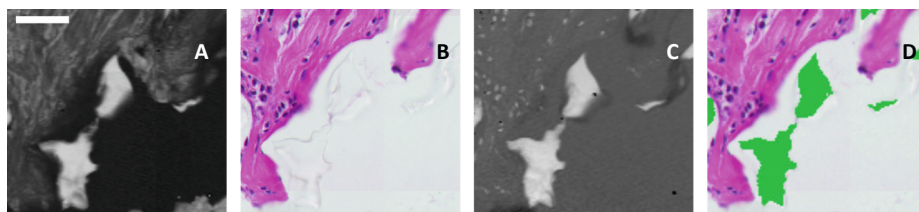


Figure 3. Comparison of silicone content before and after deparaffinization.

Figure 3A and 3C: SRS images at the 2905 cm^{-1} wavenumber depict the silicone content of a region of interest in an implant capsule (Sample # 1) before and after the deparaffinization and staining protocol. Note the apparent similarity between the silicone particles in 3A and 3C. Figure 3B shows the color image of the histology slide after deparaffinization and H&E staining. Figure 3D shows the SRS image for silicone of 3C, overlaid in green on the H&E image. Scale bar: 50 μm

Sample analysis

All four implant capsules that were analyzed (Table 1) contained measurable amounts of silicone. The capsule obtained from the ruptured implant # 1 was used as positive control due to the large amounts of silicone apparent in the bright-field image. Figure 4A shows the results of the full-slide analysis of this capsule. Relatively large agglomerations can be seen in open areas with apparent similar shape. Scanning of this relatively large sample of $27 \times 10^6\ \mu\text{m}^2$ at 1.6

μm pixel size and at two wavenumbers took approximately two hours. The area of the slide actually covered by tissue was $10.8 \times 10^6 \mu\text{m}^2$. Connected Component (CC) analysis resulted in the quantification of particle sizes. Summing of all particles showed a total silicone area of $28,000 \mu\text{m}^2$ for the entire slide, meaning a 0.26% area relative to the sample's area. Additionally, a histogram of all the particle sizes is shown in Figure 4B with $25 \mu\text{m}^2$ binning. High-resolution scans of regions of interest at $0.5 \mu\text{m}$ pixel size are shown in Figures 4C-4F.

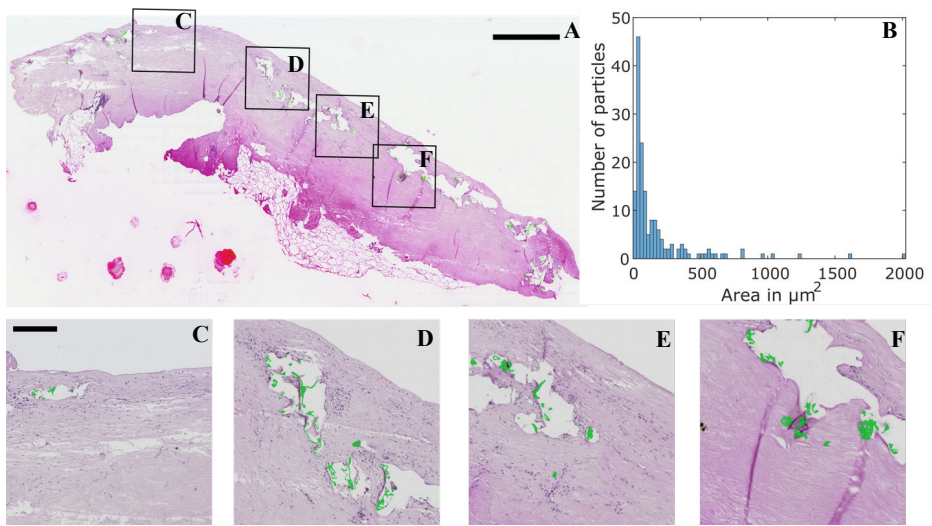


Figure 4. Fully imaged histology slide of implant capsule (Sample 1).

Figure 4A shows the fully imaged histology slide of Sample 1. Green depicts the SRS scan at silicone wavenumber, superimposed on the bright-field image of the H&E histology slide. The histogram in Figure 4B shows the distribution of particle sizes found in the full-sized image by connected component analysis of the SRS signal representing silicone. Scale bar: 1 mm. Insets scale bar: $200 \mu\text{m}$. Insets 4C, 4D, 4E, and 4F show regions of interest at higher resolution, and illustrate the extreme sensitivity of SRS to depth; only the silicone present at the focal plane elicits an SRS signal.

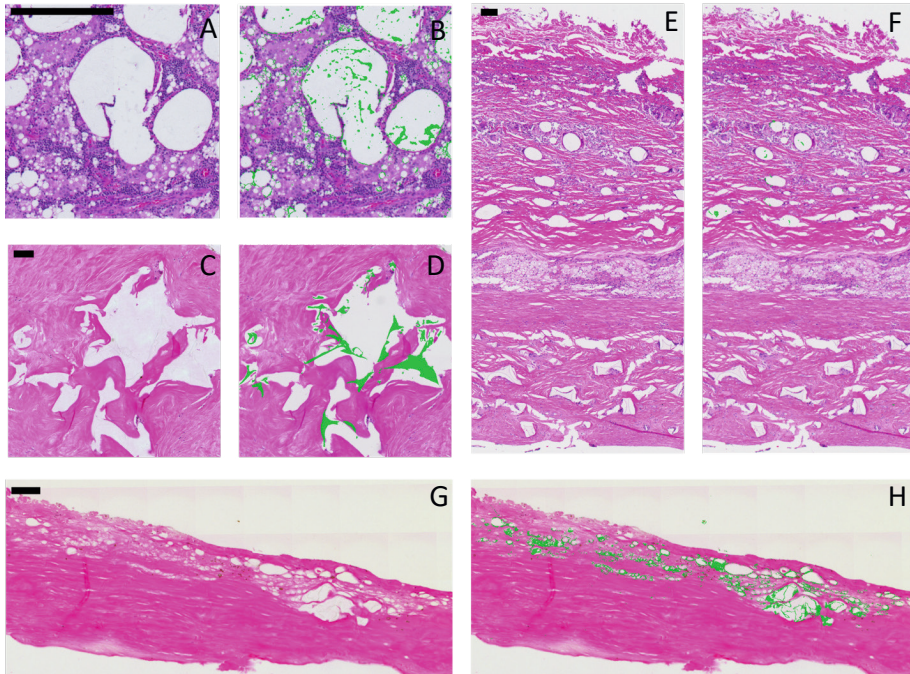


Figure 5. H&E stained tissues containing silicone.

Pairs of frames show histology images without and with the overlaid SRS false-colored image, with green depicting silicone. Figures 5A and 5B show an H&E stained slide of an axillary lymph node containing large vacuoles with a high amount of silicone particles (Sample 5). Inflammatory response in the form of multinucleated giant cells can be seen surrounding the vacuoles. Figures 5C and 5D show a periprosthetic capsule from a non-ruptured silicone gel implant with the characteristic amorphous material surrounded by a dense collagen matrix (Sample 4). A periprosthetic capsule from a PU foam-covered implant can be seen in Figures 5E and 5F, showing encapsulation of different foreign materials (Sample 3). Near the bottom of the images, a zone of translucent polygonal-shaped particles corresponds with the porous PU foam. Particles that were spectrally verified as silicone can be seen distally from the implant side of the capsule. Notice that PU does not show up on the SRS image with these SRS settings, indicating the specificity of the technique. A capsule from a non-ruptured implant, that was deemed to be 'sweating' during explantation, can be seen in Figures 5G and 5H (Sample 2). Large amounts of silicone are present at the implant side of this capsule. Scale bars: 100 μm

Figure 5 shows additional examples of silicone detection in different tissues and implant types. The axillary lymph node sample (sample # 5) in Figure 5A and 5B, an example of silicone migration to distant organs, showed an abnormal vacuolated aspect with numerous multinucleated giant cells. Large silicone particles were found in these sizeable vacuoles, while smaller vacuoles showed a crescent of material at their fringes not apparent in the standard brightfield picture. The capsule from a non-ruptured implant (Sample # 4, Figure 5C and 5D), unexpectedly revealed large agglomerations of silicone. The PU foam-covered implant capsule (Sample # 3, Figure 5E and 5F) was initially included as a potentially negative control, as PU has a different Raman spectrum and does not provide contrast in our SRS protocol. PU material in such a capsule can, however, be recognized based on its distinct morphology: polygonal and triangular shapes of translucent material. Nonetheless, SRS imaging resulted in the detection of additional silicone debris distally in the capsule, relative to the PU foam particles. This finding indicates that the foam shell cover does not stop the migration of silicone gel filling. Finally, the capsule from the 'sweating' implant (Sample # 2) is shown in Figure 5G and 5H, and was also found to contain silicone.

CONCLUSION

The SRS imaging protocol described in this manuscript makes it possible to detect and quantify silicone debris in histology slides with molecular specificity, in a fast and convenient manner. Deparaffinated and stained histological slides were found suitable for silicone quantification, as the silicone distribution in the sample is maintained when compared to unstained, paraffin embedded slides. Contrary to previous analysis techniques, SRS is non-destructive and involves no additional preparatory steps. Additionally, coverslips used in standard histology slides do not interfere with the SRS signal.

The sweating or bleeding of short-chain silicone polymers from the cohesive gel core may result in particles smaller than our size detection limit, although

there is currently a paucity of evidence concerning the distribution of this sub-micron particulate. Contrary to metal orthopedic implant debris, where particle sizes are well-documented,⁴¹ it is difficult to define a range of particle sizes because of the viscous nature of silicone gel. Hirakawa et al. looked at particle shedding from silicone-surfaced orthopedic implants and found a size distribution skewed towards sub-micron particles.⁴² Joint surfaces are subject to higher shear forces than shape-determining implants so a direct comparison of particle sizes may not be apt. Nevertheless, given the chosen pixel size for SRS imaging, the smallest detectable particle size was $2 \mu\text{m}^2$. Even though this is larger than the theoretical resolution limit of the SRS setup, smaller particles were excluded to limit the number of artifacts. It appears that this limit of $2 \mu\text{m}^2$ is more than adequate for the detection of intracellular silicone.

Although the amount of silicone material was found to remain unaffected after deparaffinization, preparatory steps prior to this may still drastically decrease the material present in the final histology slide. When looking at the large vacuoles that do contain silicone, only a fraction of the vacuole contains silicone particulate and it is presently unclear whether this is due to previous phagocytosis of silicone or washing out during the preparatory steps described earlier.

Additional uncertainty about the quantification of silicone arises from the SRS depth resolution. In a previous study we showed the full-width-at-half-max focal length in the Z dimension to be around $2.6 \mu\text{m}$ at similar wavelengths,⁴³ which is about half of the $5 \mu\text{m}$ thick histological slides. This means that some silicone can be outside of the focal volume range and will not contribute to the SRS signal. Indeed, we found some locations where silicone is observed in the color image but the edges of a particle are not detected in the SRS signal. This can be seen in the insets of Figure 4, in vacuoles in Figure 5B and to some extent in Figure 3.

Although SRS imaging of silicone exhibits excellent contrast and is generally non-destructive, some micro-sized sample damage may occur due to the pulsed and tightly focused laser beams.

The samples measured in this study showed inhomogeneity in their susceptibility to photodamage, although the relatively low power applied on the sample helped to avoid this. Nevertheless, photo-induced damage spots were sporadically observed, especially close to the edges of the tissue. These spots show up as an intense signal, allowing their removal using an upper threshold. Moreover, this occasional photodamage is the main limitation in increasing the scanning speed of the current system. That is to say, the decrease in power has to be compensated with long time constants and pixel dwell time to retain an adequate spatial resolution. Using a dual beam SRS system, as described by Heuke et al,⁴⁴ to simultaneously detect the silicone and protein peaks. This would result in a roughly two-fold increase in scanning speed.

The extent to which silicone debris from breast implants impacts women's long-term health is not fully understood. Studies that evaluate biocompatibility focus on short term effects, even though silent implant failure may go unnoticed for years. Whether a foreign body reaction to silicone particles plays a role in the most common breast implant complication, capsular contracture, or in the more rare systemic complaints is still up for debate. Until now, no fast and sensitive technique existed that spectrally determined the silicone content of histology slides down to the micrometer level.

By performing SRS analysis on stained histological slides, the extent of silicone debris contamination of the surrounding tissue can be analyzed objectively, spectrally confirming the identity of silicone material in tissue without having to rely on non-specific morphological features. This can also be done retrospectively on stored tissue samples, of which there is an ample reserve in most pathology departments, without any additional sample treatment. Furthermore, it allow the combination of SRS and conventional staining on the same slide, enabling focused research into the relationship between silicone presence and specific cells.

This approach can be used on thicker samples. Moester et al.⁴³ showed the feasibility of SRS imaging up to tens of micrometers in depth, at a cost of lower Signal-to-Noise ratio. In addition, multiple groups have described an SRS-based approach to image fresh tissue and provide label-free histology (Stimulated

Raman Histology). We are convinced that this approach is also feasible for the detection of silicone in tissue.^{45,46} Determining silicone content relative to the sample surface area allows a direct comparison between samples. The different cell types and immunological mechanisms present in the tissue surrounding silicone implants can be analyzed, while simultaneously providing a quantitative evaluation of silicone content. Comparing these processes for different implant types, surgical techniques, and patient characteristics should result in a better understanding of pathophysiological mechanisms and would enable a better assessment of the performance of both implants and surgical techniques.

REFERENCES

1. Calobrace, M.B., Schwartz, M.R., Zeidler, K.R., Pittman, T.A., Cohen, R., and Stevens, W.G. (2018) Long-term safety of textured and smooth breast implants. *Aesthetic Surg. J.*, 38 (1), 38–48.
2. The International Society of Aesthetic Plastic Surgery (2017) Annual ISAPS International Survey on Aesthetic/Cosmetic Procedures in 2017.
3. Kappel, R.M., Klunder, A.J.H., and Pruijn, G.J.M. (2014) Silicon chemistry and silicone breast implants. *Eur. J. Plast. Surg.*, 37 (3), 123–128.
4. Fleury, E. de F.C., Rêgo, M.M., Ramalho, L.C., Ayres, V.J., Seleti, R.O., Ferreira, C.A.P., and Roveda, D.J. (2017) Silicone-induced granuloma of breast implant capsule (SIGBIC): Similarities and differences with anaplastic large cell lymphoma (ALCL) and their differential diagnosis. *Breast Cancer Targets Ther.*, 9, 133–140.
5. Vaamonde, R., Cabrera, J.M., Vaamonde-Martín, R.J., Jimena, I., and Martín, J.M. (1997) Silicone granulomatous lymphadenopathy and siliconomas of the breast. *Histol. Histopathol.*, 12 (4), 1003–1011.
6. Zambacos, G.J., Molnar, C., and Mandrekas, A.D. (2013) Silicone lymphadenopathy after breast augmentation: Case reports, review of the literature, and current thoughts. *Aesthetic Plast. Surg.*, 37 (2), 278–289.
7. Klang, E., Yosepovich, A., Krosser, A., Soffer, S., Halshtok Neiman, O., Shalmon, A., Gotlieb, M., and Sklair-Levy, M. (2017) Detection of Pathologically Proven Silicone Lymphadenopathy: Ultrasonography Versus Magnetic Resonance Imaging. *J. Ultrasound Med.*, 37 (4), 969–975.
8. Carson, B., Cox, S., and Ismael, H. (2018) Giant siliconoma mimicking locally advanced breast cancer: A case report and review of literature. *Int. J. Surg. Case Rep.*, 48, 54–60.
9. Muñoz González, F., Hermoso Alarza, F., and Cano Aguirre, M. del P. (2018) Lung Siliconoma, a Rare Complication of Breast Prosthesis Rupture. *Arch. Bronconeumol.*, 54 (11), 580–581.
10. Lewin-Smith, M., Kalasinsky, V., Shilo, K., Tomashefski, J., and Cropp, A. (2012) Detection of silicone in lung tissue. *Arch. Pathol. Lab. Med.*, 136 (10), 1179–1180.
11. Levine, R.L., Allen, T.C., Cartwright, J., and Cagle, P.T. (2005) Silicone thorax due to a ruptured breast implant. *Chest*, 127 (5), 1854–1857.
12. Dragu, A., Theegarten, D., Bach, A.D., Polykandriotis, E., Arkudas, A., Kneser, U., Horch, R.E., and Ingianni, G. (2009) Intrapulmonary and cutaneous siliconomas after silent silicone breast implant failure. *Breast J.*, 15 (5), 496–499.
13. Oh, J.H., Song, S.Y., Lew, D.H., and Lee, D.W. (2016) Distant migration of multiple siliconomas in lower extremities following breast implant rupture: Case report. *Plast. Reconstr. Surg. - Glob. Open*, 4 (10), 1–3.
14. Melnick, S., Abaroa-Salvatierra, A., Deshmukh, M., and Patel, A. (2016) Calcitriol mediated hypercalcaemia with silicone granulomas due to cosmetic injection. *BMJ Case Rep.*, 2016, 2–4.
15. Narins, R.S., and Beer, K. (2006) Liquid injectable silicone: A review of its history, immunology, technical considerations, complications, and potential. *Plast. Reconstr. Surg.*, 118 (3 SUPPL.), 77–84.
16. Chong, S.J., and Deva, A.K. (2015) Understanding the etiology and prevention of capsular contracture. *Clin. Plast. Surg.*, 42 (4), 427–436.
17. Clemens, M.W., Nava, M.B., Rocco, N., and Miranda, R.N. (2017) Understanding rare adverse sequelae of breast implants: anaplastic large-cell lymphoma, late seromas, and double capsules. *Gland Surg.*, 6 (2), 169–184.
18. Headon, H., Kasem, A., and Mokbel, K. (2015) Capsular contracture after breast augmentation: An update for clinical practice. *Arch. Plast. Surg.*, 42 (5), 532–543.
19. Leberfinger, A.N., Behar, B.J., Williams, N.C., Rakszawski, K.L., Potochny, J.D., MacKay, D.R., and Ravnic, D.J. (2017) Breast implant-associated anaplastic large cell lymphoma: A systematic review. *JAMA Surg.*, 152 (12), 1161–1168.

20. De Boer, M., Van Leeuwen, F.E., Hauptmann, M., Overbeek, L.I.H., De Boer, J.P., Hijmering, N.J., Sernee, A., Klazen, C.A.H., Lobbes, M.B.I., Van Der Hulst, R.R.W.J., Rakhorst, H.A., and De Jong, D. (2018) Breast implants and the risk of anaplastic large-cell lymphoma in the breast. *JAMA Oncol.*, 4 (3), 335–341.
21. Jong, D. De, Vasmel, W.L.E., de Boer, J.P., Verhave, G., Barbé, E., Caspaire, M.K., and van Leeuwen, F.E. (2008) Anaplastic Large-Cell Lymphoma in Women with Breast Implants. *JAMA*, 300 (17), 2030–2035.
22. Peters, W., Smith, D., Lugowski, S., McHugh, A., Keresteci, A., and Baines, C. (1995) Analysis of silicon levels in capsules of gel and saline breast implants and of penile prostheses. *Ann. Plast. Surg.*, 34 (6), 578–584.
23. Peters, W. (2002) The evolution of breast imaging. *Can. J. Plast. Surg.*, 10 (5), 223–236.
24. Van Diest, P.J., Beekman, W.H., and Hage, J.J. (1998) Pathology of silicone leakage from breast implants. *J. Clin. Pathol.*, 51 (7), 493–497.
25. Pasteris, J.D., Wopenka, B., Freeman, J.J., Young, V.L., and Brandon, H.J. (1999) Medical mineralogy as a new challenge to the geologist: Silicates in human mammary tissue? *Am. Mineral.*, 84 (7–8), 997–1008.
26. Kappel, R.M., Boer, L.L., Dijkman, H., and Dijkman, H.B.P.M. (2016) Gel Bleed and Rupture of Silicone Breast Implants Investigated by Light-, Electron Microscopy and Energy Dispersive X-ray Analysis of Internal Organs and Nervous Tissue. *Clin. Med. Rev. Case reports*, 3 (1), 1–9.
27. Travis, W.D., Balogh, K., and Abraham, J.L. (1985) Silicone granulomas: Report of three cases and review of the literature. *Hum. Pathol.*, 16 (1), 19–27.
28. Krayenbühl, B.H., and Panizzon, R.G. (2000) Silicone Granuloma. *Dermatology*, 200 (4), 360–362.
29. Garrido, L., Bogdanova, A., Cheng, L.L., Pfeiderer, B., Tokareva, E., Ackerman, J.L., and Brady, T. (1996) Detection of Silicone Migration and Biodegradation with NMR, in *Immunology of Silicones*, pp. 49–58.
30. Kidder, L.H., Kalasinsky, V.H., Luke, J.L., Levin, I.W., and Lewis, E.N. (1997) Visualization of silicone gel in human breast tissue using new infrared imaging spectroscopy. *Nat. Med.*, 3 (2), 235–237.
31. Freudiger, C.W., Min, W., Saar, B.G., Lu, S., Holtom, G.R., He, C., Tsai, J.C., Kang, J.X., and Xie, X.S. (2008) Label-free biomedical imaging with high sensitivity by stimulated raman scattering microscopy. *Science.*, 322 (5909), 1857–1861.
32. Nandakumar, P., Kovalev, A., and Volkmer, A. (2009) Vibrational imaging based on stimulated Raman scattering microscopy. *New J. Phys.*, 11, 1–10.
33. Saar, B.G., Freudiger, C.W., Stanley, C.M., Holtom, G.R., and Xie, X.S. (2010) Video Rate Molecular Imaging In Vivo with Stimulated Raman Scattering. *Science.*, 330 (29), 1368–1370.
34. Fu, D., Lu, F.-K., Zhang, X., Freudiger, C., Pernik, D.R., Holtom, G., and Xie, X.S. (2012) Quantitative chemical imaging with stimulated Raman scattering microscopy. *J. Am. Chem. Soc.*, 134 (8), 3623–3626.
35. Zhang, D., Wang, P., Slipchenko, M.N., Ben-Amotz, D., Weiner, A.M., and Cheng, J.-X. (2013) Quantitative Vibrational Imaging by Hyperspectral Stimulated Raman Scattering Microscopy and Multivariate Curve Resolution Analysis. *Anal. Chem.*, 85 (1), 98–106.
36. Syed, A., and Smith, E.A. (2017) Raman Imaging in Cell Membranes, Lipid-Rich Organelles, and Lipid Bilayers. *Annu. Rev. Anal. Chem.*, 10 (1), 271–291.
37. den Broeder, M.J., Moester, M.J.B., Kamstra, J.H., Cenijn, P.H., Davidoiu, V., Kamminga, L.M., Ariese, F., De Boer, J.F., and Legler, J. (2017) Altered adipogenesis in zebrafish larvae following high fat diet and chemical exposure is visualised by stimulated Raman scattering microscopy. *Int. J. Mol. Sci.*, 18 (4), 1–21.
38. Zada, L., Leslie, H.A., Vethaak, A.D., Tinnevelt, G.H., Jansen, J.J., de Boer, J.F., and Ariese, F. (2018) Fast microplastics identification with stimulated Raman scattering microscopy. *J. Raman Spectrosc.*, 49 (7), 1136–1144.

39. Moester, M.J., Ariese, F., and De Boer, J.F. (2015) Optimized signal-to-noise ratio with shot noise limited detection in stimulated Raman scattering microscopy. *J. Eur. Opt. Soc. - Rapid Publ.*, 10.
40. Lu, F.-K., Basu, S., Igras, V., Hoang, M.P., Ji, M., Fu, D., Holtom, G.R., Neel, V.A., Freudiger, C.W., Fisher, D.E., and Xie, X.S. (2015) Label-free DNA imaging in vivo with stimulated Raman scattering microscopy. *Proc. Natl. Acad. Sci.*, 112 (37), 11624–11629.
41. Hallab, N.J., Samelko, L., and Hammond, D. (2019) The Inflammatory Effects of Breast Implant Particulate Shedding: Comparison with Orthopedic Implants. *Aesthetic Surg. J.*, 39, S36–S48.
42. Hirakawa, K., Bauer, T.W., Culver, J.E., and Wilde, A.H. (1996) Isolation and quantitation of debris particles around failed silicone orthopedic implants. *J. Hand Surg. Am.*, 21 (5), 819–827.
43. Moester, M.J.B., Zada, L., Fokker, B., Ariese, F., and de Boer, J.F. (2018) Stimulated Raman scattering microscopy with long wavelengths for improved imaging depth. *J. Raman Spectrosc.*, 1–8.
44. Heuke, S., Sarri, B., Audier, X., and Rigneault, H. (2018) Simultaneous dual-channel stimulated Raman scattering microscopy demultiplexed at distinct modulation frequencies. *Opt. Lett.*, 43 (15), 3582.
45. Sarri, B., Poizat, F., Heuke, S., Wojak, J., Franchi, F., Caillol, F., Giovannini, M., and Rigneault, H. (2019) Stimulated Raman histology: one to one comparison with standard hematoxylin and eosin staining. *Biomed. Opt. Express*, 10 (10), 5378.
46. Eichberg, D.G., Shah, A.H., Di, L., Semonche, A.M., Jimshelishvili, G., Luther, E.M., Sarkiss, C.A., Levi, A.D., Gultekin, S.H., Komotar, R.J., and Ivan, M.E. (2019) Stimulated Raman histology for rapid and accurate intraoperative diagnosis of CNS tumors: prospective blinded study. *J Neurosurg*, 6, 1–7.

SUPPORTING INFORMATION

Additional Supporting Information may be found online in the supporting information tab for this article.

Video S1: SRS wavenumber run

Video depicts a series of SRS images in the CH-stretch range (2800 – 3000 cm^{-1}), with five-wavenumber increments of a region containing silicone material in an H&E stained histological slide. The chemical contrast between silicone and the surrounding tissue is apparent, with optima at 2905 cm^{-1} for silicone and 2933 cm^{-1} for the tissue background

5

**Baker-IV capsular contracture is correlated
with an increased amount of silicone material:
an intra-patient study.**

E. de Bakker

L. Zada

R.W. Schmidt

L. van Haasterecht

A. Dick Vethaak

F. Ariese

P. Bult

H. Dijkman

S. Gibbs

F.B. Niessen

Background

Breast implant surgery is one of the most frequently performed procedures by plastic surgeons worldwide. However, the relationship between silicone leakage and the most common complication, capsular contracture, is far from understood. This study aimed to compare Baker-I with Baker-IV capsules regarding their silicone content in an intra-donor setting, using two previously validated imaging techniques.

Methods

Twenty-two donor-matched capsules from eleven patients experiencing unilateral complaints were included after bilateral explantation surgery. All capsules were examined using both Stimulated Raman Scattering (SRS) imaging and staining with Modified Oil Red O (MORO). Evaluation was done visually for qualitative and semi-quantitative assessment and automated for quantitative analysis.

Results

Using both SRS and MORO techniques, silicone was found in more Baker-IV capsules (8/11 and 11/11, respectively) than in Baker-I capsules (3/11 and 5/11, respectively). Baker-IV capsules also showed significantly more silicone content compared to the Baker-I capsules. This was true for semi-quantitative assessment for both SRS and MORO techniques ($p=0.019$ and $p=0.006$, respectively), while quantitative analysis proved to be significant for MORO alone ($p=0.026$ vs. $p=0.248$ for SRS).

Conclusions

In this study, a significant correlation between capsule silicone content and capsular contracture is shown. An extensive and continued foreign body response to silicone particles is likely to be responsible. Considering the widespread use of silicone breast implants these results affect many women worldwide and warrant a more focused research effort.

INTRODUCTION

Since their introduction, the use of silicone breast implants for reconstructive and cosmetic purposes has increased significantly and so breast implant surgery is one of the most frequently performed procedures by plastic surgeons worldwide^{1,2}. Simultaneously, extensive research efforts and lively discussions on their safety and complications continue³⁻¹². Although most of the recent attention is focused on Breast Implant-Associated Anaplastic Large Cell Lymphoma¹³ and breast implant illness¹⁴, the most common complications are still related to the capsule surrounding the implant. Capsule formation is a normal foreign body response, although excessive thickening and contracture are adverse reactions and may result in complaints experienced by the patient.

Prevalence estimates for capsular contracture (CC) range from 5-19% for breast augmentation and 19-25% for breast reconstruction, although numbers vary between studies¹⁵⁻¹⁸. Known risk factors include breast reconstructive surgery after breast cancer, irradiation of the breast, subglandular implant placement, postoperative hematoma, and a smooth implant surface^{19,20}. Over the years, innovations have been made in implant construction to prevent significant silicone bleeding through the surrounding shell²¹. High cohesive silicone gels and more durable shells were introduced, as well as novel surgical techniques. Significant gel bleed and rupture were deemed to be responsible for the high CC rates of the first and second-generation implants²². Together, this resulted in a reduced prevalence of CC compared to the first implant generations^{15,22,23}. Despite these efforts to prevent CC altogether, the actual pathophysiological mechanisms involved are still largely unknown¹⁵.

The Baker classification of CC uses a scale from I (no contracture) to IV (severe contracture) and is the most commonly used classification system for CC. Silicone bleeding, the leaking of small quantities of silicone gel into the surrounding tissue without an obvious tear of the implant, has previously been associated with a higher Baker score²⁴. However, since a reliable, selective, and sensitive detection technique for silicone was missing, the extent of the relationship between silicone bleed and CC has not been directly correlated²⁵. More

precise and sensitive methods have become available to detect silicone in tissue sections. Recently, we introduced stimulated Raman Scattering Microscopy (SRS) as a sensitive, label-free imaging technique to detect silicone particles in tissue slides that had been hematoxylin and eosin (H&E)-stained (staining is not needed but does not interfere with the SRS measurements)²⁶. Additionally, the 3-Phase technique, a combination of standard light microscopy, staining with Modified Oil Red O (MORO), and Transmission Electron Microscopy (TEM) in combination with Energy Dispersive X-ray microanalysis (EDX) has been proven to reliably measure silicone in tissue²⁷.

The plethora of silicone breast implants available, variety of implantation techniques, and patient factors all lead to a very diverse histology for CC²⁸. This makes a true comparison between CC histology samples difficult. Women who develop unilateral complaints are of particular interest to include in studies about the etiology of CC because their capsules offer the unique opportunity to study the differences between affected and unaffected capsules while all other variables remain the same. This should enable the development of a sound pathophysiological model of CC²⁸.

In a previous study using the same capsule collection as described in this study, we showed that Baker-IV capsules, compared to Baker-I capsules, were significantly thicker²⁸. They also expressed more CD68 positive cells indicating an increased influx of innate immune cells, eg macrophages, which are characteristic of foreign body granulomatous reactions observed in reaction to fillers^{28,29}. Furthermore, we observed an increase in vimentin-positive cells, indicating an increase in fibroblasts in Baker-IV. However, an increase in the myofibroblast biomarker alpha-smooth muscle actin was not observed in Baker-IV compared to Baker-I indicating that myofibroblast formation was not directly related to contracture (unpublished data).

Therefore, this study aimed to examine the relationship between Baker-I and Baker-IV capsules regarding silicone content, using both SRS and MORO techniques in an intra-individual study.

MATERIALS AND METHODS

Patient and tissue collection

Donor-matched Baker-I and Baker-IV capsules from patients undergoing explantation or revision surgery between 2010 and 2014 who had developed unilateral complaints were collected (Table 1). Patients with a history of (breast) cancer and recipients of Poly Implant Prothèse (PIP) implants were excluded. All patients had undergone cosmetic augmentation surgery with the submuscular (dual-plane, inframammary fold incision) method using high-cohesive gel textured implants. Although implant age and rupture were documented, unfortunately, the exact brand and type were not (Table 2). Clinical grading using the Baker classification, the collection of capsules, and the explantation surgery itself were performed by an experienced plastic surgeon (Niessen). Patients were included only after oral informed consent was given. These procedures were in accordance with the 'Code for Proper Secondary Use of Human tissue' as formulated by the Dutch Federation of Medical Scientific Societies³⁰. Samples were always taken from the same area of the capsule; cranial from the inframammary incision. Surgically, 5 x 5 cm samples were taken which were subsequently processed in the laboratory. Tissue samples were fixed in 4% formaldehyde for 24 h, then routinely processed and embedded in paraffin. Parallel paraffin sections (max. 20-40 µm apart) were used for both techniques.

Table 1. Patient characteristics

Number of patients	11
Age (years)	46.5 +/- 9.1
BMI	25.0 +/- 4.8
Duration of implant placement (months)	156 +/- 68
Size of implant (cc)	306 +/- 10.5
Smoker	3/11
Diabetic	2/11
[†] Tear in implant on Baker-IV side	3/11
[†] Tear in implant on Baker-I side	1/11
More than one augmentation	1/11

Mean +/- SD is shown.[†]Tear in implant observed during explantation.

Table 2; capsule grading and quantification results

patient	Baker-I			Baker-IV			Implant age		
	SRS	MORO	SRS	SRS	MORO	MORO	Grade	ppm	ppm
	grade	ppm	Grade	Grade	Grade	Grade	Grade	ppm	ppm
1†	-	138	-	295	+++	1110	+	771	132
2	-	85	-	41	++	550	+++	1218	132
3	-	127	-	1286	+++	2575	+++	4112	264
4†	-	58	-	37	++	220	++	118	264
5†	+	58	++	71	+++	10172	+++	22434	120
6	-	63	-	4	-	16	+	21	156
7	-	580	+	297	+	498	++	1270	204
8	-	87	-	11	-	0	+++	22	155
9	+	62	+	1791	+	40	++	1505	19
10	-	92	++	150	++	105	+++	547	204
11*	+	140	+	73	-	13	+	24	180
Q1		62		37		16		24	
Q3		138		297		1110		1505	
Median		87		73		220		771	
Mean		135.5		368.7		1390.8		2912.9	
SD		150.7		598.1		3011.1		6581.2	

Summary of silicone positivity in the capsules. Semi-quantitative assessment for silicone positivity was performed visually and independently by two authors for both methods (SRS and MORO) after which a common agreement was reached. Samples were graded as containing no, a little, intermediate, or a lot of positivity (-, +, ++, +++). Automated quantification was performed as described in the materials and methods section; the ratio for the positive area for silicone, relative to the total measured area of the capsule, is noted in parts per million (ppm). Implant age shown in months. Tear in implant in Baker-I side indicated with * and in Baker-IV side with †. For all quantified variables the Q1 (25th percentile) and Q3 (75th percentile) interquartile range, median, mean, and standard deviation (SD) are shown.

SRS

Histological examination was performed on deparaffinized, formalin-fixed tissue sections (5 μm) which were stained with H&E. After staining, tissue sections were analyzed using an SRS microscopy setup as described earlier^{26,31}. In short, a bright-field image was obtained of the entire slide. Next, the sample was scanned at two different wavenumbers (2905 and 2933 cm^{-1} , corresponding with the C-H stretch vibrational energies of polydimethylsiloxane (silicone) and protein, respectively) which maximized the contrast between silicone and the surrounding tissue. Then, these two SRS images were subtracted, threshold implemented, followed by processing to remove false positives. The processed images were overlaid with the corresponding histological bright-field images, where the silicone was colored green. The bright-field images were recorded as tiles and retrospectively corrected for flat- and darkfield shading³².

MORO, TEM, and EDX

For the second method of detection of silicone, we used a combination of MORO staining, TEM, and EDX. The combination of these three techniques to detect silicone in tissue has been described previously²⁷. Consecutive paraffin sections (4 μm) of the same tissue samples used for SRS analysis were cut, deparaffinized, and rehydrated for MORO staining, which binds specifically to the silicone polymers because of hydrophobic interactions²⁷. Hematoxylin was subsequently used as a counterstain. Following evaluation of the stained tissue sections, several samples were selected for TEM and EDX analysis to verify the MORO staining for quality and specificity.

A selected area of the paraffin block, positive in the MORO staining, was embedded in Epon (embedding epoxy resin) for electron microscopy. Semi- and ultrathin sections were obtained with a Leica ultramicrotome. Semi-thin 1 μm tissue sections were stained with toluidine blue for light microscopical investigation. After further selection, 90 nm ultrathin sections were cut, additionally contrasted with 4% uranyl acetate/lead citrate, and examined by electron microscopy. Uncontrasted 200 nm ultra-thin sections were used for EDX. The

samples were studied with a Jeol (JEM-1200 EX II TEM/STEM) transmission/scanning electron microscope operating at 64 kV with EDX equipment.

Silicone content evaluation & statistical analysis

After the slides were processed, both a traditional qualitative assessment and semiquantitative scoring for positivity were carried out visually and independently by two authors for both methods. Samples were scored according to the amount of silicone and the level of silicone spread within the tissue, as no silicone, localized, intermediately spread/dispersed, heavily dispersed (-, +, ++, +++).

For quantitative analysis of the SRS measurements, the silicone content in the tissues was determined with the Image segmentation app in MATLAB 2020a. The ratio of the positive silicone area relative to the tissue area measured area is expressed in parts per million (ppm).

For quantitative analysis of the MORO analyzed slides, whole-slide images were acquired at 20x, 0.5 $\mu\text{m}/\text{pixel}$ resolution, using the Vectra Polaris scanner (Akoya Biosciences, Marlborough, USA) in bright-field mode. The density of silicon particles was analyzed using QuPath Software 0.2.3 by an automated pixel classifier using the artificial neural network model³³. Regions (250.000 μm^2) from multiple samples were used to train the classifier. In all whole-slide images, a region was created meticulously surrounding the sample. The classifier was subsequently used to analyze all samples, creating a ratio for the positive area relative to the total measured area in ppm.

Both the semi-quantitative and the quantitative results of SRS and MORO analysis were statistically evaluated using the Wilcoxon signed-rank test for paired samples. A *p*-value of less than 0.05 was considered significant. For the quantified variables descriptive statistics were calculated. All statistics were performed using SPSS (IBM SPSS Statistics for Windows, Version 26.0).

RESULTS

In total, 11 patients and 22 capsules were included. Patient characteristics at baseline are shown in table 1. The mean duration of implantation was 156 months. There were three implant tears observed at the time of explantation on the Baker-IV side and one on a Baker-I side (Table 2). One patient underwent the explantation procedure because of recurrent CC (patient 11). All implants were high-cohesive gel silicone implants. There were no postoperative complications, such as hematoma or infection.

The general morphology of the capsules obtained from this patient group has been described earlier²⁸. In short; a large diversity between capsules of different patients and Baker grades I and IV was observed. Baker-IV capsules were significantly thicker and had a higher cell density compared to Baker-I capsules. All capsules were organized in multiple layers with the Baker-I capsules showing more synovial metaplasia-like layers (8/11 vs. 2/11).

SRS imaging shows increased silicone content in Baker-IV compared to Baker-I capsules

Based on visual grading, capsules obtained from 9 of the 11 donors showed elevated amounts of silicone (table 2; semi-quantitative grading of images). Silicone was detected in only three of the Baker-I capsules, whereas silicone was detected in eight of the Baker-IV capsules. In all but one donor more silicone was found in the Baker-IV capsule compared to the contra-lateral Baker-I capsule. In most Baker-IV capsules silicone was found dispersed throughout the capsule and was seen filling vacuoles (Figure 1; in green overlaid on H&E staining), whereas in Baker-I it was more focal or absent. Interestingly, in four of these capsules, a substantial increase in the amount of silicone was only found in the deeper sections of the capsule and was not found in the tissue directly bordering the implant (Figure 1, below, insets 2-3). The statistical evaluation of these semi-quantitative results shows a significant difference ($p=0.019$).

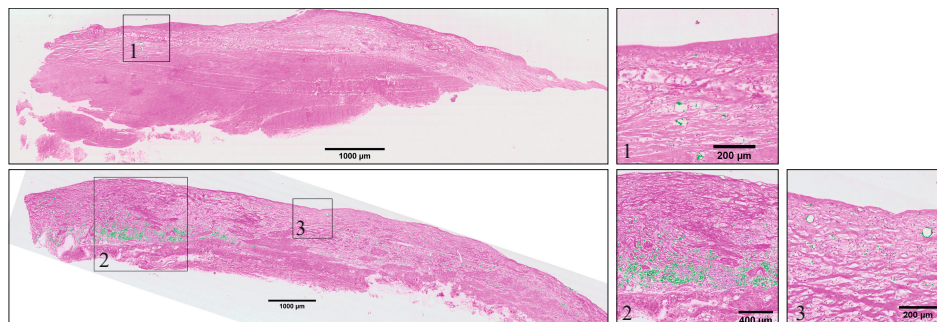


Figure 1 Overview and details of two Baker IV capsules, H&E stained and examined using the SRS technique. Implant side upwards, silicone positivity overlayed with green.

Above: Capsule from patient 4, scoring ++ with a gradual dispersion throughout the capsule and with a magnification of a designated area (inset 1), showing several vacuoles near the implant side of the capsule.

Below: Capsule from patient 5, very high silicone detection, scoring +++. Dispersion throughout and especially in the deeper layers (inset 2) and distribution at the implant side shown with two big vacuoles and multiple smaller positive spots (inset3).

Next, the amount of silicone found was quantified and calculated in ppm relative area (Table 2). Again, a great variance can be seen between capsules and patients. While the Baker-IV capsules show comparative results in semi-quantitative assessment and quantitative analysis, discrepancies exist more in the Baker-I capsules probably due to the lower amounts of silicone found in the tissues. Quantitative SRS analysis between Baker-I and Baker-IV was not able to reject the null hypothesis ($p=0.248$). However, the relative amount of silicone in the tissue showed an inconclusive trend with a higher mean ppm for Baker-IV in comparison with Baker-I (1,475 vs 135 ppm, respectively).

MORO, TEM, and EDX show increased silicone content in Baker-IV compared to Baker-I capsules

Silicone particles were detected with MORO staining in 5 out of 11 Baker-I capsules, while particles were found in all Baker-IV capsules (Table 2; Figure 2). In line with the SRS analyzed tissue sections, there was a clear increase in the number of particles found in Baker-IV capsules in comparison with Baker-I capsules. Similar to SRS, MORO staining resulted in five of the Baker-IV capsules showing a lot of positivity throughout the entire capsules (compare

Figure 2 above, Baker-I with below, Baker-IV). Like the SRS analysis, there was a dispersed pattern of positivity with a tendency to fill vacuoles or positivity in the general area of the vacuoles for most capsules (Figure 2, inset 1). Based on the light microscopy findings, the Baker-I capsule of patient 11 and the Baker-IV capsule of patient 5 were selected for TEM/EDX and to confirm accurate staining of silicone for all samples (Figure 3). The Baker-I capsule from patient 11 shows only small focal spots of positive staining. However, TEM/EDX did confirm that these small granules contain a lot of silicon-containing molecules, measuring 64,078 Si-counts (Figure 3, online supplementary material (OSM) 1, left). The Baker-IV capsule of patient 5 shows a lot of positivity in the MORO staining (++++) and an abundant amount of vacuoles. These were confirmed to contain very high counts of silicon, as the single vacuole in measuring point 014 measured 718,378 Si-counts (Figure 3, OSM 1, right). The statistical evaluation of these semi-quantitative results shows a significant difference between Baker-I and Baker-IV capsules ($p=0.006$).

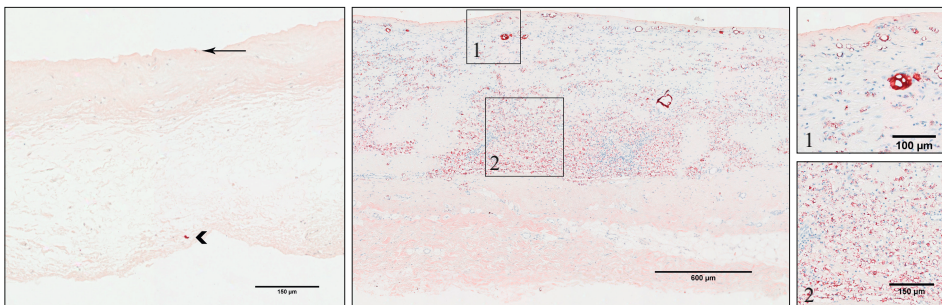


Figure 2 Overview and details of capsules Baker I & IV examined with the MORO technique. Implant side upwards, silicone positivity seen as a red dye.

Left: Baker I capsule from patient 11, scoring +. A small focal spot can be seen centrally in the image (arrow) at the implant side, while a larger focal spot is observed on the patient side of the capsule (arrowhead).

Middle: Baker IV capsule from patient 5, scoring +++ with a gradual dispersion throughout the capsule (inset 1) dispersed positivity and large vacuoles near the implant side of the capsule and large amounts of smaller granules in the deeper layers of the capsule (inset 2).

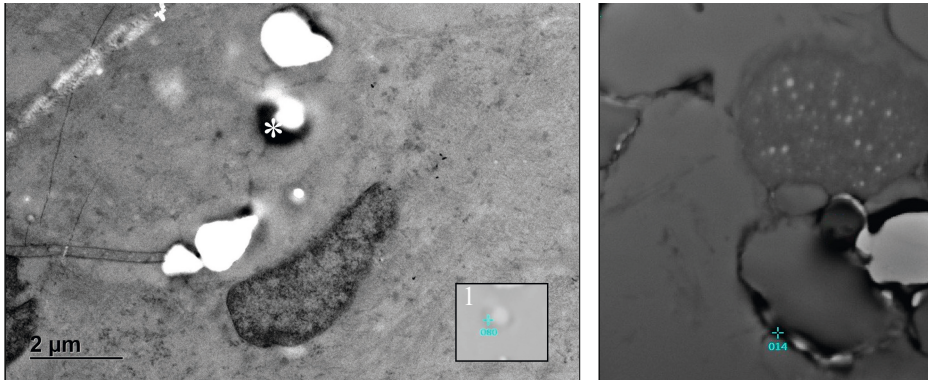


Figure 3 Overview and details of capsules from Baker I & IV examined with TEM in combination with EDX

*Left: TEM micrograph of the EDX measurement performed on the Baker I capsule from patient II, inset I showing focal measurement spot indicated with *. The measured point showed 64,078 Si-counts.*

Right: TEM micrograph of the EDX measurement performed on the Baker IV capsule from patient 5. The vacuole containing point 014 was measured to show 718,378 Si-counts.

Original microscopic magnifications figure left and right: resp. 5K and 12K. The graphs from both measurements are included in online supplementary material 1.

The quantification of these slides is in line with the other results in that they display a large variance between capsules and patients. The same incongruent pattern between semi-quantitative assessment and quantitative assessment can be seen here as well, again, especially for the Baker-I capsules. However, again there is a significant difference between Baker-I and Baker-IV capsules ($p=0.026$). Like in the SRS quantification, a higher mean ppm was seen here for Baker-IV in comparison with Baker-I (2,913 vs 369 ppm, respectively).

See Table 2 for descriptive statistics of non-parametric variables. No significant differences were found between the SRS and MORO techniques.

DISCUSSION

The multitude of articles published about CC clearly shows that it is a multifaceted process. The aim of this study, therefore, was to correlate a CC severity score (the Baker score) with silicone found in the capsule surrounding the breast implant. In current studies describing modern breast implants, silicone release and its effects are missing. By utilizing material from patients suffering from unilateral complaints, donor variation can be eliminated comparing Baker-I and Baker-IV. Here, we show that by using this concept a strong correlation is found between CC and the amount of silicone found in the capsule, which was proven to be a significant difference by two independent techniques (SRS and MORO). These results suggest that the increased deposition of silicone particles in the capsule is responsible for the extensive fibrotic capsule formation and contraction found in CC.

In asymptomatic capsule formation, macrophages and fibroblasts (among other cells) provide a foreign body response in which organized fibrous tissue layers form an initial capsule¹⁵. In these thin and supple (Baker-I) capsules, we previously demonstrated the presence of a synovial metaplasia-like inner layer, with a significantly lower presence in the Baker-IV capsules²⁸. This inner layer may serve as a protective layer, allowing the body to return to a resting state³⁴. In time and not in all patients, a secondary local process starts in which CC occurs. The amount of gel bleeding has been described to correlate with CC, indicative that the amount of silicone presented to the body plays a significant role³⁵. In this collection, patients one, four, and five had an intra-operative tear on the Baker-IV side and patient eleven on the Baker-I side (Table 2). While the Baker-IV side of patient five scored high grades and silicone counts in both SRS and MORO analysis, this was not uniformly seen for patients one and four. The Baker-I capsule of patient eleven was positive for silicone, but so were other capsules in the Baker-I collection without torn implants. Therefore, the presence of a tear cannot explain completely our results. However, imaging studies have shown that patients often have torn implants before CC exists, suggesting the silicone leakage from the tear might be responsible for the CC reaction³⁶.

Also, silicone has been shown to sweat or bleed from the implants and has been shown to contribute to capsular contracture³⁵. Patient nine was scored a + in MORO in Baker-I and a ++ in Baker-IV, the grade in SRS was the same. Objectified counts differed for these variables. As with all clinical studies, our capsule study showed a great variance (probably due to patient variation as well as the different techniques used) between some samples, so some comparisons between individual capsules might not always be in line with the results of the entire collection. CC is associated with increased numbers of cells commonly found in the foreign body reaction like T-cells, macrophages, fibroblasts, giant cells, and contractile myofibroblasts^{15,37-43}. Taken together, this indicates that a secondary foreign body reaction seems to be responsible for CC. Variations in implant placement, pressure during day-to-day activities, and quality (shell integrity) could correlate to a variation in silicone leakage into the tissue and therefore capsule formation and contracture and could explain unilateral complaints. It is notable that whereas most Baker-IV capsules show a generalized spread of silicone throughout, in some cases silicone was located primarily in the deeper regions of the capsule (away from the implant). Reasons for this are still unknown and require further investigation.

Modern techniques aid us in easy and automated quantification for both techniques used in this study. Although 'hard numbers' aid in a clear message, visual assessment is essential to obtain a more thorough analysis of the location of silicone and the characteristics of the tissue, which is why in this study both approaches were performed. A traditional semi-quantitative assessment of images performed by a pathologist involves much more than just the amount of positivity in a staining. A large single positive area will cause a high spike in automated measuring programs, while an expert will consider the total distribution rather than just localized presence in the sample. The abundance of cells and dispersed silicone pattern in some of the Baker-IV capsules indicates a more thorough response by the body than just a large uniform amount of silicone would.

The different methods used to investigate silicone amounts in tissue sections may result in diverse results. The fluidity of silicone can influence the detection

of silicone content in capsules in multiple ways. While the deparaffinization step in tissue section preparation does not seem to influence the amount of silicone found, tissue preparation before that step might cause the silicone to leak out of the sample²⁶. Silicone concentration in the capsule might be far from homogeneous, so the amount of silicone detected can be subject to sampling error. This can explain the differences between the sample sets used for SRS and MORO since the histological slides were a few microns apart. As the surface area of a capsule is more than a thousand times larger than a regular histological slide, it would be extremely time-consuming to analyze the entire capsule. However, in future studies, it would be advisable to take a limited number of biopsies from random sites within the capsule.

The Baker classification used in our study to distinguish between affected and unaffected capsules is subjective and considered unreliable as a diagnostic tool⁴⁴. It is, however, the most commonly and easily used tool in normal practice and does indicate complaints. Moreover, while used as a measure for capsular contracture, actual contracture is not measured. It's more indicative of capsule thickening and hardening. Other tools, like high-definition ultrasound and MRI, can be considered to assess implant folds and deformation as a measure of contracture^{45,46}.

The mean age of the implants (and so the capsules) is 156 months. However, age did not have a significant influence on the amount of silicone found in the capsules in this study (Table 2). For this group of patients, no advice on regular revision surgery existed. Currently, revision surgery is advised every 10-15 years, comparable with the timespan our patients had the implants⁴⁷.

While this study shows a significant correlation between silicone content and CC, these results do not necessarily mean that the implants in women with Baker-I capsules do not lose silicone to the tissue over time. Future research could also include investigating the loss of silicone out of the tissue during the different processing steps, as we saw many empty vacuoles in our samples. Capsules obtained from saline implants exhibit comparable or higher CC rates compared to full silicone implants^{19,20}. However, since only the shell is made from silicone these capsules are still interesting⁴⁸. In a study using plasma

emission spectroscopy, silicon was found in these capsules, so further analysis with the visual histological properties used in this study would be of interest in further understanding this adverse effect⁴⁹. Finally, confirmation in larger sample sizes seems a logical step as well as determining differences between implants in terms of silicone loss.

There used to be a time in which plastic surgeons told patients that silicone implants didn't need to be renewed or removed, but this has been changing over the years⁴⁷. If we consider silicone to be an essential factor in the development of CC, the role of silicone as the dominant ingredient of breast implants should be questioned. At the very least new implants should deteriorate and leak silicone as little as possible.

CONCLUSIONS

In this intra-individual Baker-I vs. Baker-IV study, we show a significant correlation between capsule silicone content and capsular contracture, with Baker-IV tissue containing more silicone than Baker-I. An extensive and continued foreign body response to silicone particles is probably responsible. Considering the widespread use of silicone in breast implants, these results are relevant to many women worldwide.

REFERENCES

- ISAPS. Isaps International Survey on Aesthetic/Cosmetic Procedures. *Isaps*. 2018:49.
- Becherer BE. *Dutch Breast Implant Registry (DBIR) Annual Report 2015 – 2017*. Leiden, the Netherlands; 2017. [https://dica.nl/media/1835/DBIR_Annual_report_\(2015-2017\).pdf](https://dica.nl/media/1835/DBIR_Annual_report_(2015-2017).pdf).
- Rohrich RJ, Kaplan J, Dayan E. Silicone Implant Illness: Science versus Myth? *Plast Reconstr Surg*. 2019;144(1):98-109. doi:10.1097/PRS.0000000000005710
- Cohen Tervaert JW, Kappel RM. Silicone implant incompatibility syndrome (SIIS): A frequent cause of ASIA (Shoenfeld's syndrome). *Immunol Res*. 2013;56(2-3):293-298. doi:10.1007/s12026-013-8401-3
- Wadat A, Rosenberg V, Tiosano S, et al. Silicone breast implants and the risk of autoimmune/rheumatic disorders: A real-world analysis. *Int J Epidemiol*. 2018;47(6):1846-1854. doi:10.1093/ije/dyy217
- Mojsiewicz-Pienkowska K, Jamrógiewicz M, Szymkowska K, Krenczkowska D. Direct human contact with siloxanes (silicones) - safety or risk part I. Characteristics of siloxanes (silicones). *Front Pharmacol*. 2016;7(MAY). doi:10.3389/fphar.2016.00132
- Katzin WE, Feng LJ, Abbuhl M, Klein MA. Phenotype of lymphocytes associated with the inflammatory reaction to silicone gel breast implants. *Clin Diagn Lab Immunol*. 1996;3(2):156-161. <http://www.pubmed-central.nih.gov/articlerender.fcgi?artid=170266&tool=pmcentrez&rendertype=abstract>.
- Lykissa E, Maharaj S. Platinum concentration and platinum oxidation states in body fluids, tissue, and explants from women exposed to silicone and saline breast implants. *J Long Term Eff Med Implants*. 2006;16(6):435-439. doi:10.1021/ac060759e
- Lykissa ED, Kala S V, Hurley JB, Lebovitz RM. Release of low molecular weight silicones and platinum from silicone breast implants. *Anal Chem*. 1997;69(23):4912-4916. doi:10.1021/ac97071ow
- Wang DG, Norwood W, Alaei M, Byer JD, Brimble S. Review of recent advances in research on the toxicity, detection, occurrence and fate of cyclic volatile methyl siloxanes in the environment. *Chemosphere*. 2013;93(5):711-725. doi:10.1016/j.chemosphere.2012.10.041
- Nanayakkara PWB, De Blok CJM. Silicone gel breast implants: What we know about safety after all these years. *Ann Intern Med*. 2016;164(3):199-200. doi:10.7326/M15-2427
- Levy Y, Ruhrman-Shahar N. The On-going Debate regarding Long-Term Safety of Silicone Breast Augmentation Rages. *Isr Med Assoc J*. 2016;18(12):754-755. doi:10.1177/000331979304400405
- de Boer M, van Leeuwen FE, Hauptmann M, et al. Breast Implants and the Risk of Anaplastic Large-Cell Lymphoma in the Breast. *JAMA Oncol*. January 2018. doi:10.1001/jamaoncol.2017.4510
- Maijers MC, de Blok CJM, Niessen FB, et al. Women with silicone breast implants and unexplained systemic symptoms: a descriptive cohort study. *Neth J Med*. 2013;71(10):534-540. <http://www.ncbi.nlm.nih.gov/pubmed/24394743>.
- Bachour Y, Verweij SP, Gibbs S, et al. The aetiopathogenesis of capsular contracture: A systematic review of the literature. *J Plast Reconstr Aesthetic Surg*. December 2017. doi:10.1016/j.bjps.2017.12.002
- Coroneos CJ, Selber JC, Offodile AC, Butler CE, Clemens MW. US FDA Breast Implant Postapproval Studies: Long-term Outcomes in 99,993 Patients. *Ann Surg*. 2019;269(1):30-36. doi:10.1097/SLA.0000000000002990
- Spear SL, Murphy DK. Natrelle Round Silicone Breast Implants. *Plast Reconstr Surg*. 2014;133(6):1354-1361. doi:10.1097/PRS.0000000000000021
- Cunningham B. The Mentor core study on silicone MemoryGel breast implants. *Plast Reconstr Surg*. 2007;120(7 SUPPL. 1):19-29. doi:10.1097/01.prs.0000286574.88752.04

19. Bachour Y, Bargon CA, de Blok CJM, Ket JCF, Ritt MJPF, Niessen FB. Risk factors for developing capsular contracture in women after breast implant surgery: A systematic review of the literature. *J Plast Reconstr Aesthetic Surg.* 2018;71(9):e29-e48. doi:10.1016/j.bjps.2018.05.022
20. Benediktsson K, Perbeck L. Capsular contracture around saline-filled and textured subcutaneously-placed implants in irradiated and non-irradiated breast cancer patients: Five years of monitoring of a prospective trial. *J Plast Reconstr Aesthetic Surg.* 2006;59(1):27-34. doi:10.1016/j.bjps.2005.08.005
21. Hillard C, Fowler JD, Barta R, Cunningham B. Silicone breast implant rupture: A review. *Gland Surg.* 2017;6(2):163-168. doi:10.21037/ggs.2016.09.12
22. Berry MG, Cucchiara V, Davies DM. Breast augmentation: Part II – adverse capsular contracture. *J Plast Reconstr Aesthetic Surg.* 2010;63(12):2098-2107. doi:10.1016/j.bjps.2010.04.011
23. Araco A, Caruso R, Araco F, Overton J, Gravante G. Capsular Contractures: A Systematic Review. *Plast Reconstr Surg.* 2009;124(6):1808-1819. doi:10.1097/PRS.obor13e3181bf7f26
24. Caffee HH. The influence of silicone bleed on capsule contracture. *Ann Plast Surg.* 1986;17(4):284-287. <http://www.ncbi.nlm.nih.gov/pubmed/3273107>.
25. Siggelkow W, Faridi A, Spiritus K, Klinge U, Rath W, Klosterhalfen B. Histological analysis of silicone breast implant capsules and correlation with capsular contracture. *Biomaterials.* 2003;24(6):1101-1109. doi:10.1016/S0142-9612(02)00429-5
26. Haasterecht L, Zada L, Schmidt RW, et al. Label-free stimulated Raman scattering imaging reveals silicone breast implant material in tissue. *J Biophotonics.* 2020;(November 2019):1-10. doi:10.1002/jbio.201960197
27. Kappel R., Boer LL, Dijkman H. Gel Bleed and Rupture of Silicone Breast Implants Investigated by Light-, Electron Microscopy and Energy Dispersive X-ray Analysis of Internal Organs and Nervous Tissue. *Clin Med Rev Case Reports.* 2016;3(1). doi:10.23937/2378-3656/1410087
28. de Bakker E, van den Broek LJ, Ritt MJPF, Gibbs S, Niessen FB. The Histological Composition of Capsular Contracture Focused on the Inner Layer of the Capsule: An Intra-Donor Baker-I Versus Baker-IV Comparison. *Aesthetic Plast Surg.* 2018;42(6):1485-1491. doi:10.1007/s00266-018-1211-1
29. Lee JM, Kim YJ. Foreign body granulomas after the use of dermal fillers: Pathophysiology, clinical appearance, histologic features, and treatment. *Arch Plast Surg.* 2015;42(2):232-239. doi:10.5999/aps.2015.42.2.232
30. FEDERA, COREON. *Human Tissue and Medical Research: Code of Conduct for Responsible Use.*; 2011. www.federa.org.
31. Moester MJ, Ariese F, De Boer JF. Optimized signal-to-noise ratio with shot noise limited detection in stimulated raman scattering microscopy. *J Eur Opt Soc.* 2015;10. doi:10.2971/jeos.2015.15022
32. Peng T, Thorn K, Schroeder T, et al. A BaSiC tool for background and shading correction of optical microscopy images. *Nat Commun.* 2017;8:1-7. doi:10.1038/ncomms14836
33. Bankhead P, Loughrey MB, Fernández JA, et al. QuPath: Open source software for digital pathology image analysis. *Sci Rep.* 2017;7(1):16878. doi:10.1038/s41598-017-17204-5
34. Fowler MR, Nathan CAO, Abreo F. Synovial metaplasia, a specialized form of repair: A case report and review of the literature. *Arch Pathol Lab Med.* 2002;126(6):727-730. doi:10.1043/0003-9985(2002)126<0727:SMASFO>2.0.CO;2
35. Moyer HR, Ghazi BH, Losken A. The effect of silicone gel bleed on capsular contracture: A generational study. *Plast Reconstr Surg.* 2012;130(4):793-800. doi:10.1097/PRS.obor13e318262f174
36. Hölmich LR, Vejborg IM, Conrad C, et al. Untreated silicone breast implant rupture. *Plast Reconstr Surg.* 2004;114(1):204-214. doi:10.1097/01.PRS.0000128821.87939.B5
37. Joseph J, Mohanty M, Mohanan P V. Role of immune cells and inflammatory cytokines in regulation of fibrosis around silicone expander implants. *J Mater Sci Mater Med.* 2010;21(5):1665-1676. doi:10.1007/s10856-010-4015-7

38. Potter EH, Rohrich RJ, Bolden KM. The Role of Silicone Granulomas in Recurrent Capsular Contracture. *Plast Reconstr Surg.* 2013;131(6):888e-895e. doi:10.1097/PRS.0b013e31828bd642
39. Kamel M, Protzner K, Fornasier V, Peters W, Smith D, Ibanez D. The peri-implant breast capsule: An immunophenotypic study of capsules taken at explantation surgery. *J Biomed Mater Res.* 2001;58(1):88-96. doi:10.1002/1097-4636(2001)58:1<88::AID-JBM130>3.0.CO;2-7
40. Bui JM, Perry T, Ren CD, Nofrey B, Teitelbaum S, Van Epps DE. Histological characterization of human breast implant capsules. *Aesthetic Plast Surg.* 2015;39(3):306-315. doi:10.1007/s00266-014-0439-7
41. Luke JL, Kalasinsky VF, Turnicky RP, Centeno JA, Johnson FB, Mullick FG. Pathological and biophysical findings associated with silicone breast implants: a study of capsular tissues from 86 cases. *Plast Reconstr Surg.* 1997;100(6):1558-1565. doi:10.1097/00006534-199711000-00029
42. Prantl L, Schreml S, Fichtner-Feigl S, et al. Clinical and morphological conditions in capsular contracture formed around silicone breast implants. *Plast Reconstr Surg.* 2007;120(1):275-284. doi:10.1097/01.prs.0000264398.85652.9a
43. Kastellorizios M, Tipnis N, Burgess DJ. Foreign Body Reaction to Subcutaneous Implants. *Adv Exp Med Biol.* 2015;865:93-108. doi:10.1007/978-3-319-18603-0_6
44. de Bakker E, Rots M, Buncamper ME, et al. The Baker Classification for Capsular Contracture in Breast Implant Surgery Is Unreliable as a Diagnostic Tool. *Plast Reconstr Surg.* 2020;146(5):956-962. doi:10.1097/PRS.0000000000007238
45. O'Toole M, Caskey CI. Imaging spectrum of breast implant complications: Mammography, ultrasound, and magnetic resonance imaging. *Semin Ultrasound CT MRI.* 2000;21(5):351-361. doi:10.1016/S0887-2171(00)90029-5
46. Zahavi A, Sklair ML, Ad-El DD. Capsular contracture of the breast: Working towards a better classification using clinical and radiologic assessment. *Ann Plast Surg.* 2006;57(3):248-251. doi:10.1097/01.sap.0000221614.32176.9a
47. Breast Implant Removal | American Society of Plastic Surgeons. <https://www.plasticsurgery.org/cosmetic-procedures/breast-implant-removal>. Accessed October 18, 2020.
48. Headon H, Kasem A, Mokbel K. Capsular contracture after breast augmentation: An update for clinical practice. *Arch Plast Surg.* 2015;42(5):532-543. doi:10.5999/aps.2015.42.5.532
49. Schnur PL, Weinzweig J, Harris JB, et al. Silicon Analysis of Breast and Periprosthetic Capsular Tissue from Patients with Saline or Silicone Gel Breast Implants. *Plast Reconstr Surg.* 1996;98(5):798-803. doi:10.1097/00006534-199610000-00007

6

**The Baker classification for capsular contracture
in breast implant surgery is unreliable as a
diagnostic tool**

E. de Bakker

M. Rots

M.E. Buncamper

F.B. Niessen

J.M. Smit

H.A.H. Winters

M. Özer

H.C.W. de Vet

M.G. Mullender

Background

Breast implants are frequently used in cosmetic and reconstructive breast surgery. Capsular contracture, the most common long-term complication, is usually graded using the Baker classification. Despite its widespread use, its reliability has never been established. The aim of this study was to determine the inter-observer reliability and agreement of the Baker classification.

Methods

Sixty women who had undergone cosmetic breast augmentation were included. They were examined independently by two plastic surgeons from an observer pool. The Baker score was determined, as well as firmness, dislocation, symmetry and pain using four-point scales. Patients were asked to complete the BREAST-Q post-augmentation module. The inter-observer reliability and agreement were calculated for all variables with a quadratic weighted Kappa.

Results

The inter-observer reliability of the Baker classification was poor (kappa: 0.55; 95% CI 0.37-0.72). Inter-observer reliability of the clinical parameters firmness (0.64; 95%CI 0.49-0.79), dislocation (0.49; 95%CI 0.26-0.73) and symmetry (0.61; 95%CI 0.34-0.88) were also poor. Pain scores seemed more reliable (0.72; 95%CI 0.56-0.89), however, most patients had no pain. The inter-observer agreement for the Baker score was 48%, in 43% the observers differed one category. In 12% the difference was more than one category.

Conclusions

Inter-observer reliability and observer agreement of the Baker classification for capsular contracture were poor. Consensus about how to adequately rate the symptoms of capsular complaints is lacking. A more reliable method of measurement or description is needed, especially for scientific research purposes, to assess the long term problems associated with breast implants.

INTRODUCTION

Breast augmentation using implants is one of the most frequently performed cosmetic surgeries. Furthermore, the most used method of breast reconstruction is implant-based. In the Netherlands, about 3.3% of women have breast implants. Between 2015-2017, approximately 11 of the 60 thousand inserted breast implants, or 25% of the procedures were for reconstructive purposes in the Netherlands. Capsular contracture (CC) is reported as a common long-term complication associated with breast implants and is usually the primary reason for reoperation¹. Reported incidences range from 0.6 to 17.4% for primary augmentations and 21.1 to 47.7% for breast reconstructions². Additionally, revision surgery in both groups is reported to result in a higher incidence of CC².

After implantation of any implant, a host response is evoked, resulting in the formation of a fibrotic capsule around the prosthesis. This is part of a normal foreign body response. Normally, the fibrous tissue remains thin and supple and most patients do not experience any complaints. However, in an adverse course, the capsule may thicken, tighten or even contract. The type of implant, surgical technique, low-grade infection, and postoperative radiotherapy are factors described to be associated with capsular problems². Clinically, these capsular changes can cause hardening of the breast or even deformation and may result in implant dislocation and asymmetry of the breasts. Some patients may experience tenderness or pain. The symptoms can occur in isolation or in any combination. Additionally, they can present at various timeframes after surgery and can progress at different rates. In other words, the presentation of capsular related complaints is very heterogeneous.

With the increasing popularity of breast implants over the last decennia, the number of patients with complaints attributed to pathological changes in the fibrous capsule has increased progressively. In medical literature, the concept of 'capsular contracture' is used as a generic term for the collation of capsule related complaints. With the recognition of these capsular problems related to breast implants, attempts were made to classify CC with regard to the severity of the symptoms. In 1978 Baker introduced a clinical classification

of CC for the first time. His original classification is still the most widely used and generally accepted³. It uses a four-point scale ranging from grade I (natural) to grade IV (severe contracture) (Table 1a). Notably, the scale does not specify how this contracture presents. The classification was later modified by Spear and Baker to accommodate for the reconstructed breast by adding sublevels I-A and I-B⁴. The Baker score is used in research settings to report incidence rates of CC in studies on the performance of implants or surgical techniques⁵⁻⁷, and it is used in more fundamental research in which clinical data (Baker scores) are correlated with biomedical data (e.g. histology, immunologic data)⁸. The classification is frequently used for clinical diagnoses in individual patients. In the Netherlands, reimbursement even depends on this classification; the CC should be classified as severe with a Baker-IV score in order to obtain (partial) reimbursement by the health insurers for surgical treatment. Pain is one of the factors deemed necessary for this reimbursement. While pain was not originally included in the Baker classification, pain has found its way into various published versions of the Baker classification published in journals and online (Table 1b). It is unclear when pain exactly appeared in the classification. Since pain can be found in multiple versions of the Baker classification, it seems that many authors consider pain to be essential to grade CC. Yet, it is remarkable that so many different versions of one classification exist.

In spite of its wide use, the reliability of the Baker classification has not yet been established. The aim of this study, therefore, was to determine the reliability of the Baker classification by determining the interobserver reliability and observer agreement of the Baker classification. In addition, the interobserver reliability of rating the separate clinical symptoms associated with CC was determined.

Table 1a: Baker classification of capsular contracture after augmentation mammoplasty

Class I	Breast absolutely natural, no one could tell breast was augmented
Class II	Minimal contracture; I can tell surgery was performed, but patient has no complaint
Class III	Moderate contracture; patient feels some firmness
Class IV	Severe contracture; obvious just from observation

Table 1b: The Baker classification as presented in various media

Grading of capsular contracture *	
Grade 1:	Grade one capsular contracture is asymptomatic (producing or showing no symptoms). The formation of scar tissue around the implant does not interfere with the size, shape or texture of the breasts. The breasts look natural and remain soft to the touch.
Grade 2:	Grade two capsular contracture usually presents itself with only minor cosmetic symptoms. The breasts will usually appear normal in shape but feel somewhat firm to the touch.
Grade 3:	Grade three capsular contracture presents itself with obvious cosmetic symptoms. The breasts will be firm to the touch and appear abnormal, e.g., they will be overly round, hard-looking and the nipples may be misshapen. However, this grade of capsular contraction often doesn't cause much (if any) pain.
Grade 4:	Like grade three capsular contracture, grade four capsular contracture causes the breasts to become hard and misshapen. Patients with grade four capsular contracture also experience breast soreness; their breasts will often be tender and painful to the touch
Baker classification **	Baker classified capsular contracture: ***
I soft	Grade I the augmented breast feels as soft as an unoperated one.
II minimal, implant palpable, not visible	Grade II minimal—implant palpable, but not visible.
III moderate, palpable and visible	Grade III moderate—implant easily palpable, and it (or distortion from it) is visible.
IV sever, hard, painful with distortion	Grade IV severe—the breast is hard, tender, painful and cold. Distortion is often marked

*Different Baker classifications from various sources, showing a large heterogeneity and discrepancy with the original classification; * from the website of the American Society of Plastic Surgeons¹², ** from the a-z of plastic surgery¹⁴, *** from Key Notes on Plastic Surgery: Second Edition¹³.*

PATIENTS AND METHODS

Study population

This was a cross-sectional observational multi-center study. Women who had undergone breast augmentation surgery >5 years prior to inclusion and without a history of breast malignancy were eligible to participate in this study. The protocol was approved by the institutional review board at each study center. All patients provided written informed consent. The study was performed in accordance with the Declaration of Helsinki and guidelines for Good Clinical Practice.

Study procedure

Eligible patients were recruited via two routes: 1) patients who underwent breast augmentation >5 years previously were identified from the hospital records and invited by phone to partake, 2) eligible patients who visited the outpatient clinic visit for complaints related to the breast implant were asked to participate. After providing informed consent patients were invited to the outpatient clinic.

Seven plastic surgeons with ample experience in breast surgery and who use the Baker classification in daily practice were asked to participate in the observer pool. Plastic surgeons were handed out the official Baker classification on paper and were instructed to classify CC as they would do in clinical practice. At the clinic, the patient's breasts were examined independently by two surgeons from the pool of observers. Breasts were scored according to the Baker classification and separately scored for the symptoms associated with CC. Patients were also asked to complete a questionnaire pertaining to the post-augmentation quality of life, the Dutch version of the BREAST-Q post-augmentation module. The BREAST-Q is a comprehensive patient-reported outcome measure (PROM), which evaluates satisfaction with breasts and impact on quality of life. It includes questions about symptoms, appearance and satisfaction. It specifically asks for visible and sensible complaints about softness of the implants and pain.

Outcomes

The main outcome was the Baker classification for capsular contraction (Table 1a). Additional outcomes were a) firmness of the breast, b) dislocation of the implant, c) pain and d) symmetry. Each of these outcomes was scored using a 4-point Likert scale for the left and right breast separately, except for d) symmetry, which was scored comparing both breasts. For each of these measures, the inter-observer reliability and the observer agreements were determined. A summed score of the items a)+b)+c) was used to test the intra-observer validity by correlating the Baker score with this summed score.

Additional outcomes were demographic data (age, date of augmentation and if applicable revision surgery and implant type and size) and patient-reported outcomes (BREAST-Q post-augmentation module).

Statistical analysis

A minimal sample size of 50 patients was estimated. This was based on a repeated measurement with two independent observers and a desired 95% confidence interval of 0.1 for an intraclass correlation coefficient (ICC) of 0.8⁹. To establish a safe margin, a target sample size of 60 participants was decided on. Descriptive statistics were used for all variables. Inter-observer reliability was determined by calculating the weighted kappa scores for the Baker classification and the individual clinical parameters using a quadratic weighting with VassarStats online statistical software¹⁰. For the cumulative clinical parameter scores, the intraclass correlation coefficient (ICC) based on one-way ANOVA was calculated¹¹. Observer agreement was calculated for all parameters which were rated using a 4-point scale. To correlate observer and patient opinion, Pearson correlation coefficients were calculated between observer scores (Baker score and the summed item score) and PROMs (Breast-Q post-augmentation module domains and question 1h which specifically asks for symmetry). All statistics were calculated using SPSS (IBM SPSS Statistics for Windows, Version 22.0).

RESULTS

Patient characteristics

Between 2017 and 2018, 60 patients were included in this cross-sectional study. Relevant patient characteristics are shown in Table 2. Nearly all (n=55, 92%) patients had received some type of silicone implant, the others had received Monobloc implants, with a silicone shell and hydrogel filling. Sixteen patients (27%) did not know what their implant size was. Three women had undergone one-sided augmentation, symmetry was not evaluated in those cases. Out of all patients, 35% had already undergone revision surgery, 13% more than once (Table 2).

Table 2: Patient characteristics (n=60)

Age (years)	mean (SD)	49 (11)
Type of prosthesis		
Silicone	n (%)	55 (92)
Other (monobloc)	n (%)	5 (8)
Size in cc (n=44, 73%)	mean (SD)	307 (88)
One-sided augmentation	n (%)	3 (1.6)
Revision surgery	n (%)	21 (35)
More than once	n (%)	8 (13)

SD = standard deviation, cc = cubic centimeter

Baker score and separate symptom scores

An overview of the distribution of all scored parameters on the used 4-point Likert scales is given in Figure 1. Baker score, firmness, dislocation, and pain were scored per breast while symmetry was scored based on both. For all parameters, data are skewed, with a higher prevalence for lower symptomatic values. This was especially true for pain, which was scored 166 times as I (no pain) and only 6 times as IV (much pain).

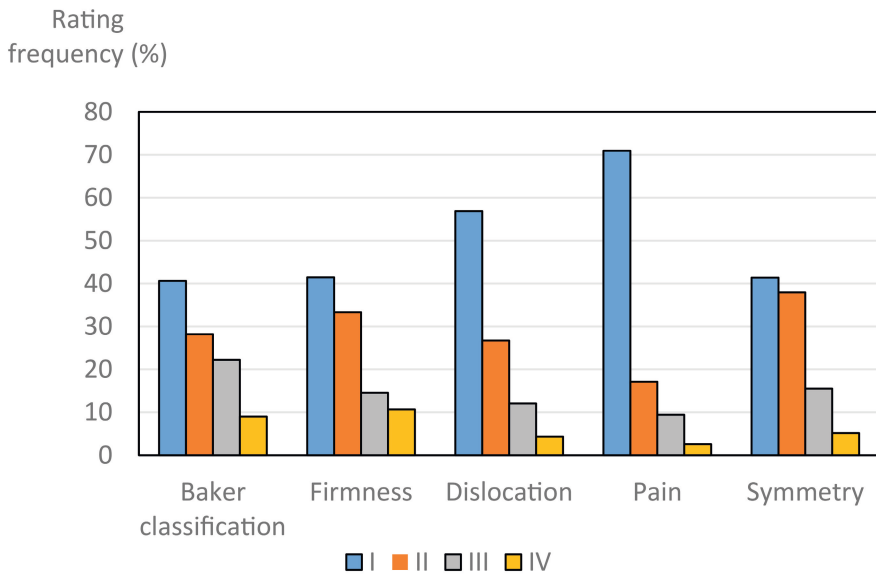


Figure 1: distribution of scored characteristics

Distribution of scored characteristics by all observers. Each breast was scored for all parameters except symmetry which was based on both breasts. It shows a skewed distribution towards fewer symptoms for most women.

Inter-observer agreement and reliability and intra-observer validity.

Inter-observer reliability and observer agreement are presented in Table 3 for all parameters. For the Baker score, the inter-observer reliability is rather low (Kappa = 0.55). The observer agreement is also low, with the same score given in only 48% of breasts. In 41% of cases, observers differ by one category while in 11% of cases they differ by two or more categories. Similar outcomes are found for the individual symptoms. The highest agreement is met when rating pain. However, it should be noted that 64% of cases this agreement was reached on having no pain (scoring I by both observers). From the BREAST-Q, domains 1 (satisfaction with breasts) and 5 (physical well-being) correlated weakly to moderately with the given Baker scores and the cumulative clinical parameter score (Pearson r between 0.295 and 0.393, Table 4). The symmetry parameter correlated weakly (Pearson $r = -0.223$) with question 1H of the BREAST-Q, which specifically asks the patient to evaluate the symmetry of her breasts. There was

a good correlation between the cumulative scores and the Baker score given by the same observer (Pearson $r = 0.84$), indicating that the intra-observer rating of CC is consistent.

Table 3: Inter-observer reliability and observer agreement. Observer agreement indicates the percentage of cases in which observers rate equally, observer agreement ± 1 indicates the percentage of cases in which there is maximally one level difference between observers.

	Inter-observer reliability			Observer Agreement	Observer Agreement ± 1
	kappa	(95% CI)			
Baker	0.55	(0.37,	0.72)	48%	89%
a) Firmness	0.64	(0.49,	0.79)	55%	92%
b) Dislocation	0.49	(0.26,	0.73)	61%	91%
c) Pain	0.72	(0.56,	0.89)	75%	97%
Symmetry	0.61	(0.34,	0.88)	52%	97%
	ICC	(95% CI)			
Summed Item Score (a+b+c)	0.72	(0.62,	0.80)		

All kappa values were calculated using quadratic weighting.

ICC = intra class correlation coefficient; CI = confidence interval.

Table 4: correlation of Baker score with BreastQ

	BreastQ1 (p)	BreastQ5 (p)	BreastQ1h (p)
Baker score (average all observers)	-0.295 (0.001)	-0.368 (0.000)	
Cumulative score (average all observers)	-0.393 (0.000)	-0.324 (0.000)	
Symmetry (average all observers)			-0.223 (0.017)

Pearson correlation coefficients with (p) between Baker and cumulative clinical parameter scores given and the BREAST-Q, domains 1 (satisfaction with breasts) and 5 (physical well-being), and between the observed symmetry and question 1h of the BREAST-Q which specifically asks for symmetry.

DISCUSSION

This study aimed to assess the inter-observer reliability of the Baker classification for capsular contracture, a well-established tool for grading CC in clinical practice as well as in research. We found that the inter-observer reliability was quite poor, as was the inter-observer agreement. In the majority of cases, the given Baker classification differed between the two observers and in 11% even more than one level.

The diverse presentation of (local) problems associated with breast implants is well-known by all plastic surgeons dealing with these implants. Most of these problems are collectively referred to as CC and graded using the Baker classification. Although widely accepted, the Baker classification is inconsistently defined in both reference works and in scientific literature^{3,12-14}. Several other methods and classifications have been proposed over the years. All, excluding applanation tonometry, are four-point Likert scales similar to the Baker classification, with similar generic descriptions¹⁵⁻¹⁸. The reliability of these classifications has not been assessed, nor have they gained broad support. Applanation tonometry is used in various studies to evaluate breast soft- or hardness and could be used to measure that one aspect of capsular related complaints more reliably. It has gained limited usage in daily clinical practice and has been described as unreliable when comparing differently shaped implants, which would severely limit its use in daily clinical practice^{19,20}.

It may be expected that grading the severity of problems with a very diverse presentation, on a single ordinal scale, poses a challenge. This was shown to be the case. To address this challenge, plastic surgeons in this study were also asked to separately grade the main symptoms associated with CC; firmness, dislocation pain and asymmetry. Remarkably, rating these specific symptoms by plastic surgeons also proved unreliable. Although there is a notion among plastic surgeons of the concept of CC and its symptoms, these ideas do not seem to match. Within the individual surgeon, a consistent rating of symptoms and the Baker score exists, but between surgeons, it seems that no consensus exists on what “firmness” or “dislocation” exactly are, or when either of those

symptoms are mild, severe or normal. In order to categorize these symptoms reliably, we need to reach consensus on the interpretation of symptoms. This may be achieved by describing these symptoms in more detail. We propose to describe the symptoms of (local) breast implant-related complaints separately, using a more qualitative approach. We suggest that using more qualitative descriptions will result in clearer communication and better comparability.

This qualitative approach should include and discriminate between physical findings such as firmness, dislocation and symmetry and experienced symptoms like pain or tenderness. We propose to refer to these complaints as ‘breast implant-related complaints’. We purposefully use the term ‘breast implant-related complaints’, because the presence of actual capsular abnormalities can only be established by operating the breast.

In order to improve the assessment of implant-related complaints, it is important to bear in mind the purpose of the classification. The Baker classification is broadly used for two main purposes: clinical and scientific. First and foremost it is used by health care professionals in clinical practice; i.e. to assess capsular complaints in individual patients, decide whether intervention surgery is necessary, and to exchange this information between colleagues. A clearer definition of symptoms may be helpful, especially with regard to communication between healthcare professionals. Yet, intervention remains a very personal preference for both patient and surgeon and depends on many factors. Therefore, we propose to refrain from labeling a certain grade as an indication for surgery.

Secondly, the Baker classification is used in scientific research. Many studies aim to compare different surgical methods or implant materials in breast implant procedures with regard to their long-term complication rate. When the measurement of CC is unreliable, this poses a major problem. For this purpose, a more reliable way of describing the presence and severity of the collation of problems associated with CC is warranted. Our expectation is that better definitions and more consensus on how these symptoms are described and classified, will improve reliability. Future exploratory studies are necessary to prove this. For scientific research, in particular, it is necessary that each study

describes the classification they used to conduct their research in detail and to use multiple observers.

The main reason why the Baker classification has become so popular is probably because it is simple. In creating a new method of classifying breast implant-related complaints a choice will have to be made between a more simple, clinical oriented classification, or a more extensive, descriptive classification. In both cases, a clear consensus and instructions are needed to improve reliability. The more descriptive measure will probably be more complex, needing more training and consensus to achieve good reproducibility. The latter is could, therefore, be less applicable in daily clinical practice.

This study has several strengths and limitations. In this study, no extensive instruction on grading using the Baker classification was given beforehand. All participating surgeons were familiar with the classification and use it in daily practice. In the study setup, it was decided to conduct the scoring as it is being performed in normal practice. Surgeons will have used the classification as they have been taught, possibly influenced by their personal experience since then. Providing extensive instructions might, therefore, improve the agreement. Not all grades of the Baker classification were equally represented in the population. In our population, women with no/few symptoms were overrepresented. Although this is a representation of the prevalence of CC, for the sake of assessing reliability a less skewed distribution might have been preferable. Each patient was rated by two observers from a pool of seven observers. Therefore, we cannot assess whether systematic differences existed between the observers. On the other hand, multiple observers mimic clinical practice and the results are more representative of all plastic surgeons than if only two observers had rated all patients.

CONCLUSIONS

In conclusion, the inter-observer reliability of the Baker classification for capsular contracture is poor. Although there is a general notion of what capsular complaints are (i.e. dislocation, firmness, asymmetry and pain), individual plastic surgeons have different interpretations about what these symptoms entail and how to grade their severity. A more reliable method of measurement or description is needed, especially for scientific research purposes.

REFERENCES

1. Handel N, Cordray T, Gutierrez J, Jensen JA, Arthur Jensen J. A Long-Term Study of Outcomes, Complications, and Patient Satisfaction with Breast Implants. *Plast Reconstr Surg.* 2006;117(3):757-767; discussion 768-72. doi:10.1097/01.prs.0000201457.00772.1d
2. Bachour Y, Bargon CA, de Blok CJM, Ket JCF, Ritt MJPF, Niessen FB. Risk factors for developing capsular contracture in women after breast implant surgery: A systematic review of the literature. *J Plast Reconstr Aesthetic Surg.* 2018;71(9):e29-e48. doi:10.1016/j.bjps.2018.05.022
3. Baker JL J. Augmentation mammoplasty. In: JQ Owsley RP, ed. *Symposium on Aesthetic Surgery of the Breast.* St Louis: Mosby. ; 1978:256.
4. Spear SL, Baker JL. Classification of capsular contracture after prosthetic breast reconstruction. *Plast Reconstr Surg.* 1995;96(5):1119-1123; discussion 1124. doi:10.1097/00006534-199510000-00019
5. Marques M, Brown S a, Oliveira I, et al. Long-term follow-up of breast capsule contracture rates in cosmetic and reconstructive cases. *Plast Reconstr Surg.* 2010;126(3):769-778. doi:10.1097/PRS.0b013e3181e5f7bf
6. Collis N, Coleman D, Foo IT, Sharpe DT. Ten-year review of a prospective randomized controlled trial of textured versus smooth subglandular silicone gel breast implants. *Plast Reconstr Surg.* 2000;106(4):786-791. doi:10.1097/00006534-200009040-00005
7. Spear SL, Murphy DK. Natrelle Round Silicone Breast Implants. *Plast Reconstr Surg.* 2014;133(6):1354-1361. doi:10.1097/PRS.000000000000021
8. Kamel M, Protzner K, Fornasier V, Peters W, Smith D, Ibanez D. The peri-implant breast capsule: An immunophenotypic study of capsules taken at explantation surgery. *J Biomed Mater Res.* 2001;58(1):88-96. doi:10.1002/1097-4636(2001)58:1<88::AID-JBM130>3.0.CO;2-7
9. de Vet HCW, Terwee CB, Mokkink LB, Knol DL. *Measurement in Medicine.* Cambridge: Cambridge University Press; 2011. doi:10.1017/CBO9780511996214
10. Richard Lowry. VassarStats statistical website. <http://vassarstats.net/kappa.html>.
11. Shrout PE, Fleiss JL. Intraclass correlations: Uses in assessing rater reliability. *Psychol Bull.* 1979;86(2):420-428. doi:10.1037/0033-2909.86.2.420
12. Tehrani K. What is capsular contracture and how can it be treated? <https://www.plasticsurgery.org/news/blog/what-is-capsular-contracture-and-how-can-it-be-treated>. Published 2018. Accessed July 23, 2019.
13. Richards A, Dafydd H. *Key Notes on Plastic Surgery.* Chichester, UK: John Wiley & Sons, Ltd; 2014. doi:10.1002/9781118757017
14. Hodges A. *A-Z of Plastic Surgery.* Oxford University Press; 2008. doi:10.1093/acref/9780199546572.001.0001
15. Berry MG, Cucchiara V, Davies DM. Breast augmentation: Part II - Adverse capsular contracture. *J Plast Reconstr Aesthetic Surg.* 2010;63(12):2098-2107. doi:10.1016/j.bjps.2010.04.011
16. Shapiro MA. Smooth vs. rough: an 8-year survey of mammary prostheses. *Plast Reconstr Surg.* 1989;84(3):449-457. <http://www.ncbi.nlm.nih.gov/pubmed/12762403>.
17. Gylbert L, Asplund O, Jurell G, Olenius M. Results of subglandular breast augmentation using a new classification method-18-year follow-UP. *Scand J Plast Reconstr Surg Hand Surg.* 1989;23(2):133-136. doi:10.3109/02844318909004505
18. Gylbert LO. Applanation tonometry for the evaluation of breast compressibility. *Scand J Plast Reconstr Surg Hand Surg.* 1989;23(3):223-229. doi:10.3109/02844318909075122
19. Edsander-Nord Å, Björklund T, Jurell G, Wickman M. Objective evaluation of two differently-shaped permanent expander prostheses used for breast reconstruction. *Scand J Plast Reconstr Surg Hand Surg.* 2004;38(4):204-208. doi:10.1080/02844310410027220
20. Gylbert L, Berggren A. Constant compression caliper for objective measurement of breast capsular contracture. *Scand J Plast Reconstr Surg Hand Surg.* 1989;23(2):137-142. doi:10.3109/02844318909004506

7

**Prognostic tools for hypertrophic scar formation
based on fundamental differences in systemic
immunity**

A prospective observational cohort study

E. de Bakker

M.A.M. van der Putten

M.W. Heymans

S.W. Spiekstra

T. Waaijman

L. Butzelaar

V.L. Negenborn

V.K. Beekman

E.O. Akpınar

T. Rustemeyer

F.B. Niessen

Unpredictable hypertrophic scarring (HS) occurs after approximately 35% of all surgical procedures and causes significant physical and psychological complaints. Parallel to the need to understanding the mechanisms underlying HS formation, a prognostic tool is needed.

The objective was to determine whether (systemic) immunological differences exist between patients who develop HS and those who develop normotrophic scars (NS) and to assess whether those differences can be used to identify patients prone to developing HS.

A prospective cohort study with NS and HS groups in which i) cytokine release by peripheral blood mononuclear cells (PBMC) and ii) the irritation threshold (IT) after an irritant (sodium lauryl sulphate) patch test was evaluated.

Univariate regression analysis of PBMC cytokine secretion showed that low MCP-1, IL-8, IL-18 and IL-23 levels have a strong correlation with HS ($p < 0.010$ - 0.004 ; AUC = 0.790 - 0.883). Notably, combinations of two or three cytokines (TNF- α , MCP-1 and IL-23; AUC: 0.942 , Nagelkerke R^2 : 0.727) showed an improved AUC indicating a better correlation with HS than single cytokine analysis. These combination models produce good prognostic results over a broad probability range (sensitivity: 93.8%, specificity 86.7%, accuracy 90.25% between probability 0.3 and 0.7). Furthermore, the HS group had a lower IT than the NS group and an accuracy of 68%.

In conclusion, very fundamental immunological differences exist between individuals who develop HS and those who do not. Whereas the cytokine assay forms the basis of a predictive prognostic test for HS formation, the less invasive, easily performed irritant skin patch test is more accessible for daily practice.

Trial registration <https://www.toetsingonline.nl>, number NL40722.029.13

Key Words: skin, wound healing, inflammation, cytokine, prognostic

INTRODUCTION

Hypertrophic scarring is one of the most common complications of all surgeries. It is estimated that about 35% of surgical skin wounds heal with a hypertrophic scar (HS)¹. Patients often experience a loss of quality of life due to physical or psychological complaints, especially when the scar is positioned over a joint^{2,3}. Hypertrophic scarring is defined as a scar raised above the skin level because of excessive collagen deposition resulting in a scar that is thick, non-pliable, itchy and painful⁴. As opposed to a keloid, a hypertrophic scar remains within the confines of the wound. It is thought that the pathological mechanisms of these aberrant scars differ, subsequently the way they are managed also differs^{3,5-8}. Much research has been focussed on discovering the pathophysiology of these scars and treatment modalities. Parallel to the need to know the processes underlying HS formation, there is a need for a prognostic tool. This would have great value in the clinic, as an early start of treatment is preferred in HS⁶. Being able to predict who is at risk to develop HS before going into surgery can help to prevent significant patient comorbidity and loss of quality of life as well as enabling better expectation management. In the case of elective, and in particular aesthetic surgery, patients and surgeons might choose to opt-out of surgery when the benefit of the concerned procedure does not outweigh the chance of developing HS.

Many risk factors, like wound location, tension and mechanical loading, young age and bacterial colonization, have been identified for the development of HS^{3,8-10}. However, it is still unknown why one individual will develop an HS after surgery whereas another will not^{7,9}. The immune system is increasingly seen as essential in answering the questions surrounding HS formation¹¹. HS formation is associated with increased numbers of inflammatory cells like mast cells and epidermal Langerhans cells and increased levels of cytokines like IL-4^{7,12,13}. Lower levels of cytokines within the wound and scar area, such as IL-1 α , IL-6, IL-8, and CXCL-8 suggest a reduced inflammatory response may be responsible^{14,15}. Considering the pivotal role of blood-derived mononuclear cells (e.g. monocytes and lymphocytes) in regulating the early inflammatory

phase once these cells infiltrate the wound bed^{13,16}, a systemic origin of the early immunological differences between normal scars (NS) and HS should be considered. Such a difference would provide both prognostic markers and targets for the development of therapeutic agents.

Notably, many of the cytokines which are regulated in the skin during HS formation are also released during skin irritation, which can be seen as microtrauma^{15,17}. Skin irritation, and thus the induction of an innate immune response, can easily be tested by determining the irritation threshold (IT) of a topically applied substance. It has been described that a range of ITs exists within a group of people with regards to their responsiveness to topically applied sodium lauryl sulphate (SLS) in a patch test¹⁸. Therefore, assuming a different (early) immune response between NS and HS formers, it would seem logical to hypothesize that the IT could be a discriminating factor between these two groups as well, and it could then subsequently be used as a predictive tool. Determining the skin IT by means of a patch test with an irritant is a non-invasive, easily applicable test with low intra-individual variation^{19,20}.

Considering this background, a prospective cohort study was performed with both an NS and HS group in which both the IT after an irritant SLS patch test and cytokine release by peripheral blood mononuclear cells (PBMC) were evaluated. Furthermore, transepidermal water loss (TEWL) and cytokines present within stratum corneum tape strips obtained from the patch test sites were assessed. Cytokine bead-based immunoassays for analysing samples were chosen after considering which cytokines would be expected to be secreted from PBMCs and which may be expected to be detectable from stratum corneum tape strips. As an example, this was based on our previous research where we showed that MCP-1 is only secreted at very low levels by epidermal keratinocytes but was secreted in high levels by monocytes²¹. This study aimed to determine whether (systemic) immunological differences exist between patients who develop HS and those who develop normotrophic scars (NS) and to assess whether those differences can be used to identify patients prone to developing HS.

MATERIALS & METHODS

Patient inclusion

Between 2014 and 2016, 31 patients were included in this prospective observational cohort study (see flow-chart depicting the inclusion, supplement figure 1). This study was performed in accordance with the Declaration of Helsinki and the guidelines for Good Clinical Practice. The independent medical ethics review boards of the participating hospitals approved the study protocol (<https://www.toetsingonline.nl>, number NL40722.029.13). Written informed consent was obtained from all participants. All patients volunteered to participate in this study and were healthy, adult females who had undergone reduction mammoplasty more than 5 months (average 11 months) prior to inclusion. The mammoplasty scars were evaluated in this study. Patients were excluded if their skin type, skin condition, medical treatment or unwillingness to adhere to life rules during the study would impede the results of patch testing (table 1a). After physical examination by an experienced plastic surgeon (FBN) the volunteers were divided into an NS group and an HS group, assigned a patient number for subsequent anonymized (blinded; not performed by FBN) data processing of IT, peripheral blood and TEWL, and baseline characteristics were collected (table 1b). Scars were scored normotrophic if they were flat at the level of the surrounding tissue and coloured like the surrounding tissue. Scars were considered hypertrophic when red and raised at least 2 mm above the skin level. All mammoplasty procedures were performed in a standard fashion. The surgical wounds were closed in layers with the cutaneous closure using absorbable intra-cutaneous suture material.

Table 1.

a. Exclusion criteria & Life rules			
Fitzpatrick photo skin type V and VI			
Skin disease, e.g. psoriasis, pemphigus vulgaris etc.			
Skin lesions, tattoos or substantial hair growth patch test site			
NS group: thickening of scars at any time after surgery			
Pregnancy/lactation during the first two years post-operatively or the patch test			
Topical immunosuppressive treatment of the upper arm in the last 7 days before the patch test			
Application of skin lotions/ointments on the upper arm in the last 6 weeks before the patch test			
Considerable exposure of the upper arm to UVR in the last 14 days before the patch test			
Systemic antibiotic treatment in the last 2 week before patch test			
Systemic immunosuppressive treatment during the first two years after surgery or in the last 6 months before the patch test			
Immunological disorders: infectious disease, immune deficiencies, auto-immune disorders			
Alcohol or drug abuse			
Smoking during the first two post-operative years			
ASA classification 3 or higher			
Participation in another clinical study			
Performing physical activities which cause heavy sweating, sauna, swimming or extreme showers or baths during the study			
b. Patient characteristics			
	NS (n=15)	HS (n=16)	
Age (years)		50 (10)	48 (8)
BMI (kg/m ²)		25.5 (3.3)	27.7 (4.0)
HS at other site		1/15	2/16
Atopic		67%	75%
Past smoker		42%	40%
Fitzpatrick skin type	I	0	1
	II	6	5
	III	6	6
	IV	3	4
	V	0	0
	VI	0	0

Table 1. Continued

c. Visual grading scale for irritation	
Score	Irritation reaction
0	No visible reaction
1	Tobacco paper-like appearance, no erythema
2	Slight patchy erythema
3	Homogeneous erythema
4	Erythema with oedema
5	Erythema, oedema and vesicles/bulla

a) exclusion criteria and life rules. b) Patient characteristics at inclusion. Mean or percentage \pm SD (standard deviation) is shown. c) Visual grading scale for irritation adopted from Basketter et al²³.

Cytokine secretion profile of peripheral blood mononuclear cells

Peripheral blood mononuclear cells (PBMC) were isolated from blood collected at inclusion using Lymphoprep[™] (Stemcell Technologies; Cambridge, UK) according to manufacturers' instructions. Cells were frozen in liquid nitrogen until use. PBMC were thawed and cultured in Iscove's Modified Dulbecco's Medium (IMDM) with 1 % penicillin/streptomycin; 1 % glutamine (100 mM) and 5 mM B-mercaptoethanol at 37° Celsius at 5 % CO₂. In a 96 well plate 2 x¹⁰⁵ PBMC were seeded per well and stimulated with 0, 1, 3.3 or 10 mg/ml lipopolysaccharide (LPS) from *Porphyromonas Gingivalis* (LPS-PG, InvivoGen, Toulouse, France) for 48 hours. LPS was chosen in this study as it is frequently used as a positive control when testing substances which may stimulate an immune response in PBMCs, since being of bacterial origin it stimulates the innate and adaptive immune systems^{21,22}. Plates were centrifuged at 300 g for 5 minutes and the supernatant was harvested and stored at -20° Celsius. The supernatant was analyzed using a bead-based immunoassay from BioLegend legendplex (BioLegend, San Diego, CA., USA). The human inflammation panel (IL-1 β , IFN- α 2, IFN- γ , TNF- α , MCP-1, IL-6, IL-8, IL-10, IL-12p70, IL-17A, IL-18, IL-23, and IL-33) was used according to the manufacturer's instructions. Samples were diluted by a factor of 50.

SLS irritation patch testing

Patch testing was performed on the non-dominant upper arm with the application of the contact irritant sodium lauryl sulphate (SLS)(0%, 0.25%, 0.5%, 1% and 2% in water). SLS is used routinely in skin patch tests in both research and clinical practice since it penetrates the stratum corneum, as opposed to LPS which is a large bacterial membrane molecule. Van der Bend® patch test chambers on Fixomull® tape were filled with 20 µl of test solution. The patch was removed 48 hours later by the participants themselves. On day four, the test was assessed by an experienced dermatologist (TR). The lowest concentration of SLS which induces an irritation reaction is the IT. The amount of irritation is graded using the visual grading scale for irritation (table 1c)²³. The percentage of SLS and the corresponding patch test gradings between the NS and HS group were then processed using ROC analysis to determine which percentage of SLS could best discriminate between the two groups in the test.

Furthermore, non-invasive measurement of transepidermal water loss (TEWL) by means of a TEWAmeter® (TM300; Courage & Khazaka, Cologne, Germany) was performed on the patch test sites to assess skin barrier disruption, which is a parameter for skin irritation¹⁶. TEWL was performed following established guidelines, with the patient resting for 10 minutes in a room free of excessive draughts, and stable temperature and moisture¹⁶. Two readings (in g/m²h) were taken from normal skin on the arm and each of the patch test sites²⁴. Measurement of skin redness by means of a DermaSpectrometer® (Cortex Technology, Hadsund, Denmark) was performed²⁵. The probe was placed on the skin and the erythema index ($E=100 \times \log(\text{intensity of reflected red light} / \text{intensity of reflected green light})$) was determined as well as a melanin index ($M=100 \times \log(1 / \text{intensity of reflected red light})$). The E parameter is used for the evaluation of vascularisation and the M parameter for pigmentation. Stratum corneum was collected via tape-stripping of the patch test sites and was analyzed for cytokine secretion as explained in supplement figure 2.

Statistical analysis

SLS patch test: it was expected that 70% of the HS group would have a high IT compared to 30% of the NS group. For clinical relevance, this means that patients with a high IT will have a 70% risk of hypertrophic scar formation. In practice, a high IT means that a person will respond with the same skin reaction to a higher dose of SLS compared to someone with a normal IT. A sample size of 30 patients per group was calculated. Thirty patients in each group would be enough to reject the null hypothesis that the probability of skin irritation for the two groups is equal with a probability (power) of 0.8. The type I error probability associated with this test of this null hypothesis is 0.05. After including 30 patients an interim analysis was performed, and due to the ample significance in this analysis, the study was concluded. Two-way ANOVA followed by Sidak's multiple comparisons test and ROC analysis were performed using GraphPad Prism version 7.00 for Windows, GraphPad Software, La Jolla California USA, www.graphpad.com. A p-value of <0,05 was considered statistically significant. This method of analysis gives a yes-no answer as to whether an individual is prone to developing a hypertrophic scar.

PBMC cytokine test: Two-way ANOVA was used for all cytokines, a p-value of <0,05 was considered statistically significant (GraphPad Prism). To form a prediction model on the PBMC data, binary logistic regression analysis was performed and a ROC curve calculated (IBM SPSS Statistics for Windows, Version 22.0). Single cytokine and cytokine combinations were analyzed in the same fashion. The data generated by measuring cytokine secretion facilitates this type of analysis. The advantage is that all data is retained in the analysis as opposed to setting a certain threshold. The disadvantage of this technique is that it means that the PBMC model and patch test model cannot be directly compared with each other. After individual analysis for each cytokine, those with a large area under the curve (AUC) and significant *p*-value were selected to create combinations with optimum prognostic value. These combinations were filtered in a similar manner. The probability of a hypertrophic scar forming can then be calculated with the formula; $p = \frac{1}{1 + e^{-LP}}$ where $LP = constant + (coefficient \times cytokine1) + (coefficient \times cytokine2)$. The cytokine

input is either pg/ml or ng/ml. Internal validation procedures were used to represent how the model would perform in new patients and to compensate for overfitting of the model on the data (RStudio Team (2015) RStudio, Inc., Boston, MA).

RESULTS

Patient characteristics are shown in table 1b. NS was observed in 15 patients and HS in 16 patients. The baseline characteristics show two groups without large discrepancies. One outlier is a patient who developed a normotrophic scar at her mammoplasty site with a formerly hypertrophic scar elsewhere on her body (her knee) which was a flat scar at the moment of inclusion.

Differential cytokine secretion in hypertrophic scar compared to normotrophic scar patients

The secretion of TNF- α , MCP-1, IL-8, IL-18 and IL-23 by unstimulated PBMC was significantly lower in the HS group compared to the NS group (Figure 1). No significant difference in the secretion of IL-1 β , IL-6, IL-10 and IL-33 by unstimulated PBMCs was observed, while secretion of IFN- α 2, IFN- γ , IL-12p70 and IL-17A remained below the detection threshold of the assay.

de Bakker et al. Figure 1

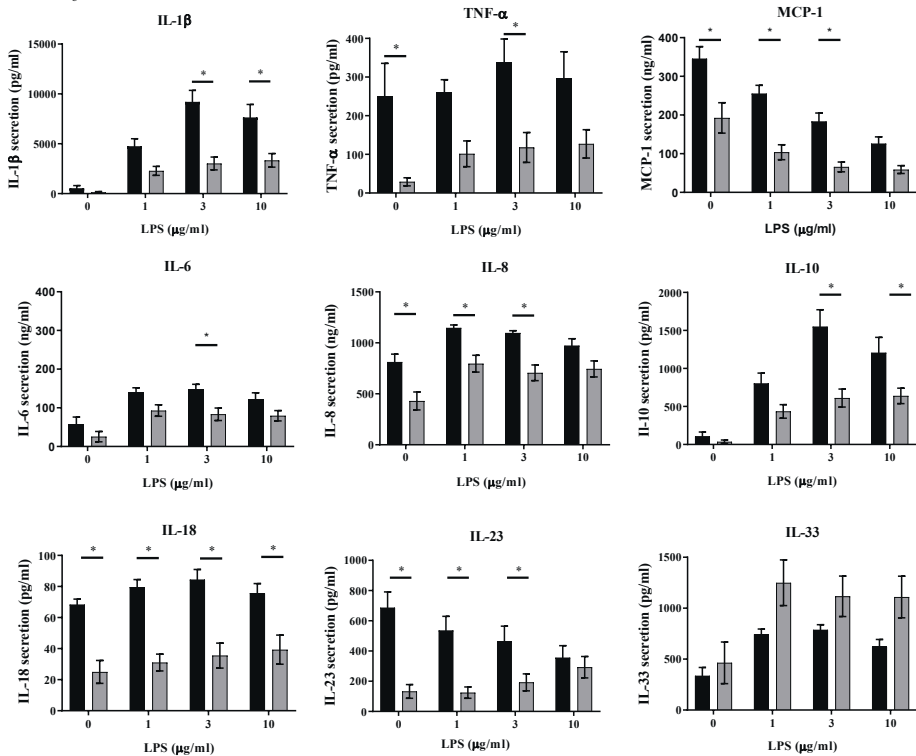


Figure 1. Cytokine secretion

Cytokine secretion by peripheral blood mononuclear cells (PBMCs) after being cultured for 48 hours and stimulated with increasing concentrations of LPS. Normotrophic patients (n=15) = bars black, hypertrophic patients (n=16) = gray bars. Mean \pm SEM (standard error of the mean) is shown. A p-value of $<0,05$ was considered statistically significant.

In order to mimic an inflammatory response, PBMC were stimulated with LPS. An increase in secretion was observed for IL-1 β , TNF- α , IL-6, IL-8, IL-10 and IL-33 in both NS and HS patients compared to unstimulated PBMC. The secretion of IL-18 was unaltered in both groups whereas MCP-1 secretion decreased in both groups. IL-23 secretion decreased in a dose-dependent manner in the NS group after stimulation while secretion increased in the HS group until secretion from the NS and HS groups was at the same level at LPS 10 mg/ml stimulation (figure 1). Notably, for IL-6, IL-8 and IL-23, the fold increase compared to unstimulated PBMC was greater in the HS group compared to the NS

group even though total protein remained lower in the HS group compared to the NS group (figure 1 and supplementary figure 3) e.g. 1 µg/ml LPS results in IL-6: 7.2 fold increase in NS group compared to 66.2 fold increase in HS group, IL-8: 1.7 fold increase in NS group compared to 3.3 fold increase in HS group and IL-23: 0.8 fold decrease in NS group compared to 56.5 fold increase in HS group at 2 µg/ml LPS.

Prediction model based on unstimulated PBMC cytokine secretion

The cytokine secretion by unstimulated PBMC was further used to develop a prediction model. The results of the univariate regression analysis of unstimulated PBMC cytokine secretion are shown in table 2a. MCP-1, IL-8, IL-18, and IL-23 have a strongly significant correlation with HS ($p < 0.010-0.004$). TNF- α , which was significant in 2-way ANOVA now showed a strong trend ($p < 0.060$). All of the five cytokines showed a good area under the curve (AUC= 0.790-0.883), confidence interval, odds ratio, and Nagelkerke R^2 (see table 2b). Next, based on the merit of the AUC and p -values of the individual cytokines, all possible combinations of these five cytokines were analysed (table 2, supplementary table 1). Notably, combinations of 2 cytokines (MCP-1 and IL-23; AUC: 0.921, Nagelkerke R^2 : 0.703) or 3 cytokines (TNF- α , MCP-1 and IL-23; AUC: 0.942, Nagelkerke R^2 : 0.727) showed clearly improved AUC indicating a better correlation with HS than single cytokine analysis (table 2). As expected with these AUC values, these combination models produce excellent prognostic results (eg sensitivity, specificity and accuracy) over a broad probability range (sensitivity: 93.8%, specificity 86.7%, accuracy 90.25% between probability 0.3 and 0.7) (table 2c; supplement table 1 for all cytokines combinations). Combinations of more than three cytokines had no further added value.

Table 2. Univariate regression analysis of unstimulated PMBC cytokine secretion

Type	Coefficient	OR	95 % CI	Nagelkerke	p	AUC	95 % CI
IL-1 β	-0.002	0.998	0.994-1.001	0.164	0.174	0.825	0.670-0.980
TNF- α	-0.014	0.986	0.972-1.001	0.357	0.060	0.820	0.667-0.973
MCP-1	-0.008	0.992	0.986-0.998	0.338	0.010	0.796	0.633-0.959
IL-6	-0.001	0.999	0.992-1.007	0.001	0.873	0.750	0.562-0.938
IL-8	-0.003	0.997	0.994-0.999	0.354	0.007	0.812	0.663-0.962
IL-10	-0.004	0.996	0.989-1.003	0.077	0.285	0.667	0.467-0.866
IL-18	-0.073	0.930	0.885-0.977	0.597	0.004	0.883	0.746-1.000
IL-23	-0.006	0.994	0.990-0.998	0.562	0.007	0.867	0.736-0.997
IL-33	0.000	1.000	0.999-1.002	0.017	0.553	0.404	0.190-0.619

Prognostic performance of cytokine combinations

Cytokines	Constant	Coefficient	OR	95 % CI	Nagelkerke	p	AUC	95 % CI	Ad.AUC	Ad. Nagelkerke
Group N=2	4.58				0.703		0.921	0.811-1.0	0.91	0.66
MCP-1		-0.009	0.991	0.982-1.000		0.041				
IL-23		-0.005	0.995	0.991-0.999		0.008				
Group N=3	4.713				0.727		0.942	0.857-1.0	0.92	0.63
TNF- α		-0.006	0.994	0.976-1.012		0.496				
MCP-1		-0.009	0.991	0.982-1.000		0.048				
IL-23		-0.004	0.996	0.992-0.999		0.022				

Prognostic characteristics of cytokine prediction models

MCP-1+IL23							
Prob	Sens	Spec	Acc	FN	FP	PPV	NPV
0.1	93.8	46.7	70.25	1	8	65.2	87.5
0.2	93.8	80	86.9	1	3	83.3	92.3
0.3	93.8	86.7	90.25	1	2	88.2	92.9
0.4	93.8	86.7	90.25	1	2	88.2	92.9
0.5	93.8	86.7	90.25	1	2	88.2	92.9
0.6	93.8	86.7	90.25	1	2	88.2	92.9
0.7	87.5	93.3	90.4	2	1	93.3	87.5
0.8	68.8	93.3	81.05	5	1	91.7	73.7
0.9	43.8	100	71.9	9	0	100	62.5

TNF- α +MCP-1+IL23							
Prob	Sens	Spec	Acc	FN	FP	PPV	NPV
0.1	93.8	46.7	70.25	1	8	65.2	87.5
0.2	93.8	66.7	80.25	1	5	75	90.9
0.3	93.8	86.7	90.25	1	2	88.2	92.9
0.4	93.8	86.7	90.25	1	2	88.2	92.9
0.5	93.8	86.7	90.25	1	2	88.2	92.9
0.6	93.8	86.7	90.25	1	2	88.2	92.9
0.7	93.8	93.3	93.55	1	1	93.8	93.3
0.8	62.5	93.3	77.9	6	1	90.3	70
0.9	43.8	100	71.9	9	0	100	62.5

a) Binary logistic regression analysis of unstimulated PBMC cytokine secretion after 48 hr culture identifies patients with a hypertrophic scar. MCP-1, IL-8, IL-18, IL-23 and TNF- α were selected to form stronger combinations on the merit of strong AUC and p value. b) Prognostic performance of cytokine combinations. Internal validation procedures were used to represent how the model would perform in new patients and to compensate for overfitting of the model on the data (RStudio Team (2015). RStudio, Inc., Boston, MA). See Materials and Methods, section Statistical Analysis. c) Prognostic characteristics of cytokine prediction models at increasing probability of developing a hypertrophic scar. Abbreviations and terms: OR, odds ratio; CI, confidence interval; AUC, area under the curve; Ad., adjusted value after inter validation procedures; coefficient for the constant; Nagelkerke R²; prob, probability; sens, sensitivity; spec, specificity; acc, accuracy; FN, false negative; FP, false positive; PPV, positive predictive value; NPV, negative predictive value.

Prediction model based on irritation threshold

In both patient groups increasing visual erythema correlated to increasing SLS concentration with the dose-dependent increase in patch test score being greater for HS than for NS (figure 2a). Notably, the difference between NS and HS was significant for SLS 1% ($p < 0.027$; range patch test score: NS 0-3 vs HS 1-4) and 2% ($p < 0.014$; range patch test score: NS 0-4 vs HS 2-4) concentrations indicating that the HS group has a lower IT than the NS group (figure 2b). In figure 2b all visual erythema grading scale scores are visualized with a scatter plot. After ROC curve analysis following 2-way ANOVA, both 1% and 2% SLS showed good discriminatory characteristics when using a cut-off of ≥ 2 on the visual irritation scale. With a 1% SLS solution, sensitivity and specificity are 60% and 73% respectively, with an overall accuracy of 66.7%. Increasing the percentage to 2% results in higher sensitivity (80%) while lowering the specificity (46.7%), with an overall accuracy of 63.3%. The grading scores at concentrations of SLS lower than 1% were too similar between the two groups to be useful (see figure 2b). No significant difference was observed between the control (vehicle water) exposed sites of the NS and HS groups which both scored negative (0) according to the visual irritation grading scale (table 1c).

The normotrophic patient with a formerly hypertrophic scar on her knee interestingly had a non-conclusive score in both patch testing (scoring visual erythema grades of 2 for 1% and 3 for 2% SLS) as well as in the cytokine panel (lower than average for NS secretion of TNF- α (48.5 vs 249.5 pg/ml), MCP-1 (120.0 vs 345.8 ng/ml), IL-6 (6.0 vs 59.1 ng/ml) and IL-8 (242.0 vs 811.5 ng/ml)).

In contrast to the visual irritation grading, neither the TEWL nor the dermatospectrometry measurements were able to distinguish the HS from the NS group based on IT (supplement figure 2). Cytokines extracted from the stratum corneum also did not show significant differences between the two groups (see supplement figure 4).

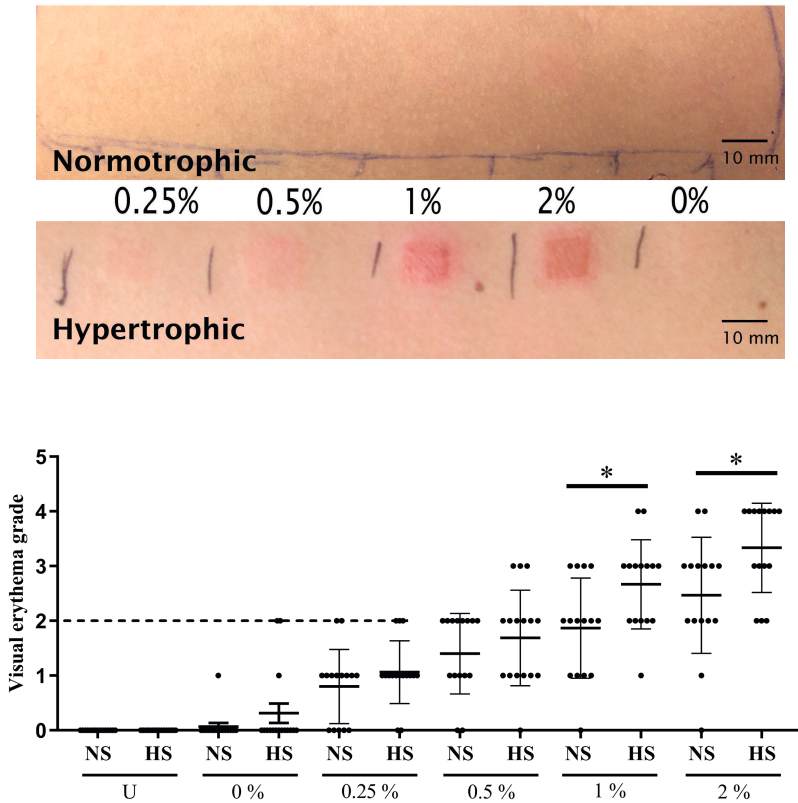


Figure 2: patch test results

a) Representative results of reaction to SLS patch testing in an HS and a NS patient. SLS concentrations of 0.25%, 0.5%, 1%, 2% and 0% in water. The duration of the patch test was 48 hours and the readout was at 96 hours. Erythema grades given were 0 (0.25%), 1 (0.5%), 2 (1%), 2(2%) and 0 (0%) for the NS patient and 2 (0.25%), 3 (0.5%), 4 (1%), 4 (2%) and 0 (0%) for the HS patient, see grading scale in Table 1.

b) Scatter plot with standard error of the mean (SEM) of all visual erythema grading scores of unexposed skin (U) and patch test sites exposed to percentage of SLS in water. Black bar = HS, gray bar= NS. Normotrophic patients (n=15) = bars black, hypertrophic patients (n=16) = gray bars. 2-way ANOVA performed in GraphPad Prism.

DISCUSSION

Here we show that very fundamental immunological differences exist between individuals who develop HS and those who do not. More importantly, the suppressed PBMC cytokine secretion observed in HS individuals compared to NS individuals is the basis of a novel predictive prognostic test for HT formation. The less invasive and easily performed irritant skin patch test showed a differentiating induction response in HS individuals compared to NS individuals and therefore, provides a more accessible option for daily practice.

Of the 13 cytokines studied in the stimulated PBMC assay, 5 cytokines (TNF- α , MCP-1, IL-8, IL-18, and IL-23) had potential prognostic value due to the clearly lower levels detected in unstimulated PBMC cultures derived from HS individuals compared to NS individuals. These individual cytokines had, in logistic regression analysis, an AUC ranging from 0.796 - 0.883. When combining these individual cytokines into a panel of two (MCP-1 and IL-23) or three (add TNF- α) cytokines, the AUC increased to 0.921 and 0.942 respectively, while the accuracy of these combinations was >90 % over a large range. All of these are excellent values for a prognostic tool.

Many studies implicate the roles of TNF- α , MCP-1, IL-6 and IL-8 in wound healing. MCP-1, IL-6 and IL-8 have been described to be a chemoattractant for monocytes and neutrophils which regulate the inflammatory phase of wound closure^{26,27}. All four are mitogens and stimulate re-epithelialization²⁸. In contrast, IL-18 and IL-23 are not well-known cytokines in wound regulation. IL-18 has been associated with (cutaneous) inflammatory skin diseases like psoriasis, allergic contact dermatitis and atopic dermatitis^{29,30}, in addition to keloid formation³¹. It is produced by keratinocytes and plays a key role in innate immunity and inflammasome activation although its role in wound healing has not yet been reported³². IL-23 is closely related to IL-18 and can be produced by activated macrophages and dendritic cells³³, it has been linked to autoimmunity and is involved in the differentiation of Th17 cells^{32,34,35}. In line with our current findings, we previously described a local suppressed inflammatory mRNA expression (TNF- α , IL-1 α , IL-1RN, CCL2, CCL3, CXCL2, CXCR2, C3, and IL-10)

within the early healing wound and the young scar over a 52-week follow-up period as well as significantly lower concentrations of inflammatory proteins in the post-surgical wound site in hypertrophic scars^{15,36}. This suggested a reduced inflammatory response which conflicted with the existing belief that HS is related to increased inflammation^{15,37,38}. Despite the low basal cytokine secretion in HS individuals, when PBMCs were stimulated, the fold increase in IL-6, IL-8 and IL-23 cytokine secretion was greater than in NS individuals. IL-23 is of particular interest as the HS group shows a 56.2 fold increase whereas the NS group actually shows a small 0.8 fold decrease. Importantly, this increase in secretion did not result in a higher absolute secretion compared to NS patients and would therefore still present as a reduced inflammatory response when comparing NS and HS directly. HS patients have in a resting state a lowered inflammatory cytokine profile, but upon triggering, a clear cytokine response is initiated. Further studies are required to determine whether the low basal cytokine secretion followed by a potential increased inflammatory reaction is also a contributory factor to HS formation.

Our finding that a functional difference of the immune system at a systemic level is an important factor in HS formation is a critically different approach to focussing on the biology within the local site of injury. While acknowledging risk factors like age and allergy status^{3,8-10}, there is a group of individuals who are susceptible to developing HS despite these risk factors and who will be predisposed to develop HS regardless. The immune suppression which we describe in this study may now be considered as a potent risk factor. This further expands the puzzle of HS formation in which we know that injury in the deep dermis is predictive for HS development as well as the fact that scars are often partially hypertrophic and normotrophic³⁹. Our results showed that both unstimulated and stimulated PBMCs from the HS group secreted lower amounts of IL-10 than the NS group. IL-10 is a potent anti-inflammation regulatory cytokine and has been described extensively in the context of hypertrophic scar formation and therefore has generated interest as a potential anti-scarring agent^{36,40}. Although further research is required, these first results may provide a link between HS

formation and the more inflammatory irritation patch test result that was observed in the HS group.

Although some of the results described in our study and the existing body of research seem contradictory, most of the current literature focusses on the local site of injury as opposed to these systemic processes⁴¹⁻⁴⁴. Indeed a different population of immune cells are present in the skin (e.g. Langerhans Cells, macrophages and resident T cells) compared to their counterparts in the blood since immune cell plasticity and the influence of the micro-environment determine immune cell phenotype and their cytokine secretome⁴⁵. This may be the reason that we observe an increased inflammatory response in HS patients upon a localized skin irritant challenge and a decreased baseline cytokine secretion from PBMCs in the same HS group. This finding cannot be considered a discrepancy since two totally different stand-alone methods were used, one which assesses a local skin immune reaction and the other a systemic peripheral blood immune reaction. To our knowledge, there are no publications describing an irritant patch test response for other forms of fibrosis e.g. in keloid patients or the stimulation of keloid derived PBMCs with LPS. However, it has been described that IL-18 secretion was reduced in both unstimulated and LPS-stimulated monocytes from patients with atopic dermatitis⁴⁶. This is an interesting subject for a follow-up study as it will indeed determine whether our observations are specific for HS patients or more general for fibrosis and other inflammatory skin diseases e.g. Rosacea, keratosis pilaris, eczema and psoriasis. Although, in the past, we have investigated IL-6 and IL-8 secretion from healthy and keloid derived monocytes and did not observe a decreased baseline secretion in the keloid monocytes⁴⁷. Also, TNF-alpha and IL-6 have also been reported to be increased in LPS stimulated healthy PBMC⁴⁸ although we only observed a moderate increase, and in contrast to our results, it has been described that LPS increases secretion of MCP-1 from PBMCs derived from healthy donors²². The expanding knowledge on the mechanisms of hypertrophic scar formation would seem to indicate that it is an intricate process in which individual cells and cytokines act in both stimulatory and suppressive roles at certain moments over the entire course of scar maturation and therefore

this may also explain some of the discrepancies which we find with reports of others^{15,36}. In our study, we only included mature NS and HS scars resulting from the same surgical intervention.

Although slightly less impressive, patch testing the skin with an irritant also resulted in clear differences between the NS and HS groups. It should be noted that this is a more subjective test, requiring an experienced dermatologist to assess the patch test sites. Based on earlier research describing cytokine mRNA expression in skin tissue biopsies, we had expected a higher IT, which would correlate with a suppressed local immune reaction to trauma in the HS group^{15,36}. The fact that we observed a lower IT in HS individuals does, however, reflect the changes in the PBMC cytokine profiles where HS patients responded more substantially with a greater fold induction compared to NS individuals. Our patch test findings cannot be explained by HS individuals having an inferior barrier function compared to NS individuals since cytokines isolated from stratum corneum tape strips, visual erythema and TEWL showed no significant differences, indicating that the difference originates deeper in the skin.

In this study, we describe two prognostic tests to determine whether an individual may be prone to developing HS after surgery. The PBMC test reaches 93 % accuracy, however, it is an invasive test that requires peripheral blood and expertise in cell culture and therefore is relatively time-consuming to implement into routine procedures. The patch test, whilst being slightly less accurate (63-68 %) than the PBMC test has the advantage that it is minimally invasive and does not require a cell culture laboratory. However, it does require an experienced dermatologist to score the patch test. Further studies might well improve the accuracy and clinical usability of the patch test, e.g. by testing distinct more skin irritants, different concentrations and different time intervals^{49,50}. Whereas both tests have their specific pros and cons, they do both provide easily accessible tools to estimate the chance of an individual developing HS after surgery. In addition to providing an option not to undergo surgery if it is not essential, extra attention can be given to patients at risk during and directly after surgery e.g. by performing extra meticulous surgery and using reduced tension skin stitching methods, as well as the start of silicone application at two weeks

following surgery. The PBMC cytokine secretion profiles need further confirmation in larger cohorts, but our results clearly suggest that these mediators can be critical predictors. Furthermore, these cytokines offer new insights into pathophysiological mechanisms and, hence, these findings stimulate future research into prevention and treatment.

These prognostic markers have proven strong in our cohort, but prospective research is needed in a larger group of patients including males and all skin types, including patients who have not yet developed a significant scar to further strengthen these results. Similar research should be considered in the keloid patient group considering the greater influence on the quality of life. Furthermore, if measuring cytokines directly in serum proves equally effective, the more time laborious process of PBMC isolation and culture could be omitted.

In conclusion, our results indicate that HS patients exhibit a systemically suppressed immune status with lower PBMC cytokine secretion. After stimulation, a more pronounced response than in NS patients is seen but still falls short of cytokine secretion of individuals who form NS. Ultimately this may result in a failure to successfully complete the normal wound healing process. These findings enable a very potent model to predict the formation of hypertrophic scars.

REFERENCES:

- [1] B. Mahdavian Delavary, W. M. van der Veer, J. A. Ferreira, F. B. Niessen, *J. Plast. Surg. Hand Surg.* **2012**, *46*, 95.
- [2] M. C. T. Bloemen, W. M. van der Veer, M. M. W. Ulrich, P. P. M. van Zuijlen, F. B. Niessen, E. Middelkoop, *Burns* **2009**, *35*, 463.
- [3] S. Monstrey, E. Middelkoop, J. J. Vranckx, F. Bassetto, U. E. Ziegler, S. Meaume, L. Téot, *J. Plast. Reconstr. Aesthetic Surg.* **2014**, *67*, 1017.
- [4] C. C. Finnerty, M. G. Jeschke, L. K. Branski, J. P. Barret, P. Dziewulski, D. N. Herndon, *Lancet (London, England)* **2016**, *388*, 1427.
- [5] F. B. Niessen, P. H. Spauwen, J. Schalkwijk, M. Kon, *Plast. Reconstr. Surg.* **1999**, *104*, 1435.
- [6] H. J. Lee, Y. J. Jang, *Int. J. Mol. Sci.* **2018**, *19*, DOI 10.3390/ijms19030711.
- [7] B. Berman, A. Maderal, B. Raphael, *Dermatologic Surg.* **2017**, *43*, S3.
- [8] A. E. Slemper, R. E. Kirschner, *Curr. Opin. Pediatr.* **2006**, *18*, 396.
- [9] L. Butzelaar, M. M. W. Ulrich, A. B. Mink van der Molen, F. B. Niessen, R. H. J. Beelen, *J. Plast. Reconstr. Aesthet. Surg.* **2016**, *69*, 163.
- [10] R. S. Chiang, A. A. Borovikova, K. King, D. A. Banyard, S. Lalezari, J. D. Toranto, K. Z. Paydar, G. A. Wirth, G. R. D. Evans, A. D. Widgeow, *Wound Repair Regen.* **2016**, *24*, 466.
- [11] S. H. Kwon, G. C. Gurtner, *Exp. Dermatol.* **2017**, *26*, 133.
- [12] F. B. Niessen, J. Schalkwijk, H. Vos, W. Timens, *J. Pathol.* **2004**, *202*, 121.
- [13] Z. Zhu, J. Ding, Z. Ma, T. Iwashina, E. E. Tredget, *Wound Repair Regen.* **2016**, *24*, 644.
- [14] L. J. Van Den Broek, F. B. Niessen, R. J. Scheper, S. Gibbs, *ALTEX* **2012**, *29*, 389.
- [15] L. Butzelaar, D. P. M. Schooneman, E. A. Soykan, W. Talhout, M. M. W. Ulrich, L. J. van den Broek, S. Gibbs, R. H. J. Beelen, A. B. Mink van der Molen, F. B. Niessen, *Exp. Dermatol.* **2016**, *25*, 797.
- [16] S. Suda, H. Williams, H. J. Medbury, A. J. A. Holland, *J. Burn Care Res.* **2016**, *37*, 265.
- [17] S. W. Spiekstra, M. J. Toebak, S. Sampat-Sardjoepersad, P. J. van Beek, D. M. Boorsma, T. J. Stoof, B. M. E. von Blomberg, R. J. Scheper, D. P. Bruynzeel, T. Rustemeyer, S. Gibbs, *Exp. Dermatol.* **2005**, *14*, 109.
- [18] D. A. Basketter, H. A. Griffiths, X. M. Wang, K. P. Wilhelm, J. McFadden, *Contact Dermatitis* **1996**, *35*, 208.
- [19] H. R. Smith, M. Rowson, D. A. Basketter, J. P. McFadden, *Contact Dermatitis* **2004**, *51*, 26.
- [20] M. J. C. Nagtegaal, S. E. Pentinga, J. Kuik, S. Kezic, T. Rustemeyer, *Contact Dermatitis* **2012**, *67*, 28.
- [21] S. A. Koppes, S. Ljubojevic Hadzavdic, I. Jakasa, N. Franceschi, R. Jurakić Tončić, B. Marinović, R. Brans, S. Gibbs, M. H. W. Frings-Dresen, T. Rustemeyer, S. Kezic, *Br. J. Dermatol.* **2017**, *176*, 1533.
- [22] T. Yoshimura, M. Takahashi, *J. Immunol.* **2007**, *179*, 1942.
- [23] D. A. Basketter, J. Miettinen, A. Lahti, *Contact Dermatitis* **1998**, *38*, 253.
- [24] R. Darlenski, J. Kazandjieva, N. Tsankov, J. W. Fluhr, *Exp. Dermatol.* **2013**, *22*, 752.
- [25] L. J. Draaijers, F. R. H. Tempelman, Y. A. M. Botman, R. W. Kreis, E. Middelkoop, P. P. M. van Zuijlen, *Burns* **2004**, *30*, 103.
- [26] D. E. A. Komi, K. Khomtchouk, P. L. Santa Maria, *Clin. Rev. Allergy Immunol.* **2019**, DOI 10.1007/s12016-019-08729-w.
- [27] B. M. Delavary, W. M. van der Veer, M. van Egmond, F. B. Niessen, R. H. J. Beelen, *Immunobiology* **2011**, *216*, 753.
- [28] I. Pastar, O. Stojadinovic, N. C. Yin, H. Ramirez, A. G. Nusbaum, A. Sawaya, S. B. Patel, L. Khalid, R. R. Isseroff, M. Tomic-Canic, *Adv. Wound Care* **2014**, *3*, 445.
- [29] J. H. Lee, D. H. Cho, H. J. Park, *Int. J. Mol. Sci.* **2015**, DOI 10.3390/ijms161226172.
- [30] S. Gibbs, E. Corsini, S. W. Spiekstra, V. Galbiati, H. W. Fuchs, G. DeGeorge, M. Troese, P. Hayden, W. Deng, E. Roggen, *Toxicol. Appl. Pharmacol.* **2013**, *272*, 529.

- [31] D. V. Do, C. T. Ong, Y. T. Khoo, A. Carbone, C. P. Lim, S. Wang, A. Mukhopadhyay, X. Cao, D. H. Cho, X. Q. Wei, G. Bellone, I. Lim, T. T. Phan, *Br. J. Dermatol.* **2012**, *166*, 1275.
- [32] S. F. Martin, P. R. Esser, F. C. Weber, T. Jakob, M. A. Freudenberg, M. Schmidt, M. Goebeler, *Allergy Eur. J. Allergy Clin. Immunol.* **2011**, *66*, 1152.
- [33] Y. Iwakura, *J. Clin. Invest.* **2006**, *116*, 1218.
- [34] E. Duvallet, L. Semerano, E. Assier, G. Falgarone, M. C. Boissier, *Ann. Med.* **2011**, *43*, 503.
- [35] R. Conway, L. O'Neill, G. M. McCarthy, C. C. Murphy, A. Fabre, S. Kennedy, D. J. Veale, S. M. Wade, U. Fearon, E. S. Molloy, *Ann. Rheum. Dis.* **2018**, *0*, annrheumdis.
- [36] L. J. van den Broek, W. M. van der Veer, E. H. de Jong, S. Gibbs, F. B. Niessen, *Exp. Dermatol.* **2015**, *24*, 623.
- [37] J. Wang, K. Hori, J. Ding, Y. Huang, P. Kwan, A. Ladak, E. E. Tredget, *J. Cell. Physiol.* **2011**, *226*, 1265.
- [38] J. Ding, E. E. Tredget, *Adv. Wound Care* **2015**, *4*, 673.
- [39] C. S. J. Dunkin, J. M. Pleat, P. H. Gillespie, M. P. H. Tyler, A. H. N. Roberts, D. A. McGrouther, *Plast. Reconstr. Surg.* **2007**, *119*, 1722.
- [40] A. King, S. Balaji, L. D. Le, T. M. Crombleholme, S. G. Keswani, *Adv. wound care* **2014**, *3*, 315.
- [41] V. W. Wong, K. C. Rustad, S. Akaishi, M. Sorkin, J. P. Glotzbach, M. Januszzyk, E. R. Nelson, K. Levi, J. Paterno, I. N. Vial, A. A. Kuang, M. T. Longaker, G. C. Gurtner, *Nat. Med.* **2012**, *18*, 148.
- [42] G. G. Gauglitz, H. C. Korting, T. Pavicic, T. Ruzicka, M. G. Jeschke, *Mol. Med.* **2011**, *17*, 113.
- [43] S. Liu, L. Jiang, H. Li, H. Shi, H. Luo, Y. Zhang, C. Yu, Y. Jin, *J. Invest. Dermatol.* **2014**, DOI 10.1038/jid.2014.169.
- [44] R. M. Salgado, L. Alcántara, C. A. Mendoza-Rodríguez, M. Cerbón, C. Hidalgo-González, P. Mercadillo, L. M. Moreno, R. Álvarez-Jiménez, E. Kröttsch, *Burns* **2012**, DOI 10.1016/j.burns.2011.12.012.
- [45] J. E. Glim, M. Van Egmond, F. B. Niessen, V. Everts, R. H. J. Beelen, *Wound Repair Regen.* **2013**, *21*, 648.
- [46] N. Higashi, B. Gesser, K. Thestrup-Pedersen, S. Kawana, N. Higashi, *J. Allergy Clin. Immunol.* **2001**, *108*, 607.
- [47] G. C. Limandjaja, T. Waaijman, S. Roffel, F. B. Niessen, S. Gibbs, *Arch. Dermatol. Res.* **2019**, *311*, 615.
- [48] L. Janský, P. Reymanová, J. Kopecký, *Physiol. Res* **2003**, *52*, 593.
- [49] H. Löffler, R. Happle, *Contact Dermatitis* **2003**, *48*, 26.
- [50] J. Aramaki, C. Löffler, S. Kawana, I. Effendy, R. Happle, H. Löffler, *Br. J. Dermatol.* **2001**, *145*, 704.

8

PART I: HYPERGRANULATORY TISSUE IN BREAST IMPLANT SURGERY

Wound healing is an intricate process involving a magnitude of cells to enable tissue to return to homeostasis and normal function after injury. The most desirable outcome of this process is newly formed tissue that functions exactly like the tissue it replaces or surrounds. In breast surgery, this means thin, supple, and barely visible scars in the operated skin and thin and supple scar tissue or capsule surrounding an implant deeper in the breast.

Excessive scar formation or fibrosis in breast surgery causes hypertrophic scars, capsular contracture, breast deformation, and pain and poses a significant psychological burden. While the relative number of women suffering from these complaints has become fewer thanks to improvements in surgical techniques, implants, and a general better understanding of risk factors, the absolute number has seen a significant increase. Early detection of breast cancer and the rise in popularity of breast implants (both in reconstruction and, primarily, in augmentation) all mean that there is a significant increase in the number of these procedures performed worldwide^{1,2}.

Cosmetic, as well as reconstructive surgery, should be as safe as possible with as few as possible side effects. Due to the increase in the number of breast implant surgeries since they were introduced in 1963, it should come as no surprise that research into surgery and complications gained traction from the start, be it with ups and downs³⁻⁵. Silicone implants have been in continuous development right from the start, with the design being tweaked over time. This was mainly due to the numerous controversies regarding implant safety because of leaking implants, suspicions of immunological or connective tissue diseases, the usage of industrial (lower) grade silicone in the PIP implant scandal, and, recently, breast implant-associated anaplastic large cell lymphoma (BIA-ALCL)^{3,6-8}. Discussion notwithstanding, there is a clear market demand for breast implants, both in reconstructive and augmentation surgery. Driven by demand to objectify satisfaction rates there are now multiple studies using

patient-reported outcome measures, like the Breast-Q. These confirm that there are indeed many satisfied recipients of breast implant surgery^{9,10}.

After surgery, postoperative complications can occur. Infection, hematoma, seroma, wound rupture, skin deformation, implant folds, numbness of the skin, and prolonged pain occur as short-term or immediate complications, but are generally rare complications¹¹. Capsular contracture (CC) is the aggregate term used to describe capsular-related complaints. As explained in more detail in the introduction of this manuscript, the formation of a capsule surrounding the implant is a physiological process and serves as a barrier shielding the implant from the body while also keeping it in place. In an adverse course, capsules may thicken and/or contract, resulting in asymmetry, hardening, and or deformation of the breast and painful breasts. Rarely an early complication, CC is most commonly seen in the medium to long-term follow-up (>1-2 years)^{12,13}. CC is usually graded according to Baker's classification for capsular contracture, a four-point scale ranging from grade I (natural look and feel), to grade IV (severe contracture). The symptomatic, Baker-IV capsule (hardened, contracted) has been the predominant focus of research into CC. Women who develop unilateral CC complaints are an interesting group to study in this respect. However, a direct, inpatient comparison of symptomatic, Baker-IV capsules and asymptomatic, Baker-I capsules was missing until recently. In chapter II we studied the differences in a collection of capsules. Comparing 10 sets of capsules (20 in total), stainings were performed for CD-68 (macrophages, cytokeratin (epithelial cells), vimentin (fibroblasts), and, unpublished, alpha smooth-muscle actin (asma, myofibroblasts). Baker-IV capsules were significantly thicker, consistent with what the clinical presentation of these Baker-IV capsules would suggest. A clear distinction was seen in the inner layer of the capsules, the layer directly facing the implant. Described in varying degrees in research by others, this layer is often described as an epithelial-like or pseudo-epithelial layer, or as synovial metaplasia^{14,15}. While both look similar, with a row of palisaded cells, the actual cells should be different. Our research significantly identified the layer as a synovial metaplasia structure consisting

of macrophages and fibroblasts and being mainly present in Baker-I capsules (research question 1). In only a few of the Baker-IV capsules, remnants of these structures could also be seen.

Silicone itself has always been of particular interest in CC research as liquid silicone and silicone bleed were deemed responsible for the high CC rates in the first generations of implants^{14,16–18}. A significant pathophysiological connection between CC and (at least fluid) silicone seems probable. Historically, identifying silicone histologically has always been troublesome, and reliable staining methods did not exist. Silicone was just assumed to be in the capsule as there were, for example, vacuolated macrophages with retractile material, and silicone was seen as birefringent material with brightfield microscopy^{19,20}.

New techniques have taken a different approach when identifying substances within a tissue. Confocal Raman-microspectroscopy (CLRM) is one such new technique and uses a laser to identify silicone in tissue^{21–23}. In chapter III this technique was used to confirm the presence of silicone in an axillary lymph node and a capsule, coexisting with Schaumann antibodies in a patient suffering from sarcoidosis. This case study was the first to report this. A limitation of CLRM is that it is very time-consuming (multiple seconds per pixel) and requires the specific preparation of tissues. Therefore, it is well suited to case reports and investigating small sample sizes, but less suited to paired comparisons of entire collections of capsules.

Preferably, the specificity for silicone detection using a technique like Raman-microspectroscopy should be combined with the accessibility characteristic of using high throughput regular histological analysis. In chapter IV, therefore, we explored the feasibility of using stimulated Raman scattering (SRS) microscopy to detect silicone faster and on a larger scale. SRS uses two laser beams to excite (stimulate) the tissue, speeding up the detection significantly with pixel dwell times of microseconds as opposed to seconds. A specific part of the spectrum is chosen to stimulate and thereby specifically detect a substance on a molecular level. The spectral response, i.e. the digital image, is akin to spontaneous Raman spectroscopy, enabling comparisons between the two techniques. Normally, Raman spectroscopy is performed on unstained

and uncovered tissue. On a per-sample basis, this is not a huge problem, although the long processing times involved do mean the sample will dry out and generally will have to be discarded afterward. Therefore, this causes problems with the analysis of multiple samples which arrive in the laboratory at different timeframes, as is to be expected when sample collection is dependent on specific surgeries being performed. It also makes analysing existing sample collections near impossible as these have generally been pre-collected to perform normal (immuno)histological preparations on paraffin and freeze samples. Staining with hematoxylin and eosin (H&E) is one of the most basic, most-performed stainings in a pathology lab and research setting. In chapter IV we showed that SRS can analyze these existing H&E slides mostly without damage, enabling the reliable and relatively fast detection of silicone in the tissue (research question 2).

Advancements in histological staining to detect silicone in tissue have also been made. When combined with Transmission Electron Microscopy (TEM) and Energy Dispersive X-ray microanalysis (EDX) to measure elemental Silicon (Si), a histological staining with Modified Oil O Red (MORO) can be used to detect silicon in the tissue²⁴.

The next logical step in this research line was undertaken for chapter V, in which the same collection of capsules used in chapter II was now analyzed for the presence of silicone. The study was strengthened by our choice to use both available techniques in two independent centers. After processing, both qualitative and automated quantitative assessments were performed. Both techniques found significantly more Baker-IV capsules with silicone. Furthermore, the amount found in the Baker-IV capsules was also significantly higher compared to the Baker-I capsules. For the first time, a clear correlation between silicone content and Baker-IV CC was found (research question 3).

Taken together, the results of chapters II and V suggest that the increased amount of silicone found in Baker-IV capsules is either responsible for, or is caused by, the extensive and ongoing foreign body response (FBR) creating the fibrotic capsule formation and contracture found in CC.

CC rates were significantly higher in the first generations of silicone breast implants, which suffered from silicone bleeding through the shell and the risk of rupture due to a vulnerable shell²⁵. More durable, cross-linked silicone elastomer shells and high cohesive gel fillings were the main improvements made in modern implants to prevent silicone bleed and implant rupture^{14,16-18}. The subsequent drop in CC rates suggested a pivotal role of silicone in the fibrotic process. The findings in chapters II and V are consistent with this role and suggest that, despite numerous improvements, silicone bleed is still an issue causing CC.

Macrophages might play a role as well, by trying to digest the initial implant which will eventually result in silicone being released from the implant.

The synovial metaplasia-like layer (SMLL) on the implant side of the Baker-I capsules found in chapter II may serve as a protective layer, essentially succeeding and preventing fibrosis at the outset of the FBR, or preventing an ongoing FBR. Conversely, the SMLL might disappear if the FBR becomes too advanced, for reasons as yet unknown. When Baker-IV capsules form, the layer could be lost as fibrosis and thickening of the capsule progresses resulting in a hypoxic environment. If a SMLL does play such a protective role, it probably does so in shielding the body effectively from the actual foreign body (the implant). It seems likely that a SMLL is formed in the initial FBR to textured implants, as this layer has been less frequently described in capsules of smooth implants^{19,21,23,26}. The surface profile of the implant more than likely seems to play a role in the formation and shape of a SMLL, as well as the movement of the foreign body²⁷. Interestingly, smooth implants are 2.3 times more likely to be associated with CC in comparison with textured implants². This further suggests the texturing of implants might result in less CC through the formation of the SMLL and shielding the body from the implant (and silicone) for a longer time.

For the approximately 60 years during which CC has been investigated, the Baker scale for capsular contracture has become the standard for the communication of CC in medical files and scientific research. In this manuscript too, much of the results are correlated with Baker's classification scale for CC from¹⁹⁷⁸²⁸ (Table 1). Ideally, such a widely used diagnostic tool should have good

interobserver reliability. In short, the better the interobserver reliability, the more consistent different observers will assess the same situation. Unfortunately, in chapter VI we found the Baker classification to be unreliable as a diagnostic tool, with poor interobserver reliability. In the study, sixty women who had undergone cosmetic breast augmentation were independently examined by two plastic surgeons, noting the Baker score and firmness, dislocation, symmetry, and pain on a comparable four-point scale. For all these parameters poor interobserver reliability results were calculated.

As Table 1 shows, the Baker score uses fairly vague wording and does not set stringent boundaries between the different classes. After the symposium at which dr. Baker presented his classification, no formal article was published. There were written reports from the symposium with the classification in writing, but even today these original documents are hard to find.

Even a modest search through the medical databases reveals an evident lack of consensus on how the different classes should be formulated. Different definitions and wording can be found throughout different articles, teaching books, and websites of national plastic surgery societies. A few examples are given in Tables 2 through 4. As CC is an aggregate of symptoms, the choice was made to evaluate firmness, dislocation, symmetry, and pain separately, hoping that the interobserver reliability of these individual parameters would be better. Unfortunately, the individual symptoms had comparable interobserver reliability scores to the Baker score. The interobserver agreement is a lot higher when observers are allowed to disagree by one level (so I and II, II and III, etc.). This indicates that observers do agree on the same end of the spectrum, but the exact grade is difficult to agree on. This is a problem when these grades are used as distinct classes and a one-level difference is deemed significant. For example, currently, in the Dutch healthcare insurance regulations, reimbursement for explantation/re-implantation procedures is (partially) granted in Baker-IV cases, but not in Baker-III cases. When comparing Baker-I with Baker-IV cases, as in the rest of this thesis, the consequences are arguably less significant. Inclusions in those instances may vary and cause differences within a cohort when the inclusions are done by multiple clinicians independently and between co-

horts. Evaluating multiple capsule-related complaints on a single four-point Likert scale is likely to be difficult, especially when the definition of the individual scales is vague and not discriminatory enough. Formulating a good and useful clinical classification that has a broad application is always difficult in medicine. In the case of the Baker classification, usage spiraled from a simple initial classification to enable easy communication between colleagues to a scale used in clinical and scientific practice and to even obtain (partial) reimbursement from health insurance for surgical treatment. Evaluation of a breast containing an implant can have many different factors; local complaints like firmness, dislocation, and symmetry may differ in seriousness or implication to both patient and observer and can also differ between cultures. These may also differ significantly per implant type, surgical technique, and especially in augmentation surgery versus (oncological) reconstruction. Experienced symptoms like tenderness and pain are patient-reported and should be separately considered. Although there seems to be a rough consensus about symptomatic versus asymptomatic capsules there is a clear need for a more reliable method of measurement or description, especially for scientific purposes. As it is, it seems very important to discuss what is considered symptomatic or asymptomatic in CC research manuscripts.

Table 1: Baker classification of capsular contracture after augmentation mammoplasty *

Class I	Breast absolutely natural, no one could tell breast was augmented
Class II	Minimal contracture; I can tell surgery was performed, but patient has no complaint
Class III	Moderate contracture; patient feels some firmness
Class IV	Severe contracture; obvious just from observation

*From Baker JL Jr. *Augmentation mammoplasty*. In: Owsley JQ Jr, Peterson RA, eds. *Symposium on aesthetic Surgery of the Breast*. St. Louis: Mosby; 1978:256–263

Table 2: from the website of the American Society of Plastic Surgeons²⁹

Grade 1:	Grade one capsular contracture is asymptomatic (producing or showing no symptoms). The formation of scar tissue around the implant does not interfere with the size, shape or texture of the breasts. The breasts look natural and remain soft to the touch.
Grade 2:	Grade two capsular contracture usually presents itself with only minor cosmetic symptoms. The breasts will usually appear normal in shape but feel somewhat firm to the touch.
Grade 3:	Grade three capsular contracture presents itself with obvious cosmetic symptoms. The breasts will be firm to the touch and appear abnormal, e.g., they will be overly round, hard-looking and the nipples may be misshapen. However, this grade of capsular contraction often doesn't cause much (if any) pain.
Grade 4:	Like grade three capsular contracture, grade four capsular contracture causes the breasts to become hard and misshapen. Patients with grade four capsular contracture also experience breast soreness; their breasts will often be tender and painful to the touch

Table 3: from the *a-z of plastic surgery*³⁰

I	soft
II	minimal, implant palpable, not visible
III	moderate, palpable and visible
IV	sever, hard, painful with distortion

Table 4: from *Key Notes on Plastic Surgery: Second Edition*³¹

Grade I	the augmented breast feels as soft as an unoperated one.
Grade II	minimal—implant palpable, but not visible.
Grade III	moderate—implant easily palpable, and it (or distortion from it) is visible.
Grade IV	severe—the breast is hard, tender, painful and cold. Distortion is often marked

Future perspectives;

As reliable methods now have been established to identify silicone in tissue, it would be very interesting to see the journey of silicone through the capsule into the body and the influence of capsule type and synovial metaplasia on this migration. As large empty vacuoles were seen in chapter V there remain questions on the loss of silicone when processing tissue. Investigating the same tissue fresh and after processing in the same spot would be helpful in this aspect. Breast implant-related complaints deserve a better diagnostic tool. A qualitative approach to this problem will probably be able to better communicate these complaints between both physicians and scientists.

PART II: HYPERGRANULATION TISSUE IN SKIN SCAR FORMATION

After breast surgery, the skin scar is often the most visible aspect. Even the most minimally invasive implantation techniques leave a visible skin scar, while most breast reconstructive techniques, especially breast reduction, leave quite large visible scars. While the primary downside to a hypertrophic scar (HS) on the breast after surgery will be aesthetic, the skin irritation commonly associated with HS can also hinder comfortable bra wearing. Moreover, the psychological impact of HS is associated with symptoms of depression, anger, anxiety, and post-traumatic stress^{32,33}.

Predicting HS formation is currently limited to known risk factors like wound location, tension, mechanical loading, age, and bacterial colonization³⁴⁻³⁶. These are helpful to identify certain patients at risk of HS formation, mainly those undergoing elective surgery. Nevertheless, many of these risk factors don't apply to patients undergoing breast reduction, reconstruction, or augmentation surgery. Many more have no choice in receiving accidental cuts, burn wounds, or surgical wounds causing HS formation. Since an early treatment start is preferred in HS a good prognostic tool would be useful for both groups³⁷. Nearly all known risk factors are about the location of the scar,

while the presentation profile of HS suggests there must also be systemic components of HS formation. Unfortunately, little is known about systemic factors influencing HS formation³⁸.

The local wound bed has been the subject of extensive research, so many cytokines involved are known by now. Interestingly, many of these cytokines are also found in skin irritation. Skin irritation can be considered a micro-trauma of the skin and can be induced with an irritant patch test, also producing an irritation threshold (IT) figure. This is the amount of irritant which is needed to provoke a reaction, or erythema, from the patient's skin. Since the two processes seem similar, we hypothesized a correlation could be found between HS formation and a different reaction to an irritant patch test. Mononuclear cells, like lymphocytes and monocytes, play a pivotal role in primarily the early inflammatory phase of wound healing. Although their local role has been described in HS research, they migrate into the wound bed and are of a systemic origin. So in addition, we hypothesized that systemically derived monocytes (e.g. from a venipuncture) could show a difference between HS and normotrophic scar (NS) patient groups.

In chapter VII we describe a prospective observational cohort study comprising 31 patients. All had undergone breast reduction mammoplasty and half of them developed a HS. The local skin response was measured with a patch test to determine the IT, as well as measuring transepidermal water loss (TEWL, a way to assess skin barrier disruption, a parameter for skin irritation), measuring skin redness using a DermaSpectrometer and stratum corneum collection via tapestripping for cytokine analysis. To analyze systemic differences a venipuncture was performed from which peripheral blood mononuclear cells (PBMC) were isolated. These cells were later stimulated with lipopolysaccharide (LPS), stimulating both the innate and adaptive immune systems. The supernatant from these cells was consequently used with a bead-based immunoassay to measure an inflammation panel of cytokines (IL-1 β , IFN- α 2, IFN- γ , TNF- α , MCP-1, IL-6, IL-8, IL-10, IL-12p70, IL-17A, IL-18, IL-23, and IL-33).

Irritation patch testing was indeed able to discriminate between the HS and NS group. When stimulated with the same irritating substance, patients

in the HS group showed a significantly higher visual erythema score and also a differentiating induction response when stimulated with a higher dose of the irritant LPS. Interestingly, the five most strongly differentiating cytokines, TNF- α , MCP-1, IL-8, IL-18, and IL-23, were secreted at significantly lower levels in HS patients as compared to NS patients.

The roles of MCP-1, IL-6, and IL-8 as chemoattractants for monocytes and neutrophils as regulators in the inflammatory phase of wound closure are well described^{39,40}. Together with TNF- α , these are also mitogens stimulating re-epithelialization⁴¹. IL-18 has been associated with psoriasis, allergic contact dermatitis, and atopic dermatitis, all inflammatory skin diseases and its role in wound healing had not yet been documented⁴²⁻⁴⁴. IL-23 is closely related to IL-18 but is produced by macrophages and dendritic cells as opposed to keratinocytes. This is the first time IL-18 and -23 have been explicitly linked to HS formation, possibly broadening the research into the pathophysiology of HS formation.

In the current body of literature a remarkable inconsistency exists, as there is both literature to support HS formation correlates with an increased inflammatory response as well as to support a reduced inflammatory response^{38,45-51}. With the red, inflamed appearance that a HS has an increased inflammatory response seems evident, yet in an ample amount of research, the opposite was found. This means that both are probably true and a more complete picture was missing.

Stimulating the PBMCs of HS and NS patients enables a more dynamic way to look at a specific piece of wound healing. Interestingly, the response in the HS group was indeed far stronger compared to the NS group, suggesting a hyperinflammatory state. At the same time, the absolute secretion of the same cytokines was still lower than it was in the NS group. The entire course of scar maturation seems to be an intricate process involving multiple types of cells and cytokines that act in both stimulatory and suppressive roles at different moments. This could also be the basis for the discrepancies found in the current literature.

The initial outset of this project was to assess whether a prognostic model could be created for HS formation, other than the known non-specific risk factors discussed earlier. Both irritation patch testing and the PMBC secretion

assay were able to discriminate between the NS and HS groups well enough to create a prognostic model. The PBMC model in particular was shown to be a very potent prognostic model, reaching a 93% accuracy. With current therapeutic strategies, there is a (limited) benefit to identifying those at risk; early treatment seems to be adequately beneficial³⁷.

For those contemplating cosmetic surgery knowing their HS risk status with a reliable prognostic marker can be a decision-changing piece of information. As cosmetic surgery experiences a surge in quantity, a proper marker could predict HS formation, and as a consequence contra indicate surgery and prevent dissatisfied patients. This could be a genuine advantage for cosmetically oriented practices, wanting to keep satisfaction high and preventable complications as low as possible.

Future perspectives

Both the patch test and cytokine assay will need further validation in a prospective trial. This research shows that HS formation is more than just a wound simply being located in the wrong place and in a hyper-inflammatory state. Further research into the systemic immunological differences between individuals developing HS and those who do not, should be a key subject for future HS projects. As pathophysiological pathways are unraveled, doors to therapeutic options will open and we might be able to prevent or cure HS for a far larger group of patients than we currently are. As most of our current strategies are only crude and often just treat the symptoms, these require repeated or prolonged treatment and are prone to recurrent complaints. Ideally, we would want to be able to identify the patient at risk, know why they are at risk, and if there are possibilities to manage that risk before undergoing a surgical procedure. After further finetuning in a prospective clinical trial, these predictive markers that identify those prone to develop HS could have a huge benefit in clinical (and shared) decision-making.

REFERENCES

1. Jalalabadi, F., Doval, A. F., Neese, V., Andrews, E. & Spiegel, A. J. Breast Implant Utilization Trends in USA versus Europe and the Impact of BIA-ALCL Publications. *Plast. Reconstr. Surg. - Glob. Open* 1–9 (2021). doi:10.1097/GOX.0000000000003449
2. DBIR. Dutch Breast Implant Registry (DBIR) Annual Report 2019. (2020).
3. Rohrich, R. J., Kaplan, J. & Dayan, E. Silicone Implant Illness: Science versus Myth? *Plastic and reconstructive surgery* 144, 98–109 (2019).
4. Patel, B. C., Wong, C. S., Wright, T. & Schaffner, A. D. *Breast Implants. StatPearls* (2021).
5. Tanne, J. H. FDA approves silicone breast implants 14 years after their withdrawal. *BMJ* 333, 1139.1-1139 (2006).
6. de Boer, M. *et al.* Breast Implants and the Risk of Anaplastic Large-Cell Lymphoma in the Breast. *JAMA Oncol.* (2018). doi:10.1001/jamaoncol.2017.4510
7. Nanayakkara, P. W. B. & De Blok, C. J. M. Silicone gel breast implants: What we know about safety after all these years. *Annals of Internal Medicine* 164, 199–200 (2016).
8. Majijers, M. C. & Niessen, F. B. The clinical and diagnostic consequences of Poly Implant Prothèse silicone breast implants, recalled from the European market in 2010. *Plast. Reconstr. Surg.* 131, (2013).
9. Lancien, U., Leduc, A., Tilliet Le Dentu, H., Perrot, P. & Duteille, F. Evaluation of satisfaction and well being with Breast-Q® of aesthetic breast augmentations by implants using the 'Dual Plane' technique: A serie of 191 cases. *Ann. Chir. Plast. Esthet.* 66, 314–319 (2021).
10. Noorizadeh, H. & Bari, B. The effect of breast augmentation surgery on quality of life, satisfaction, and marital life in married women using BREAST-Q as a validation tool. *J. Fam. Med. Prim. Care* 9, 711 (2020).
11. Henriksen, T. F. *et al.* Incidence and Severity of Short-Term Complications After Breast Augmentation. *Ann. Plast. Surg.* 51, 531–539 (2003).
12. Stevens, W. G. *et al.* Risk Factor Analysis for Capsular Contracture. *Plast. Reconstr. Surg.* 132, 1115–1123 (2013).
13. Dancey, A., Nassimzadeh, A. & Levick, P. Capsular contracture - What are the risk factors? A 14 year series of 1400 consecutive augmentations. *J. Plast. Reconstr. Aesthet. Surg.* 65, 213–8 (2012).
14. Berry, M. G., Cucchiara, V. & Davies, D. M. Breast augmentation: Part II - Adverse capsular contracture. *J. Plast. Reconstr. Aesthetic Surg.* 63, 2098–2107 (2010).
15. Moyer, K. E. & Ehrlich, H. P. Capsular Contracture after Breast Reconstruction. *Plast. Reconstr. Surg.* 131, 680–685 (2013).
16. Bachour, Y. *et al.* The aetiopathogenesis of capsular contracture: A systematic review of the literature. *J. Plast. Reconstr. Aesthetic Surg.* (2017). doi:10.1016/j.bjps.2017.12.002
17. Hillard, C., Fowler, J. D., Barta, R. & Cunningham, B. Silicone breast implant rupture: A review. *Gland Surg.* 6, 163–168 (2017).
18. Caffee, H. H. The influence of silicone bleed on capsule contracture. *Ann. Plast. Surg.* 17, 284–7 (1986).
19. Prantl, L. *et al.* Clinical and morphological conditions in capsular contracture formed around silicone breast implants. *Plast. Reconstr. Surg.* 120, 275–84 (2007).
20. Potter, E. H., Rohrich, R. J. & Bolden, K. M. The Role of Silicone Granulomas in Recurrent Capsular Contracture. *Plast. Reconstr. Surg.* 131, 888e-895e (2013).
21. Luke, J. L. *et al.* Pathological and Biophysical Findings Associated with Silicone Breast Implants: A Study of Capsular Tissues from 86 Cases. *Plast. Reconstr. Surg.* 100, (1997).
22. Kidder, L. H., Kalasinsky, V. F., Luke, J. L., Levin, I. W. & Lewis, E. N. Visualization of silicone gel in human breast tissue using new infrared imaging spectroscopy. *Nat. Med.* 3, 235–7 (1997).
23. L. Garrido, A. Bogdanova, L. L. Cheng, B. Pfeiderer, E. Tokareva, J. L. Ackerman, T. B. *Immunology of silicones.* (Springer, Berlin, 1996).

24. Kappel, R. ., Boer, L. L. & Dijkman, H. Gel Bleed and Rupture of Silicone Breast Implants Investigated by Light-, Electron Microscopy and Energy Dispersive X-ray Analysis of Internal Organs and Nervous Tissue. *Clin. Med. Rev. Case Reports* 3, (2016).
25. Kappel, R. M., Klunder, A. J. H. & Pruijn, G. J. M. Silicon chemistry and silicone breast implants. *Eur. J. Plast. Surg.* 37, 123–128 (2014).
26. Bassetto, F., Scarpa, C., Caccialanza, E., Montesco, M. C. & Magnani, P. Histological Features of Periprosthetic Mammary Capsules: Silicone vs. Polyurethane. *Aesthetic Plast. Surg.* 34, 481–485 (2010).
27. Fowler, M. R., Nathan, C. A. O. & Abreo, F. Synovial metaplasia, a specialized form of repair: A case report and review of the literature. *Arch. Pathol. Lab. Med.* 126, 727–730 (2002).
28. Baker JL, J. Augmentation mammoplasty. in *Symposium on Aesthetic Surgery of the Breast. St Louis: Mosby.* (ed. JQ Owsley, R. P.) 256 (1978).
29. Tehrani, K. What is capsular contracture and how can it be treated? (2018). Available at: <https://www.plasticsurgery.org/news/blog/what-is-capsular-contracture-and-how-can-it-be-treated>. (Accessed: 23rd July 2019)
30. Hodges, A. *A-Z of Plastic Surgery.* (Oxford University Press, 2008). doi:10.1093/acref/9780199546572.001.0001
31. Richards, A. & Dafydd, H. *Key Notes on Plastic Surgery.* (John Wiley & Sons, Ltd, 2014). doi:10.1002/9781118757017
32. Ngaage, M. & Agius, M. The psychology of scars: A mini-review. *Psychiatr. Danub.* 30, S633–S638 (2018).
33. Lawrence, J. W., Mason, S. T., Schomer, K. & Klein, M. B. Epidemiology and impact of scarring after burn injury: a systematic review of the literature. *J. Burn Care Res.* 33, 136–46
34. Slemper, A. E. & Kirschner, R. E. Keloids and scars: a review of keloids and scars, their pathogenesis, risk factors, and management. *Curr. Opin. Pediatr.* 18, 396–402 (2006).
35. Butzelaar, L., Ulrich, M. M. W., Mink van der Molen, A. B., Niessen, F. B. & Beelen, R. H. J. Currently known risk factors for hypertrophic skin scarring: A review. *J. Plast. Reconstr. Aesthet. Surg.* 69, 163–9 (2016).
36. Chiang, R. S. *et al.* Current concepts related to hypertrophic scarring in burn injuries. *Wound Repair Regen.* 24, 466–477 (2016).
37. Lee, H. J. & Jang, Y. J. Recent Understandings of Biology, Prophylaxis and Treatment Strategies for Hypertrophic Scars and Keloids. *Int. J. Mol. Sci.* 19, (2018).
38. Zhu, Z., Ding, J., Ma, Z., Iwashina, T. & Tredget, E. E. Systemic depletion of macrophages in the subacute phase of wound healing reduces hypertrophic scar formation. *Wound Repair Regen.* 24, 644–656 (2016).
39. Komi, D. E. A., Khomtchouk, K. & Santa Maria, P. L. A Review of the Contribution of Mast Cells in Wound Healing: Involved Molecular and Cellular Mechanisms. *Clin. Rev. Allergy Immunol.* 58, 298–312 (2020).
40. Delavary, B. M., van der Veer, W. M., van Egmond, M., Niessen, F. B. & Beelen, R. H. J. Macrophages in skin injury and repair. *Immunobiology* 216, 753–762 (2011).
41. Pastar, I. *et al.* Epithelialization in Wound Healing: A Comprehensive Review. *Adv. Wound Care* 3, 445–464 (2014).
42. Lee, J. H., Cho, D. H. & Park, H. J. IL-18 and cutaneous inflammatory diseases. *International Journal of Molecular Sciences* (2015). doi:10.3390/ijms161226172
43. Do, D. V. *et al.* Interleukin-18 system plays an important role in keloid pathogenesis via epithelial-mesenchymal interactions. *Br. J. Dermatol.* 166, 1275–1288 (2012).
44. Martin, S. F. *et al.* Mechanisms of chemical-induced innate immunity in allergic contact dermatitis. *Allergy* 66, 1152–1163 (2011).
45. Berman, B., Maderal, A. & Raphael, B. Keloids and Hypertrophic Scars. *Dermatologic Surg.* 43, S3–S18 (2017).
46. Niessen, F. B., Schalkwijk, J., Vos, H. & Timens, W. Hypertrophic scar formation is associated with an increased number of epidermal Langerhans cells. *J. Pathol.* 202, 121–129 (2004).

47. Van Den Broek, L. J., Niessen, F. B., Scheper, R. J. & Gibbs, S. Development, validation, and testing of a human tissue engineered hypertrophic scar model. *ALTEX* **29**, 389–402 (2012).
48. Butzelaar, L. *et al.* Inhibited early immunologic response is associated with hypertrophic scarring. *Exp. Dermatol.* **25**, 797–804 (2016).
49. van den Broek, L. J., van der Veer, W. M., de Jong, E. H., Gibbs, S. & Niessen, F. B. Suppressed inflammatory gene expression during human hypertrophic scar compared to normotrophic scar formation. *Exp. Dermatol.* **24**, 623–9 (2015).
50. Wang, J. *et al.* Toll-like receptors expressed by dermal fibroblasts contribute to hypertrophic scarring. *J. Cell. Physiol.* **226**, 1265–1273 (2011).
51. Ding, J. & Tredget, E. E. The Role of Chemokines in Fibrotic Wound Healing. *Adv. Wound Care* **4**, 673–686 (2015).

9

LIST OF PUBLICATIONS

The Histological Composition of Capsular Contracture Focussed on the Inner Layer of the Capsule: An Intra-Donor Baker-I Versus Baker-IV Comparison.

E. de Bakker, L.J. van den Broek, M.J.P.F. Ritt, S. Gibbs, F.B. Niessen
Aesthetic Plast Surg 2018;42:1485–91. doi:10.1007/s00266-018-1211-1

Prognostic tools for hypertrophic scar formation based on fundamental differences in systemic immunity.

*E. de Bakker**, *M.A.M. van der Putten**, *M.W. Heymans, S.W. Spiekstra, T. Waaijman, L. Butzelaar, V.L. Negenborn, V.K. Beekman, E.O. Akpınar, T. Rustemeyer, F.B. Niessen*
Experimental Dermatology. doi: 10.1111/exd.14139

The Baker classification for capsular contracture in breast implant surgery is unreliable as a diagnostic tool.

E. de Bakker, M. Rots, M.E. Buncamper, F.B. Niessen, J.M. Smit, H.A.H. Winters, M. Özer, H.C.W. de Vet, M.G. Mullender.
Plastic and Reconstructive Surgery. doi: 10.1097/PRS.0000000000007238.

Label-free stimulated Raman scattering imaging reveals silicone breast implant material in tissue.

L. van Haasterecht, L. Zada, R.W. Schmidt, E. de Bakker, E. Barbé, H.A. Leslie, A. Dick Vethaak, S. Gibbs, J.F. de Boer, F.B. Niessen, P.P.M. van Zuijlen, M. L. Groot, F. Ariese.
Journal of Biophotonics. 2020;e201960197 doi: 10.1002/jbio.201960197

**Additional invasive techniques in scar management (ed Luc Téot et al),
Textbook on scar management; State of the art management and emerging
technologies.**

Springer Nature. ISBN: 978-3-030-44765-6

E.de Bakker, M.C.E. van Leeuwen, O.W.M. Meijer, F.B. Niessen

**A case of silicone and sarcoid granulomas in a patient with ‘highly cohesive’
silicone breast implants: a histopathologic and laser raman micro-
probe analysis.**

*T.I. Todorov, E. de Bakker, L.C. Langenberg, L.A. Murakata, M.H.H. Kramer,
P.W.B. Nanayakkara and J.A. Centeno.*

International journal of Enviromental research and Public Health 2021, 18,
4526. doi: 10.3390/ijerph18094526

**Baker-IV capsular contracture is correlated with an increased amount of
silicone material: an intra-patient study.**

*E. de Bakker, L. Zada, R.W. Schmidt, L. van Haasterecht, H.A. Leslie, A. Dick
Vethaak, J.F. de Boer, P.P.M. van Zuijlen, M.L. Groot, F. Ariese, P. Bult, H. Dijkman,
S. Gibbs, F.B. Niessen.*

submitted and accepted in Plastic and Reconstructive Surgery, december
2021

DANKWOORD

Ik ben over het algemeen niet iemand die moeite heeft om ergens woorden voor te vinden. Toch is het bijzonder om aan dit dankwoord te beginnen. Ik ben dolblij dat er een strik om dit project kan en heb erg uitgezien naar de afronding. Uitdagingen zoals deze vormen je, maar zijn soms ook erg lastig. Ik kan echter vooral terugkijken op vele geslaagde samenwerkingen, ontmoetingen, talloze leermomenten en een enorme groei als arts, maar bovenal als mens.

De artikelen en achtergrond van dit proefschrift zijn over vele schijven gegaan. Dat moet ook haast wel als je er bijna 8 jaar over doet, al was dat met horten en stoten. Het spreekt dan ook voor zich dat dit dankwoord verre van compleet is, toch wil ik een poging doen iedereen te bedanken die in deze lange periode belangrijk voor mij en dit proefschrift is geweest. Ik ben namelijk aan velen dank verschuldigd voor, vaak belangeloze, hulp en samenwerking. Of tenminste toch een luisterend oor tijdens de vele kopjes koffie (en biertjes) die het cement vormen van elk proefschrift.

In de medische wereld werken we (te) vaak in een duidelijk afgebakend stukje vakgebied. Met mijn immer brede interesse vond ik het prachtig om in dit onderzoek juist heel multidisciplinair te werken. Ik verdeelde mijn tijd en aandacht al tussen de afdeling Plastische, Reconstructieve en Handchirurgie en het DermaLab, inmiddels onderdeel van de Moleculaire Celbiologie en Immunologie (MCBI). Naast die twee afdelingen heb ik gedurende de jaren ervaren dat het belangrijk en waardevol is om overal je licht op te steken en met mensen uit allerlei vakgebieden te blijven praten. Het resultaat is dat ik in die periode heb samengewerkt met een hoop afdelingen en instanties. Ik ben ze alle dank verschuldigd en ik vrees dat ik er nog een paar vergeten ben: het Cancer Center Amsterdam, de Dermatologie, Interne Geneeskunde en afdeling Pathologie van het Amsterdam UMC, het LaserLab, de Faculteit der Bètawetenschappen, de afdeling Medische Statistiek en de Omgevingswetenschappen van de Vrije Universiteit Amsterdam, de Brandwondenstichting, het Department of Envi-

ronmental and Infectious Disease Sciences, Division of Biophysical Toxicology, Armed Forces Institute of Pathology in Washington en de FDA.

Prof.dr. Gibbs, beste Sue, toen ik via via bij jou aankwam om een leuke wetenschappelijke stage te versieren hadden we denk ik allebei niet kunnen voorstellen dat het in dit boekje zou eindigen. Jouw eerste reactie op mijn onderzoeksvoorstel was eigenlijk glashelder; een enkeltje terug naar de tekentafel en is zo'n lab stage nou wel wat voor jou. Ik denk dat jij zelf ook niet verwacht had dat je het een goed idee zou vinden als ik zou komen promoveren. Inmiddels zijn we (vele) jaren verder en dan eindelijk aangekomen bij mijn promotie. Hoe de start ook moge zijn geweest, ik kan weinig anders dan lof hebben voor hoe je mij geholpen hebt door de jaren heen. Je draagt je promovendi een warm hart toe, blijft ze wanneer ze dat nodig hebben aan de jas trekken en sleept ze erdoor heen. Voor al deze dingen ben ik je enorm dankbaar.

Dr. Niessen, beste Frank, vanaf het eerste moment ben je betrokken bij het onderzoek wat ik aan de VU heb gedaan. Jouw enthousiasme is aanstekelijk en zonder jouw onderzoekende geest was de basis voor al het kapselcontractie onderzoek in het lab simpelweg niet aanwezig geweest. Je staat terecht bekend als de man in Platisch Nederland die een hoop doet voor het littekenonderzoek en het lijkt me leuk hier over te blijven nadenken met je. Ik ben je dankbaar voor alle uitgebreide besprekingen, updates, hulp en discussies. Zonder twijfel heb je meer theorieën dan dat er ooit promovendi beschikbaar zullen zijn om deze uit te zoeken. Wellicht word je hier af en toe in geremd, maar laat het je niet stoppen, want er komen regelmatig prachtige dingen uit voort!

Prof.dr. Ritt, beste Marco, als promotor heb je me, ondanks dat jouw inhoudelijke deskundigheid op een heel ander vlak ligt, toch vaak kunnen helpen en me wegwijs gemaakt in de wondere wereld van de academische geneeskunde. Je bent altijd bereid om mee te denken over zowel de inhoudelijke als de politieke zaken die kunnen spelen. Toen ik zelf een handletsel had stond je vooraan om me van advies te voorzien waardoor ik een stuk eerder aan mijn revalidatie kon

beginnen dan eerder het plan was (en mogelijk dus ook succesvoller). Dank dat je zo bereikbaar en open opstelt naar je promovendi.

Beste Lenie, ik was echt een jong labkuikentje toen je me onder je hoede nam. Eerst als student en later aan het begin van mijn promotie. Samen hebben we talloze kleuringen, ELISA's, FACS en celkweken gedaan. Allemaal onderwerpen waarbij ik echt op nul ben begonnen in het lab. Zonder al jouw geduld en hulp was de basis van dit proefschrift vast en zeker niet gelegd.

Prof.dr. Middelkoop, beste Esther, regelmatig zaten we tegenover elkaar in het mooie hoekkantoor van de Plastische. Ik wil je dan ook bedanken voor de gezellige en dikwijls nuttige gesprekken en kopjes koffie. Bedankt dat je hebt willen plaatsnemen in mijn leescommissie en nu ook oppositie.

Geachte leden van de leescommissie en oppositie, prof.dr. J.W.M. Niessen, prof. dr. M.A.M. Mureau, prof.dr. E. Middelkoop, prof.dr. R.R.J.W. Van der Hulst en dr. C. van Montfrans. Veel dank voor het beoordelen van mijn proefschrift en uw bereidheid plaats te nemen in de oppositie.

Mijn paranimfen Floris en Aarent: Floris! Al sinds de middelbare school ben je een van mijn beste vrienden. We kennen elkaar door dik en dun en je bent altijd bereid te helpen. Het was niet meer dan logisch je te vragen als paranimf en ik ben blij dat je daarmee instemde.

Aarent, toen wij elkaar in een moment van puur escapisme vonden in de bibliotheek van het Catharinaziekenhuis zat er maar één ding op: een biertje pakken in de lokale buurtkroeg en een enorme bak plezier maken. Ik ben blij dat we daar sindsdien niet mee gestopt zijn. Je bent een goeie vent en ik ben je dankbaar voor alle gesprekken, advies, tips, diepe poedersnieuw en reizen die we samen gedeeld hebben. Vandaag voegen we daar mijn promotie aan toe en hopelijk in de nabije toekomst ook de jouwe.

Het dermalab, ondertussen Skinlab bij de MCBI, heb ik ervaren als een warm bad en heel open en op leren gerichte omgeving. Eerst naast de brug naar het ziekenhuis in het poli gebouw van het VUmc en later in een prachtig nieuw gebouw en in een veel grotere groep. Zeker in het begin is er denk ik niet een iemand geweest die mij niet af en toe heeft geholpen bij wat voor hen ongetwijfeld simpele problemen waren. Er zijn dan ook veel mensen die ik wil bedanken. Allereerst uiteraard de echte onvolprezen helden van het lab, de analisten: Sander, Sanne, Taco en Maria. Jullie zijn echt nooit te beroerd om een helpende hand of meedenkend brein te bieden en zijn van onschatbare waarde voor alle promovendi, ikzelf inclusief!

Al mijn mede promovendi, Niels, Charlotte, Elisabetta, Jeroen. In hetzelfde schuitje zitten vormt altijd een sterke band, maar bovenal hebben we het erg gezellig gehad. Jullie waren altijd bereid om iets uit te leggen aan een weinig aan het lab gewende arts zoals ik, of uiteraard om een goede borrel te doen op z'n tijd.

Aan de overkant van de straat bij de Plastische: Margriet, inmiddels (terecht) professor Mullender, dank voor alle gesprekken, brainstorms en hulp bij het schrijven van een mooi artikel, je bent veelzijdig en essentieel voor het onderzoek van de hele afdeling.

Vera, Floyd en Maeghan mijn wisselende kamergenootjes en medepromovendi: dank voor alle gezelligheid en meer dan enkele lange gesprekken tijdens biertjes, wijntjes en koffie! Ook wil ik alle AIOS en plastisch chirurgen van de afdeling, danken voor de gezelligheid en leerzame momenten.

Prabath, Christel en Lisette voor de brainstorms tijdens de siliconen meetings en het schrijven van een mooi artikel samen.

Pim, Martin, Dick en vele anderen van verschillende afdelingen in het O2 gebouw en de VU. Ons project om siliconen lekkage te meten in een fysiolo-

ogische omgeving vereiste samenwerking, een bovengemiddeld percentage MacGyver en creativiteit. Ondanks dat het voor niemand van jullie een gebruikelijke onderzoeksrichting is, wilden jullie allemaal graag een handje helpen. Het was mooi geweest om het resultaat in dit boekje te mogen publiceren, maar ik blijf optimistisch om het project met de siliconen prothesen in weckpotten tot een goed einde te volbrengen!

Het part-time werken bij de Nederlandse Obesitas Kliniek heeft dit proefschrift mede mogelijk gemaakt, de lieve collegae daar maakten het echter ook een hele leuke en leerzame periode waar ik met plezier op terugkijk (en het leukste afscheidsfilmpje ooit).

Alle toppers van de chirurgie in het Spaarne Gasthuis wil ik graag bedanken voor een leerzame tijd en een continue stroom aan plezier maken die hopelijk voorlopig nog niet opgedroogd is.

Lieve mam, bedankt voor alle liefde, zorg en tijd die je altijd beschikbaar maakt. Je steun is onvoorwaardelijk en dat is heel erg fijn. We lijken op elkaar en kunnen eindeloos discussiëren en filosoferen samen wat ik echt op prijs stel.

Lieve pap, alhoewel we soms pittige discussies kunnen hebben, juist over wetenschap, weet ik dat je me steunt in de dingen die ik doe en daar ben ik je dankbaar voor. We delen een hele leuke hobby, het spijt me dat dit proefschrift daar kostbare tijd vanaf gesnoept heeft. Ik hoop dat we daar de komende periode meer tijd voor kunnen vinden.

Lieve Marleen en Carien, mijn lieve zusjes. Jullie hebben beiden een totaal andere richting gekozen met de muziek. Ik ben waanzinnig trots op hoe jullie je ontwikkelen en succes hebben in de muzikale wereld die soms toch wat overeenkomsten vertoont met de medische wereld. Gelukkig weten we elkaar heel goed in gemeenschappelijke interesses te vinden en ik weet dat ik altijd op jullie kan rekenen.

Lieve Jop, dank voor de gezelligheid en de passie voor (jazz)muziek die we delen. Dank ook voor het onderdak in Amsterdam toen ik begon met de wetenschappelijke stage die de basis heeft gelegd voor dit proefschrift. Ik heb enorm respect voor hoe je uit het niks inmiddels drie bedrijven gaande houdt en bovendien een prachtig gezin hebt.

Mijn lieve 'schoon'familie: Marion, John, Eveline en Richard, we kennen elkaar inmiddels al een hele tijd. Dank voor alle momenten bij de open haard en skivakanties waarbij meer dan eens mijn carrière en promotie besproken zijn. Het is bijzonder, maar tegelijkertijd ook heel vanzelfsprekend dat Marion nu zelfs mijn collega is.

Floris, Jeroen, Jiri, Mark, Maurits, Pepijn, Robert en Wiebe. Ik voel me gezegend dat we na al die jaren nog zo'n hechte vriendengroep zijn. Iedereen heeft ruim verhalen van me moeten aanhoren tijdens talloze gesprekken en borrels. Robert bleef desondanks met me fietsen. Mark en Maurits ben ik eeuwig dankbaar voor het samen organiseren van het Kantje-Boord bootfestival, wat een ervaring is dat geweest! Samen gaan we hopelijk nog vaak skiën, borrelen en plezier maken.

De mannen van Coïtus Caelestis, #1! Alex, Bas, Boudewijn, Daan, Gijs, Lars, Olav, Reinoud, Rik en Tibor. Dankzij jullie was mijn studie in Maastricht een briljante tijd. We hebben allemaal talloze uurtjes op 'de Kaap' doorgebracht en de vereniging was er een stukje mooier door. Ons lustrumfeest blijft een van de mooiste feestjes ooit daar. Gelukkig wordt er nu tijdens fietstochten met Gijs, Rik, Daan en Bou nog volop afgezien en gelachen, iets waar ik heel blij mee ben.

Mijn vrienden oud-bestuursgenootjes van Pulse Master mogen natuurlijk niet ontbreken. Na een onovertroffen succesvolle reeks co-borrels zijn we vrolijk doorgegaan met weekendjes zeilen en korte reisjes. Jullie zijn stuk voor stuk toppers en we vullen elkaar op een leuke manier aan. Een combi tussen een multidisciplinaire medische hulplijn en gezelligheid, touché!

Tot slot lieve, lieve Roos. Het is heel simpel, zonder jou had ik hier nu niet gestaan. Je hebt me gesteund door dik en dun en jij als geen ander weet dat het soms best frustrerend is geweest. Ik heb hier te weinig pagina's om uit te leggen hoeveel je voor mij betekent. We hebben al een hoop avonturen samen mogen delen en vinden elkaar gelukkig moeiteloos in onze liefde voor de bergen, reizen, sport, lekker eten en nog veel meer. Op naar nog vele, vele avonturen samen!

ABOUT THE AUTHOR

Erik de Bakker was born in Blaricum on the 10th of June 1989. After graduating from the *Gemeentelijk Gymnasium* in Hilversum in 2007 he started his study of Medicine at Maastricht University. During his bachelor he got in touch with Plastic-, Reconstructive- and Handsurgery during an elective course in the anatomy of the hand and arm. In his master he did an elective rotation in Plastic Surgery and later went on to do his final clinical rotation (semi-arts) in Plastic surgery as well. His final scientific rotation was at the Dermatology Laboratory of the VUmc, which has become part of the Molecular Cell Biology and Immunology as the Skinlab. In continuation of the initial research started in his scientific rotation, he started a combined PhD under the supervision of prof. dr. S. Gibbs (MCBI), prof.dr. M.J.P.F. Ritt (Plastic Surgery) and dr. F.B. Niessen (Plastic Surgery) in 2015 next to clinical work in the following years in Surgery, the Dutch Obesity Clinic and Dermatology.



